

**Society of Automotive Engineers: Mini Baja**  
**The City College of New York**  
**Senior Design II: ME 47300**  
**Professor: Peyman Honarmandi**  
**Faculty Advisor: Prof. Ali Sadegh**



**Team Members:**  
Umut Ayyildiz, Alessandro Belaj, Daniel Cohen, Fathema Islam,  
Brian Kazi, David Kim, Yusuf Wong

# Table of Contents

<b>Introduction</b>	<b>4</b>
<b>Chassis</b>	<b>5</b>
What is the Chassis?	5
Customer Requirements	5
Driver	6
Primary Members	7
Secondary Members	8
Measurements/Constraints	9
Design	9
2020 Chassis	10
2021 Iteration	13
FEA Analysis	17
Calculations	18
Boundary Condition	18
Rear Impact	19
Front Impact	19
Side Impact	20
Roll Over	20
Result	20
<b>Suspension and Steering</b>	<b>21</b>
What is Suspension?	21
What is Steering?	24
Rack and Pinion:	24
Ackerman Steering	25
Suspension Customer Requirements	26
Components	27
Knuckles:	27
Shocks and Springs:	28
Wheels:	29
Ideal Spring Rate Calculations	29
Front Suspension and Steering	31
Design	32
Drop Test:	40
Rear Suspension	49
FEA	53

Final Design Comparison	55
<b>Powertrain</b>	<b>56</b>
What is the Powertrain?	56
Overview of current setup	57
Customer Requirements	58
Component Specifications	59
Engine	59
Continuously Variable Transmission (CVT)	60
Old Gearbox	61
New Gearbox	63
Front Differential	67
Rear Differential	67
U Joints	70
<b>Brakes</b>	<b>78</b>
What are Brakes?	78
Braking System Function	79
Brake System Philosophy	80
Inboard Brakes vs Outboard Brakes	82
Adjusting Shaft (Bias Bar) vs Proportioning Valve	84
Fixed Calipers vs Floating Calipers	86
Vertical Brake Assembly	88
Traction Assisted Cornering	89
Upside-down Brake Assembly	89
Final Brake Design	90
Throttle Assembly	92
Recap of Previous Brake Design	93
CAD Design	93
Rotors	93
Assembly:	94
Brake System Analysis	95
Heat Transfer Analysis	95
Brake Force Calculations	96
Updated Design with Brake Assembly	99
<b>Electronics</b>	<b>100</b>
What is an AWD System?	100
What is a Clutch Pack & Torque Transfer Theory?	100

Flaws in the Previous EM Clutch Design	103
BMW's XDrive Clutch System	105
Lever Arm Mechanical Advantage	106
Cylindrical Ramp Mechanical Advantage	107
Stepper Motor Requirements	108
Final Assembly of XDrive Clutch Design	109
FEA Analysis	109
Manufacturing Plan	111
<b>Conclusion</b>	<b>113</b>
<b>References</b>	<b>115</b>
<b>Appendix</b>	<b>116</b>
Electronics MATLAB Codes	116
Lever_Arm_Torque_Motor.m	116
Powertrain MATLAB Codes	116
Shaft Stress analysis code	116

# Introduction

The purpose of this project is to develop an offroad vehicle for the annual Baja SAE competition, where students design, manufacture, and race a single-seater off road vehicle in a 4 day long competition. In this competition, the team will be expected to give a cost report, design presentation, and a business presentation on the viability of the vehicle as a potential mass-manufactured vehicle for the recreational market.

Overall, the development of an offroad vehicle takes into consideration many different factors that can affect the handling/performance of the vehicle. Because of this, many of the subsystems will require several iterations of redesign as we design the vehicle around the rulebook and the challenges we will have to face in the dynamic events of the competition. Weekly meetings were held to make sure every system was in communication with each other and understood how each systems affects the other.

As each separate system has its own requirements, each system will be described as its own product which will later be combined to create the entire Baja. A functional diagram of the vehicle is detailed below

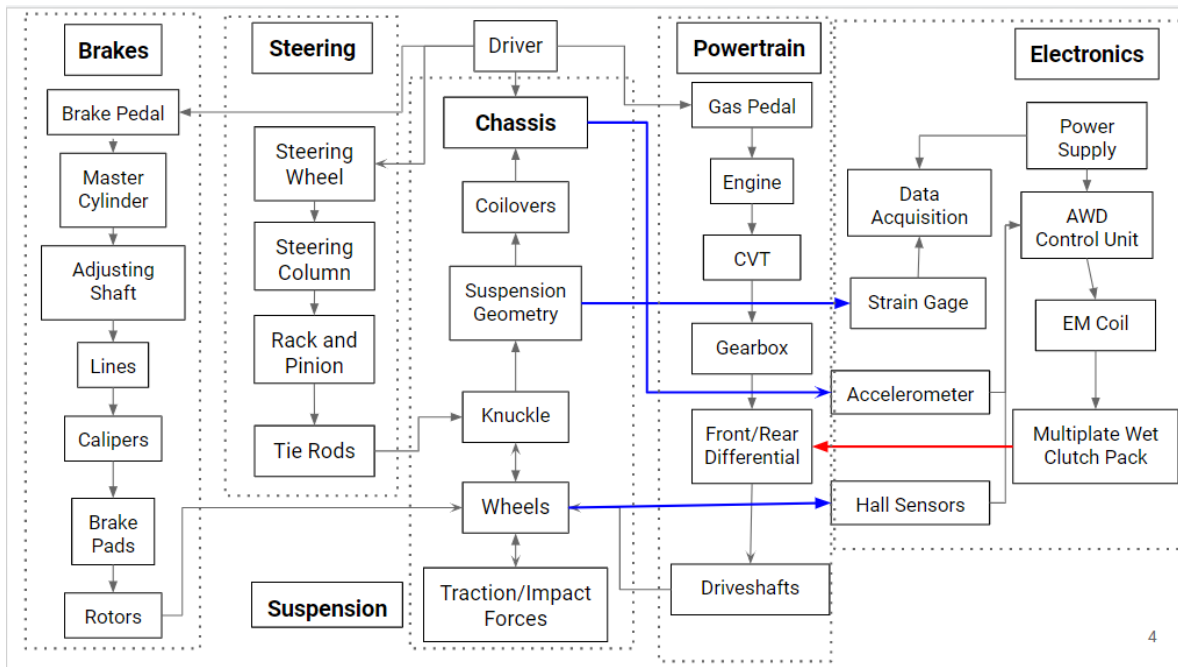


Figure 1: Baja Functional Diagram

# Chassis

Some important terminology to note for this section of the report is outlined below:

- Frame: The entire tubular structure including all non-contilevered tubes.
- Roll Cage: Primary and Secondary members that protect the driver.
- Member: A Primary or Secondary member that ends and begins at a named point.
- Named Point: The intersection of the Centerlines of two or more joining members.

## *What is the Chassis?*

The chassis is the core component in the Baja vehicle. Its primary function is to protect the driver during normal use and in the event of a crash. Along with the safety of the driver, it houses the other systems, thus it is also used to protect the systems which include the engine, transmission, suspension, etc. The subsystems dictate how the frame must be designed along with the restrictions set aside by the SAE Baja Competition rule book. With both of these in mind, it'll allow for the design of a successful frame. The following *Figure 2* is the chassis functional diagram.

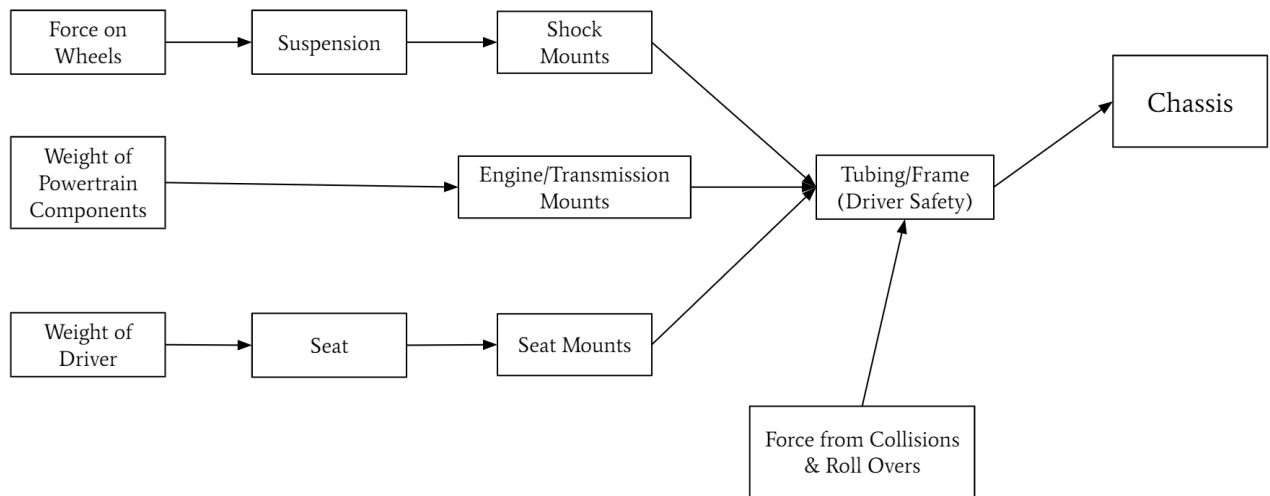


*Figure 2: Chassis Functional Diagram*

## *Customer Requirements*

The chassis must be designed and fabricated to prevent any failure of the frame's structure during normal use, collision, or rollover. The roll cage must be a space frame of tubular steel. The roll cage and frame members must be fully welded together. The welds cannot be ground,

sanded, or modified. Roll cage members that are bent, must not have any wrinkles, dents, or detrimental deformation to the cross-section.

Roll cage members may be straight or bent. Straight members cannot extend longer than 1016 mm (40 in) between named points and bent members may not be longer than 838 mm (33 in) between named points. Bent members cannot have a bend greater than 30 degrees. Bend radii less than 152 mm (6 in) that end at named points are expected and are not considered to make a member bent. Named points are shown in *Figure 3*.

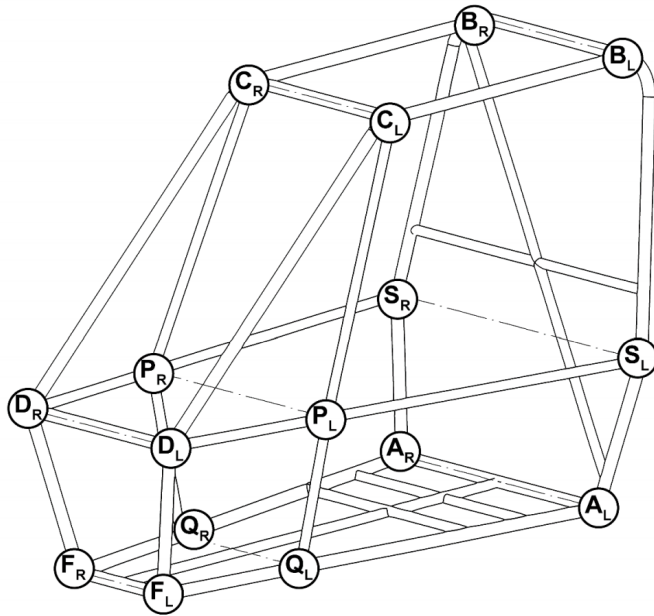


*Figure 3: Named Points*

### *Driver*

The Baja vehicle must be able to accommodate drivers of all sizes from the 95th percentile male and 5th percentile female. The driver must be able to fit comfortably and meet the minimum clearances. The minimum space is based on clearances between the driver and a straight edge which is applied to any two points on the outside edge of a roll cage member. The lateral space rule states that the driver's helmet must have 152 mm (6 in) clearance. The driver's shoulders, torso, hips, thighs, knees, arms, elbows, and hands must have a clearance of 76 mm (3 in) clearance. The vertical space rule states that the driver's helmet must have a minimum of 152 mm (6 in) from any two points among the members that make up the top of the roll cage. In a side view of the vehicle, no part of the driver's body, shoes, and clothing may extend beyond the envelope of the roll cage.

## **Primary Members**

Primary roll cage members and members used for bracing must be made out of circular steel tubing with an outer diameter of 25 mm (0.984 in) and a wall thickness of 3 mm (0.118 in) and a carbon content of at least 0.18%.

It may also be a steel shape with bending stiffness and strength greater than that of a circular steel tube with an outside diameter of 25 mm (0.984 in) and a wall thickness of 4 mm (.118 in). The wall thickness must be at least 1.57 mm (0.062 in) and the carbon content must be at least 0.18%.

Primary members are shown in *figure 4* and are listed below:

- RRH: Rear Roll Hoop
  - The rear roll hoop (RRH) is a planar structure that defines the boundary between the front-half and rear-half of the Baja. It is located behind the driver's back. It has to be inclined up to 20 degrees from vertical. The minimum width of the RRH is 736 mm (29 in) located 686 mm (27 in) above the seat bottom. The vertical members may be straight or bent.
- RHO: Roll Hoop Overhead Members
  - The rearward ends of the roll hoop overhead (RHO) members intersect the RRH within 51 mm (2 in) of points BR and BL defined by BLC. The forward ends of the RHO members intersect with the CLC at points CR and CL. Members CLC, BLC, and RHO must be coplanar. Bends at the rearward ends of the RHO members are not allowed.
- FBM: Front Bracing Members
  - Front bracing members (FBM) connect to the RHO, SIM, and the LFS at points C, D, and F. The FBM must be continuous tubes and the angle between the upper front bracing member and the vertical must be less than or equal to 45 degrees.
- LC: Lateral Cross Members
  - Lateral cross members (LC's) are denoted by the points they connect (e.g. ALC, BLC, etc.). LC's cannot be less than 203.5 mm (8 in) long. LC's cannot have a bend but they can be part of a larger bent system. The LC's are listed below.
    - ALC: Aft Lateral Cross Member
    - BLC: Overhead Lateral Cross Member
    - CLC: Upper Lateral Cross Member
    - DLC: SIM Lateral Cross Member
    - FLC: Front Lateral Cross Member
- LFS: Lower Frame Side Members

- The lower frame side members define the lower right and left edges of the roll cage. They are joined at the bottom of the RRH at point A and extend forward up until the driver's heels. The LFS intersects the FLC at points FR and FL.

### ***Secondary Members***

There are two types of secondary members; a circular secondary member and a square secondary member. The circular secondary members are circular tubes with an outside diameter of at least 25.4 mm (1 in) and a thickness of 0.889 mm (0.035 in). The square secondary members are square tubes with a thickness of 0.889 mm (0.035-in) and have a width and length of 25.4 (1-in).

Secondary members are shown in *figure 4* and are listed below:

- **LDB: Lateral Diagonal Bracing**
  - The lateral diagonal bracing (LDB) member is used to diagonally brace the RRH from one RRH vertical member to the other. The top and bottom intersections between the LDB members and the RRH vertical members must be no more than 127 mm (5 in) from points A and B. Also, the angle between the LDB members and RRH vertical members must be greater than or equal to 20 degrees.
- **SIM: Side Impact Members**
  - The two side-impact members (SIM) lie on a horizontal mid-plane within the roll cage. They extend forward from point S on the RRH up to the driver's toes. In the case of a front braced roll cage, the SIM extends forward to point D. The members must be between 203 mm (8 in) and 356 mm (14 in) above the seat bottoms between points S and D.
- **FAB: Fore/Aft Bracing Members**
  - Fore/aft bracing (FAB) must be used to restrain the RRH from rotation and bending in the side view. Rear bracing restrains point B from longitudinal displacement in the event of failure of the joints at points C. Front bracing restrains point C from longitudinal and vertical displacement, supporting points B through the RHO members. Members used in the FAB must not be longer than 1016 mm (40 in) in unsupported length. Triangulation angles from the side view 20 degrees between members.
- **USM: Under Seat Member**
  - The under-seat member (USM) must be placed in a way so it can prevent the driver from passing through the plane of the LFS. There are two options for the USM, one is called the lateral USM, and the other the longitudinal USM. The lateral USM joins the LFS from below the driver. The longitudinal USM joins the ALC and FLC members longitudinally.
- **RLC: Rear Lateral Cross Member**

- The rear lateral cross member (RLC) must follow the minimum lengths described for LC members.
- Any tube that is used to mount the safety belts or fuel tank or protect the fuel system

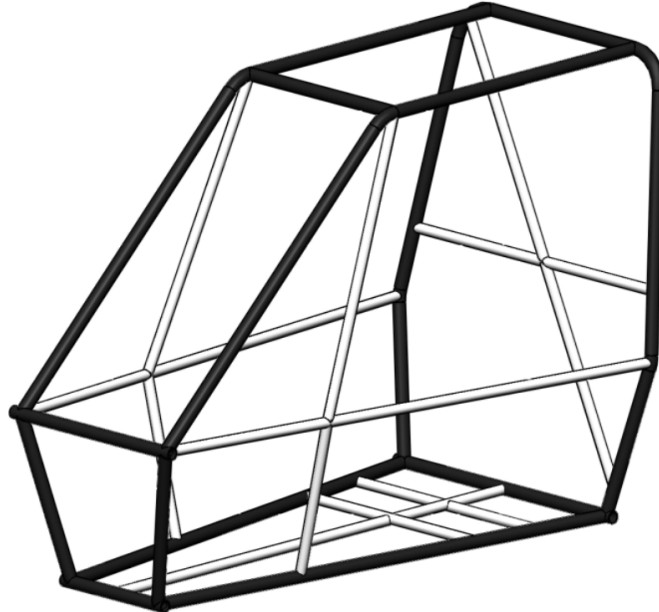


*Figure 4: Primary Members Highlighted in Black and Secondary Members are in White.*

## *Measurements/Constraints*

The design process for the Baja frame began by taking detailed measurements of three different people to fulfill the customer requirements. Ergonomic measurements such as sitting length, sitting height, and width of the driver were recorded. Measurements were taken when the drivers were sitting in their car. Measurements of possible seat options were taken, a carbon fiber coated seat and an aluminum seat. The constraints of the steering and brake system were recorded. The dimensions of the engine and transmission were also recorded to get a visual of the constraints of the rear.

## *Design*

The Baja frame went through multiple iterations of modifications to reflect the new constraints from the different subsystems and decisions made about the integration of the powertrain. The initial design was made using the 3D sketch feature on SolidWorks. With the proper constraints, modifications to the design were made when needed without much adversity. The vehicle had gone through 12+ different designs. It was decided during winter break to redo the entire design of the chassis. This was because prior to winter break, it was believed we would be allowed back in school to continue where the prior design team had left off with the manufacturing of the

chassis. Since we were not manufacturing anything, it was decided that we should design a new chassis without the limitations of what was already manufactured. The final 2020 and 2021 chassis designs are the primary focus of this report.

### 2020 Chassis

The 2020 chassis began with the design of the RRH. Using the size constraint of the new drivers and the lateral/vertical space rule, the design of the 2020 RRH was modified. The driver constraint measurements can be seen in *figure 5*. The ALC member was given a length of 30 inches, which is enough space for the width of the driver. The height of the RRH was reduced from what it was in 2019's design, from 49 to 45 inches, because the driver is shorter. The RRH initially had an angle of 18 degrees in the frame. All bends in the design are 4.5 inches due to manufacturing limitations.

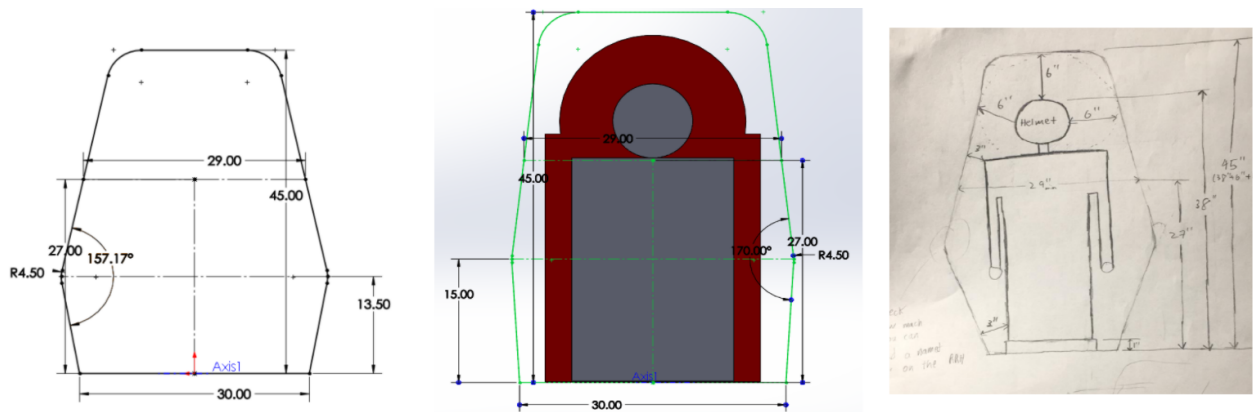


*Figure 5: Design of the RRH*

After the design of the RRH was complete, next up was the LFS and the USM. The constraints used for this were taken from the brakes and steering shown in *figure 6*. From the dimensions, the LFS was chosen to be 32 inches from points A to Q. The overall extension of the LFS is 48 inches. The USM had one longitudinal member and a lateral member six inches from the RRH. The lateral member was situated so that an extra member would be in place to support the seat in the event of a seat failure.

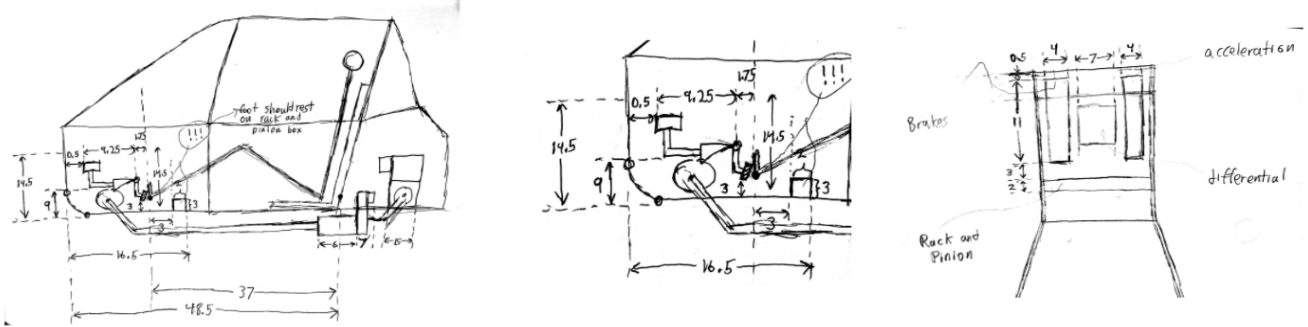


Figure 6: Constraints of Brakes and Steering

Next in the design process was the SIM. The design of the SIM initially had an extension of 35.5 inches in the center of the frame shown in *figure 7*.

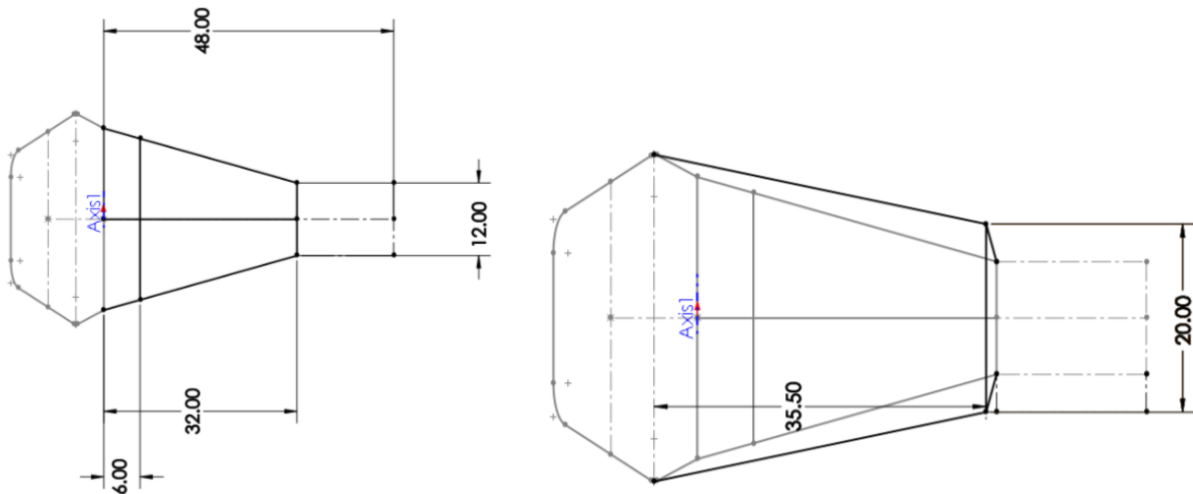
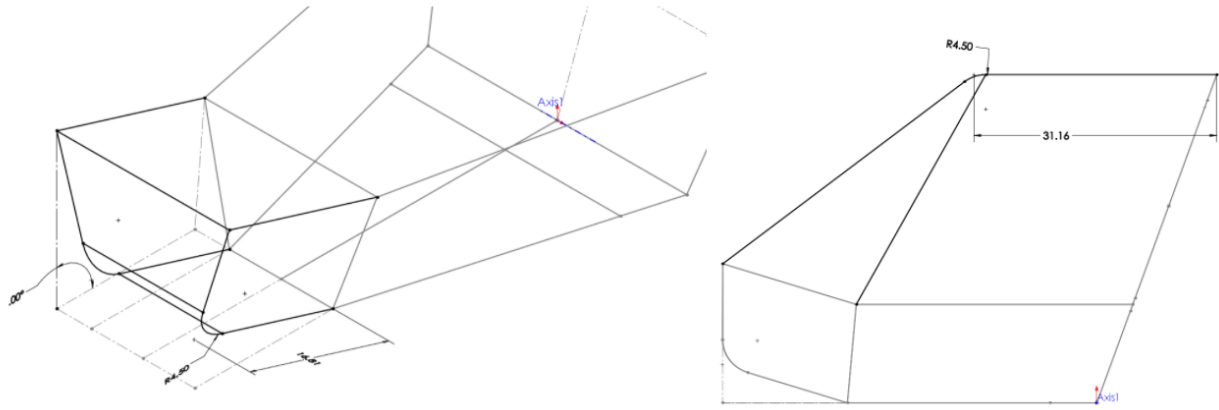


Figure 7: Base and SIM Design (Top View)

Next up was the design of the overhead members which is limited by the design choices of the other members. The design was made to ensure the overhead members were shorter than 40 inches between named points. In *figure 8* the front and the overhead members are shown.



*Figure 8: Front and Overhead Members Shown, Isometric and Side View*

Next is the rear of the chassis. Due to the need of constant modifications in the 3D sketch, the rear was kept open ended so for now it is based off the 2019 baja vehicle shown in *figure 9*.

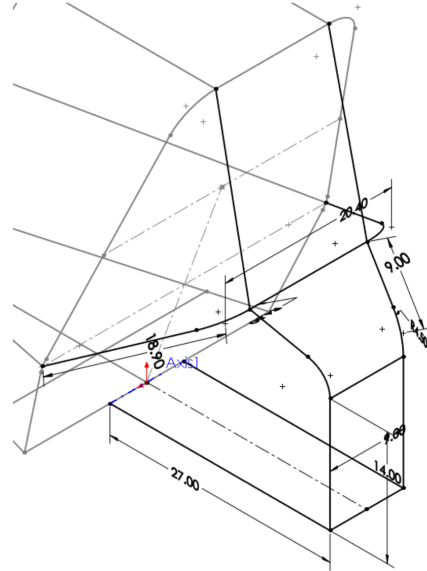


*Figure 9: Rear Design of Chassis*

The tubes were added to the design after the frame was complete. Physical models of the brakes, powertrain, engine, template, etc were inserted into the assembly to have a visual of the constraints.

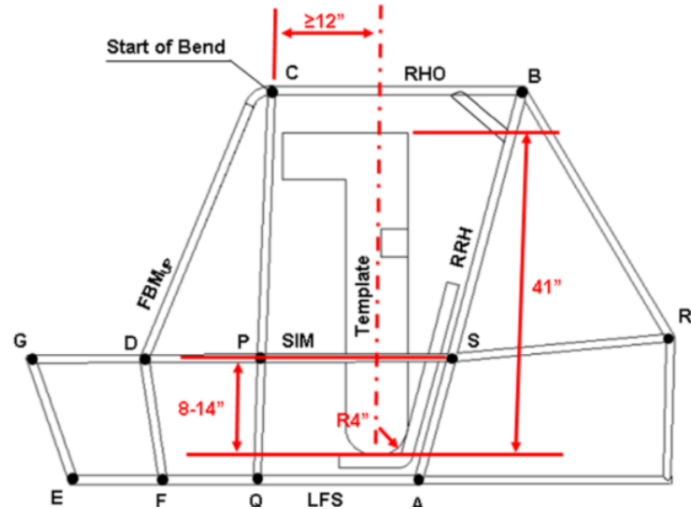
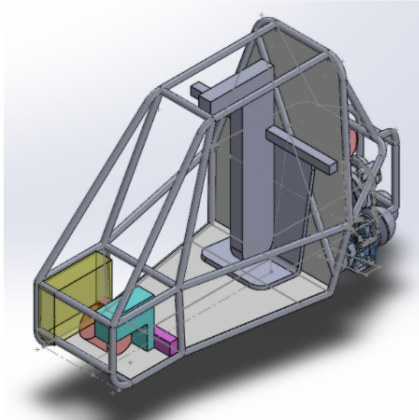


Figure 10: Constraint Design

### 2021 Iteration

After many design decisions, the Baja is at its final iteration. We wanted to reduce weight and use space efficiently with our new design. We started our design process by measuring the smallest person in our group.



Figure 11: Driver Measurements

Then we went about reducing members of the previous design and optimizing to be lighter but just as strong. So first we optimized the front so every space was used where the drivers feet and pedals would go highlighted in red in *Figure 12*.

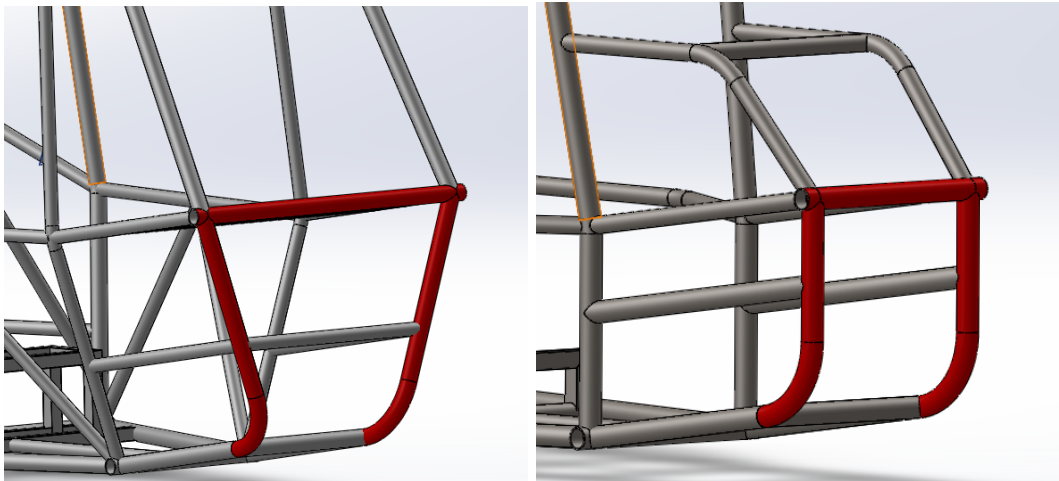


Figure 12: Front Modifications (Left is 2020 and right is 2021)

Next we modified the RRH by making it angled to the maximum amount allowed by the competition,  $18^\circ$ . By doing this we reduced the height of the RRH which brought the overhead members down. This was done to meet the minimum clearance requirements from the drivers head to the overhead members. The shape of the RRH was also optimized to meet the lateral clearance rules,

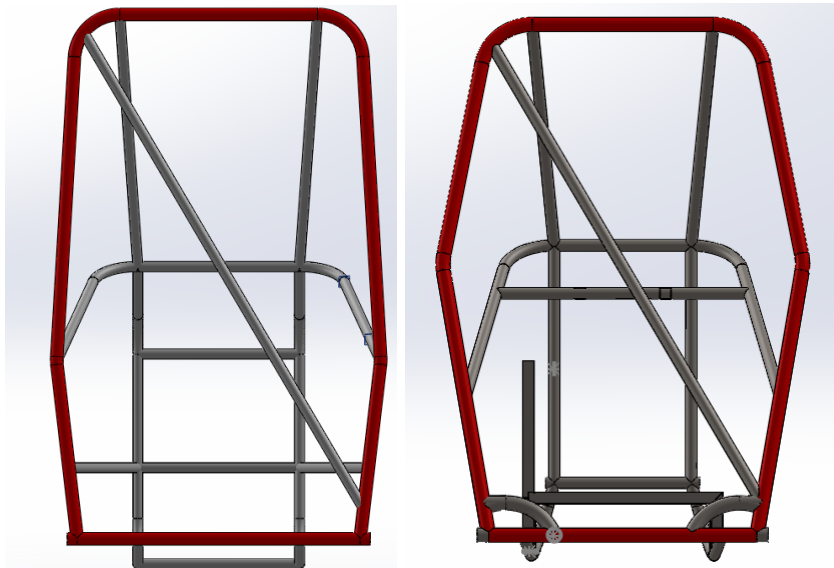
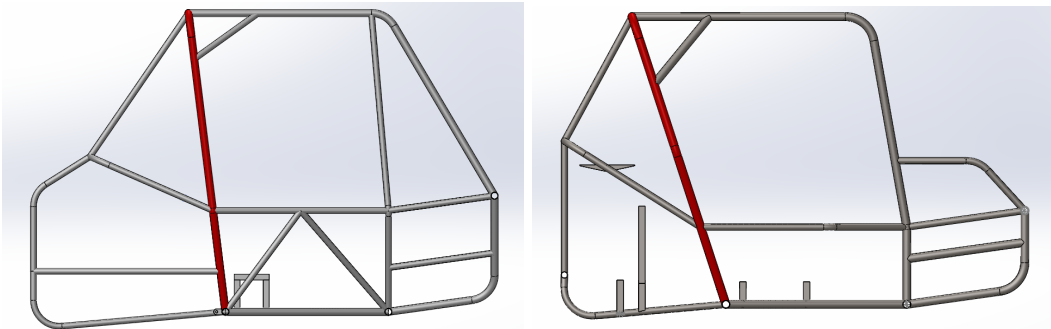
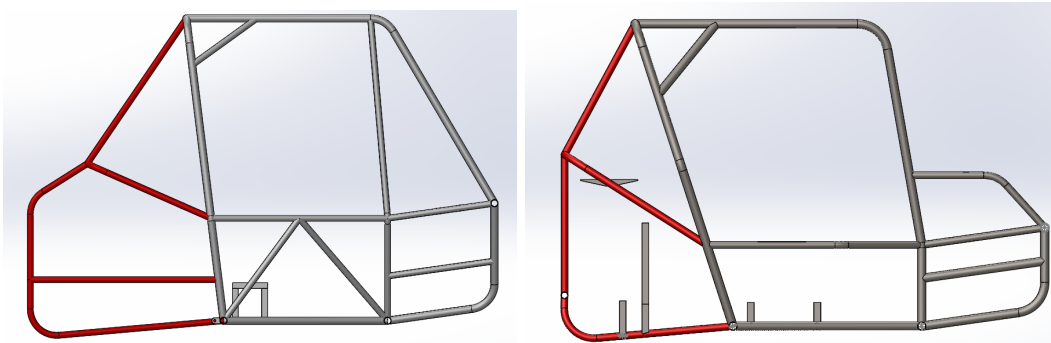


Figure 13: RRH Modifications Front View (Left is 2020 and right is 2021)



*Figure 14: RRH Modifications Side View (Left is 2020 and right is 2021)*

From the side view we can see that the rear was drastically altered. It was noted that the previous design had too much empty space so in the 2021 design it was optimized so the space was used efficiently. The alteration of the rear is highlighted in red in the following figure.



*Figure 15: Rear Modifications Side View (Left is 2020 and right is 2021)*

The most important factor in the design of the final iteration was the way all the components would be mounted to the chassis, particularly the powertrain and suspension. The powertrain was mounted as shown below, serving the purpose of mounting both the engine and the sprocket mounting bearings.

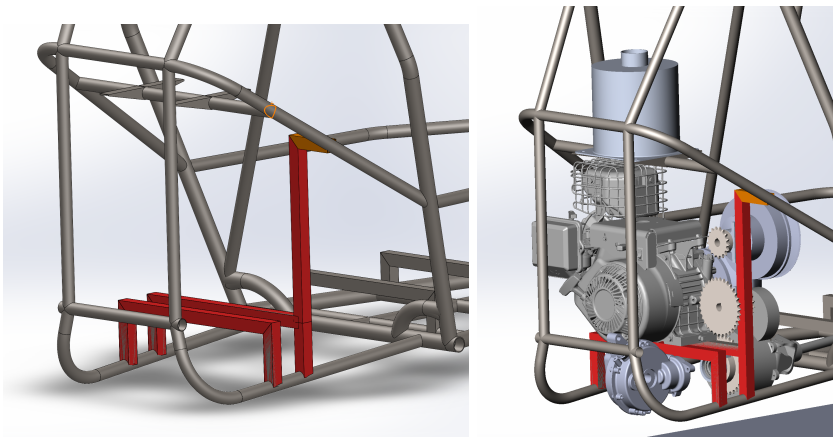


*Figure 16: Powertrain Mounting Points*

The rear had to be modified in order to allow the rear suspension to articulate as well, and in accordance with the suspension team's LOTUS analyses, a mounting point for the front pivot of the trailing wheel had to be created on the RRH.

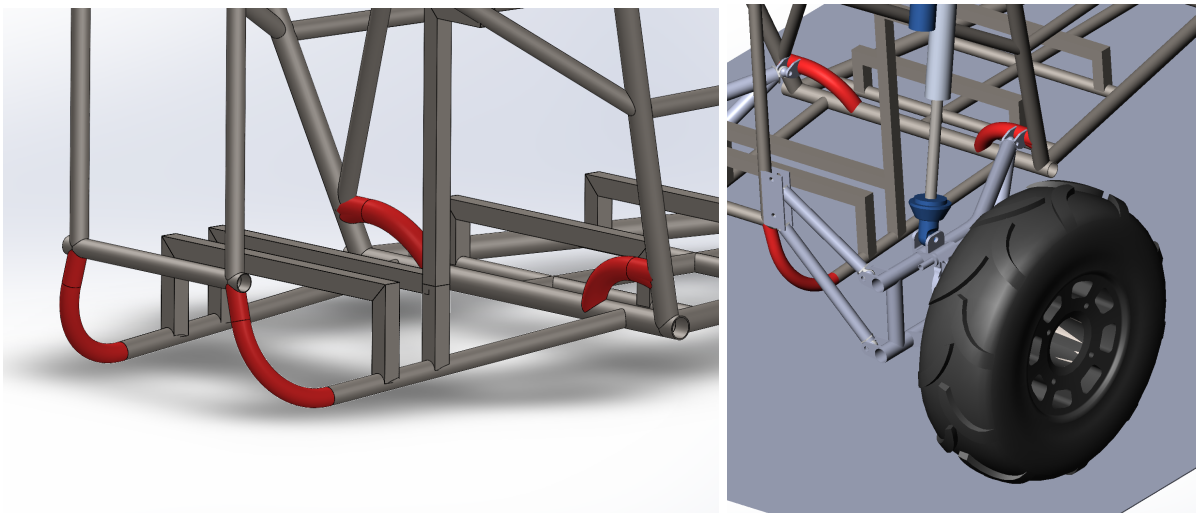


*Figure 17: Trailing Arm Mounts*

Finally, the front suspension required the shocks to be mounted in an area that wasn't on a rear-braced version of the chassis, so additional tubing had to be added for the upper A-arm and the top shock mount. This new front suspension design had a more rectangular front face, so changes were made to the 3D sketch to account for the LOTUS analysis.

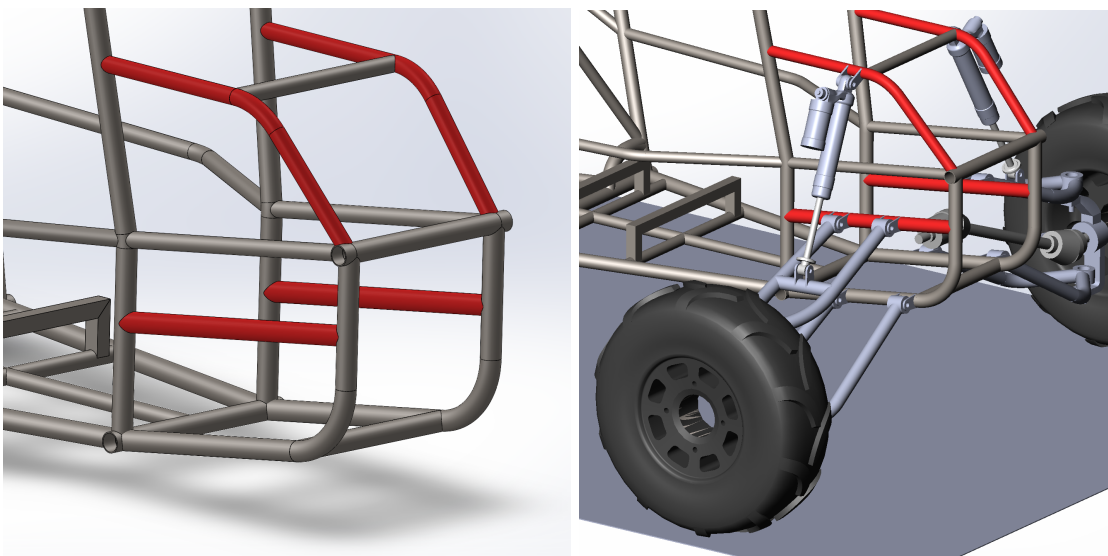


*Figure 18: Front Suspension Mounts*

The final design of the chassis is shown below and reflects the work that has been done to allow next year's team to manufacture a vehicle that is ready for fabrication. The new chassis is 4.1 kg lighter and 6.9 inches shorter in height compared to the 2020 design.

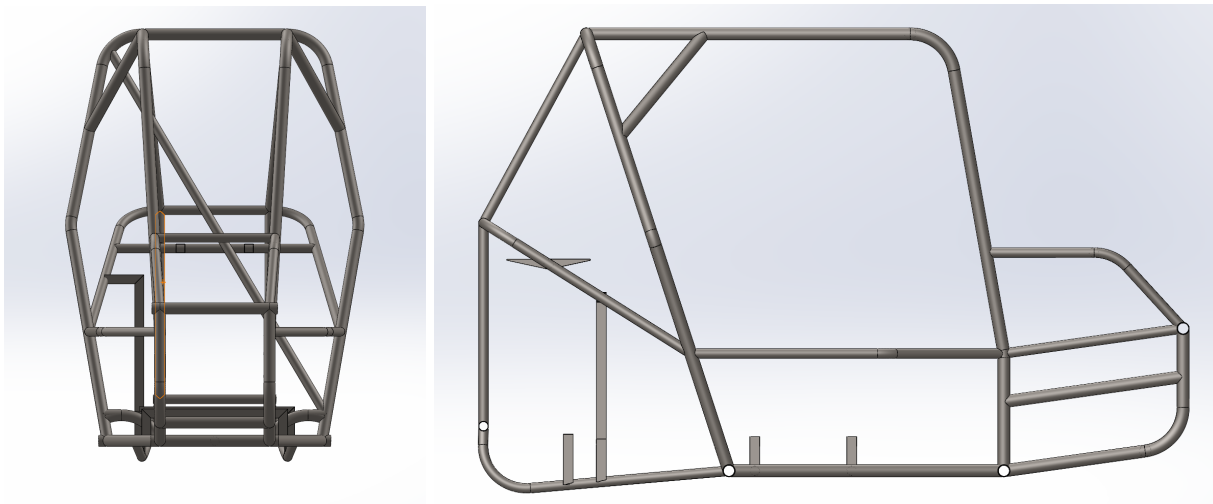


*Figure 19: Front and Side View of Chassis*

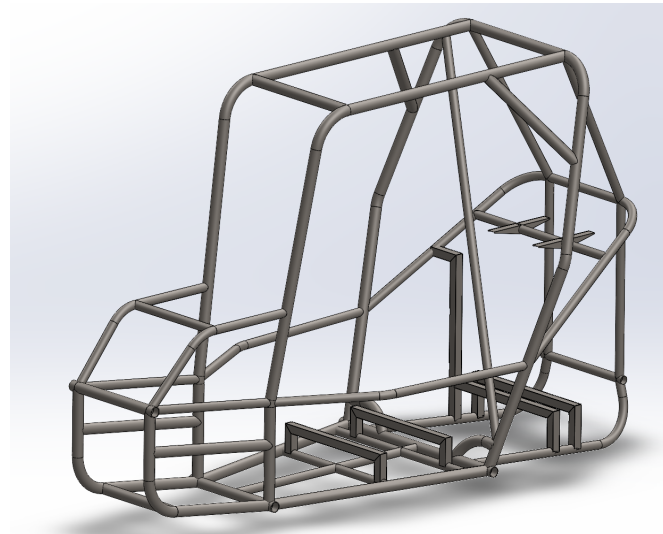


*Figure 20: Arbitrary View of Chassis showing all features*

### *FEA Analysis*

The underlying design rule followed was to keep the driver safe. FEA was conducted to determine if the frame did just that. There were four different scenarios: front impact,

side-impact, rear impact, and rollover. The first steps were to get the parameters needed. Hand calculations were done.

### ***Calculations***

The mass of the chassis is 291 kg. A velocity of 15.65 m/s was chosen because it is a value close to the max speed, this creates a safer and better design for the worst possible outcome. The factor of safety chosen was 1.25 for each analysis. The force for the front, side, and rear impact can be determined with a single calculation. The force for the rollover was different as it needed to withstand three times the vehicle's weight. The following table shows the parameters used.

<b>Mass</b>	291 kg
<b>Velocity</b>	15.65 m/s
<b>Factor of Safety</b>	1.25
<b>Force for Front, Side, and Rear</b>	FS*45541.5 N = 56926 N
<b>Force for Roll Over (3x Baja Weight)</b>	FS*8555.4 N = 106943 N
<b>Impact Time</b>	0.1 s

*Table 1: Parameters used to find the force*

The formula used to find the force was the impulse formula derived from Newton's second law shown below.

$$F = ma = \frac{mv}{t}$$

In the case of a rollover, the force was calculated following the rules put down by the National Highway and Traffic Safety Administration. A five-star crash rating requires that the vehicle must be able to withstand three times its weight without deforming 4 inches. All the forces were multiplied by a safety factor of 1.25.

### ***Boundary Condition***

All the boundary conditions were set with the assumption that the vehicle would remain stationary but in reality, the vehicle would move in the direction it was hit. With a vehicle that is fixed, the forces produced by an impact would be larger than that of a vehicle with no restrictions. Since the boundary condition applied to the model is fixed on certain locations, rather than free to move, this will induce a larger stress on the vehicle, thus having a conservative analysis on the impact. We were limited to setting the boundary conditions on the joints only.

### Rear Impact

Fixture was set at front members and the force was applied onto the rear members as shown in figure 17.

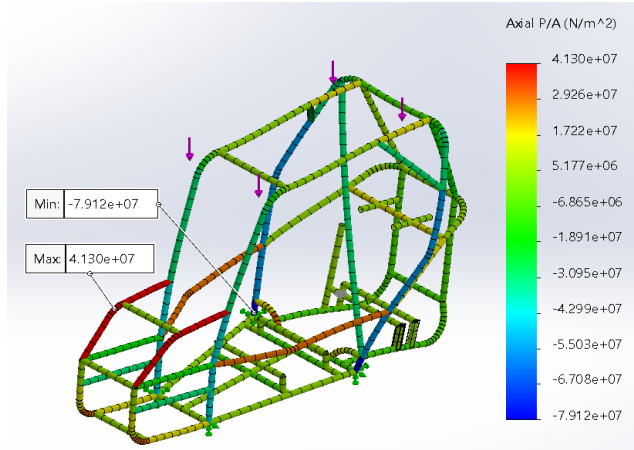


Figure 21: Rear impact FEA

### Front Impact

Fixture was set at rear members and the force was applied onto the rear members as shown in figure 18.

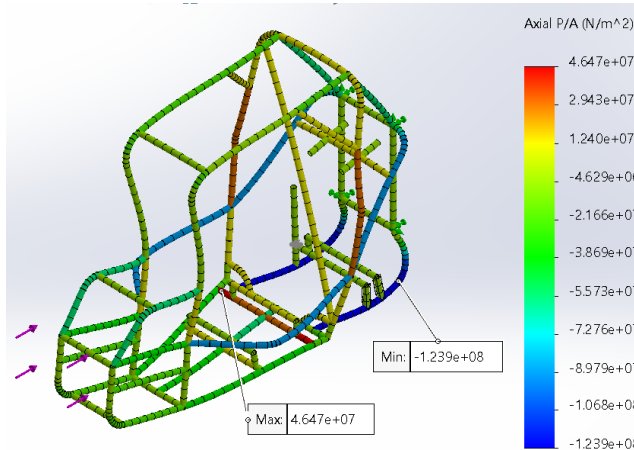


Figure 22: Front impact FEA

### *Side Impact*

Fixture was set at one side member and the force was set at the opposite side member.

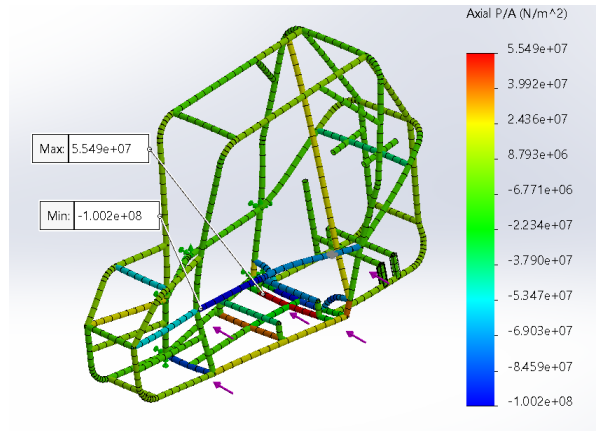


Figure 23: Side impact FEA

### *Roll Over*

The fixture was set at the bottom members and the force was set on the top members.

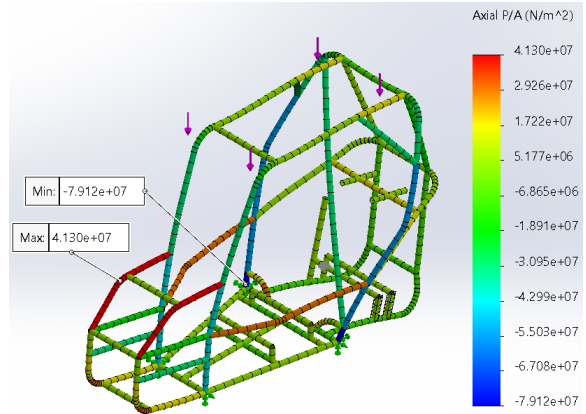


Figure 24: Roll over FEA

### *Result*

FEA was done using SolidWorks and Ansys. In both software we ran into singularities located in the joints of the 2021 design. SolidWorks only allowed us to use boundary conditions at weldment joints using 1D studies. When we tried to fix this issue on Ansys by including weld fillets, it ruined our mesh topology. Even though our study on the 2021 design couldn't produce proper data, we are confident that the design can withstand impact forces with a FOS of 2+ due to the rulebook enforcing a strong and robust design especially when paired with 4140 alloy steel. The goal for next year would be to continue FEA on the 2021 design to ensure it is ready. Due to not being able to get a finite result, the following is the FEA on the 2020 design.

A shell mesh was used for all the studies because it decreased the computing time and power. In *table 2* the results are shown. None of the tests reached the yield stress of the material used. The roll over study only deformed by 0.55 inches which is well below the 4 inches set by the National Highway and Traffic Safety Administration.

<b>Impact</b>	<b>Max Stress (psi)</b>	<b>Yield Stress (psi)</b>	<b>Deformation (in)</b>
<b>Front</b>	58885	63100	0.39
<b>Side</b>	32633	63100	0.57
<b>Rear</b>	82236*	95434	0.55
<b>Roll Over</b>	82091*	95434	0.55

\* Primary Members

*Table 2: FEA results with yield stress shown for material used*

## Suspension and Steering

### *What is Suspension?*

The role of a good suspension system is to keep the driver comfortable and confident in the vehicle's handling while keeping the vehicle planted on the road. In a competitive setting like the SAE Baja competition, both the front and rear suspension must be up to the task of smoothing out the multitude of bumps we will see throughout the course while being lightweight enough to give our car a competitive advantage. Each component in the suspension system has their own role to play in the dynamics of the vehicle, and will each have pros and cons that will determine how we design our suspension. The functional diagram for the suspension system (both front and back) is shown in Figure 21 below.

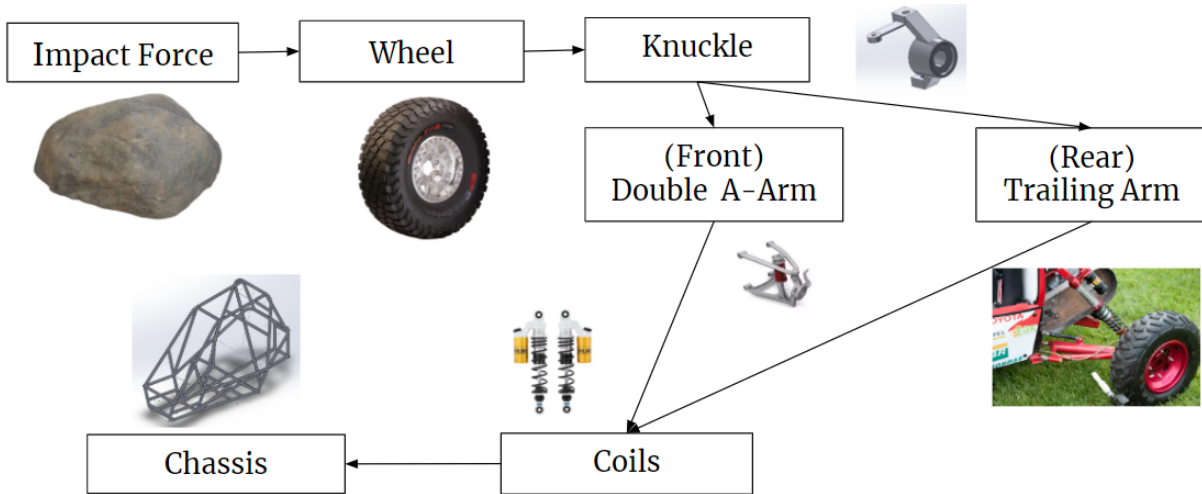


*Figure 25: Suspension Functional Diagram*

As seen in the functional diagram, the suspension mainly deals with impact forces from rocks or bumps in the road. This impact force goes through the wheel into the knuckle, which is attached via bolts or ball joints to the suspension geometry. In our vehicle, the front suspension utilizes a double a-arm suspension while the rear has a trailing arm suspension with two lateral (camber) links. The suspension geometry is then finally attached to the chassis via a shock and spring (or coilovers in our case). While the functional diagram starts off with impact forces, our main goal is to improve the dynamics of our vehicle in corners, which is why it is imperative to understand the implications of certain suspension terms.

To understand how to design our suspension geometry, we needed to understand some basic vehicle dynamics theory, which involves a lot of new jargon like caster, camber, toe, etc. The diagrams below show pictures of what these each mean for better understanding.

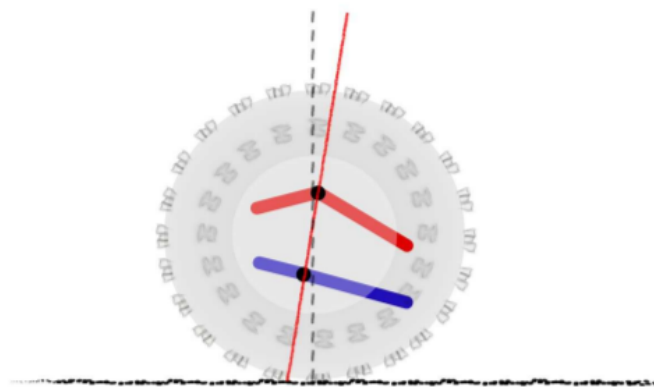


*Figure 26: Positive Caster (Negative Caster is opposite of this)*

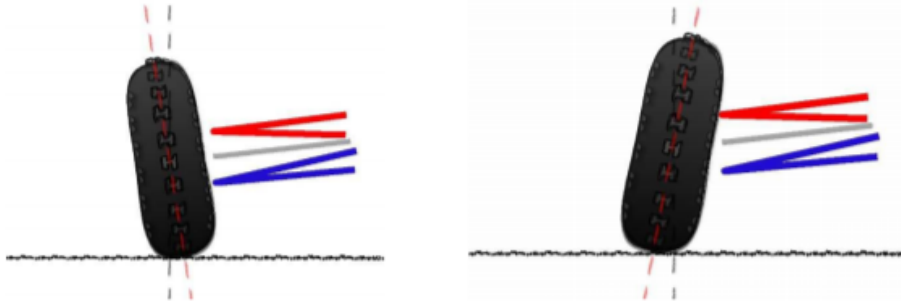


Figure 27: Positive and Negative Camber (shown left to right)

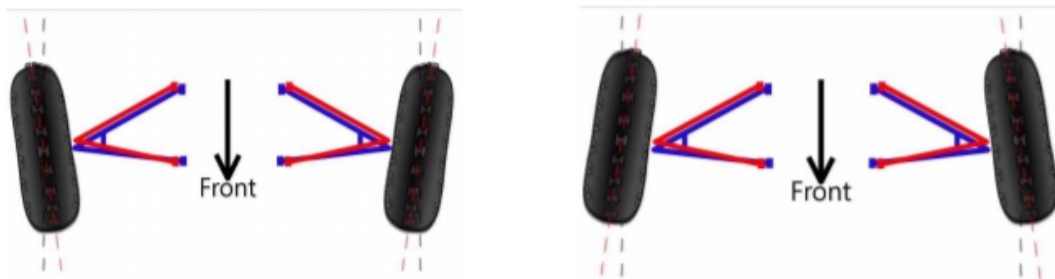


Figure 28: Toe In and Toe Out (shown left to right)

The implications for each will also help determine how we set up our suspension geometry as we move forward. Castor has implications on steering as with higher degrees of positive caster, more force is required to move the steering wheel, but less is required from the driver to bring the vehicle back to a straight line. Camber has implications during cornering, as during roll, the wheel will tilt towards the outside of the corner, so implementing negative camber will help vehicle stability and speed in corners. Finally, toe has implications in general vehicle stability as toe-out can lead to a very unstable vehicle if implemented in the rear, but while toe in is much more stable, it leads to increased tire wear

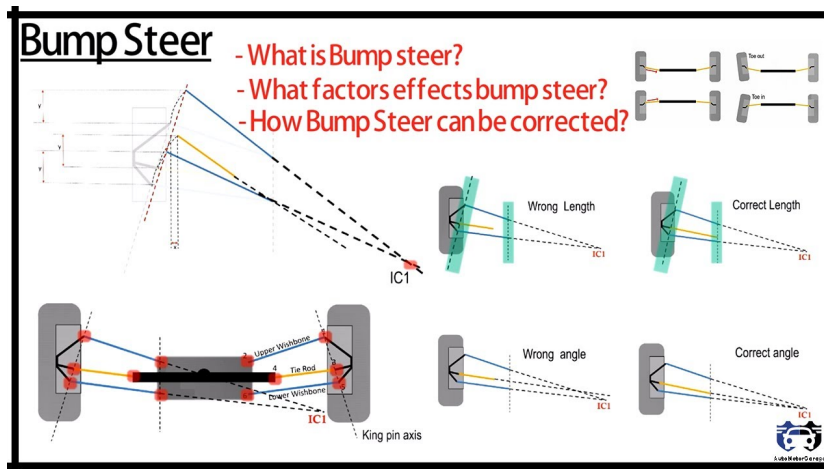
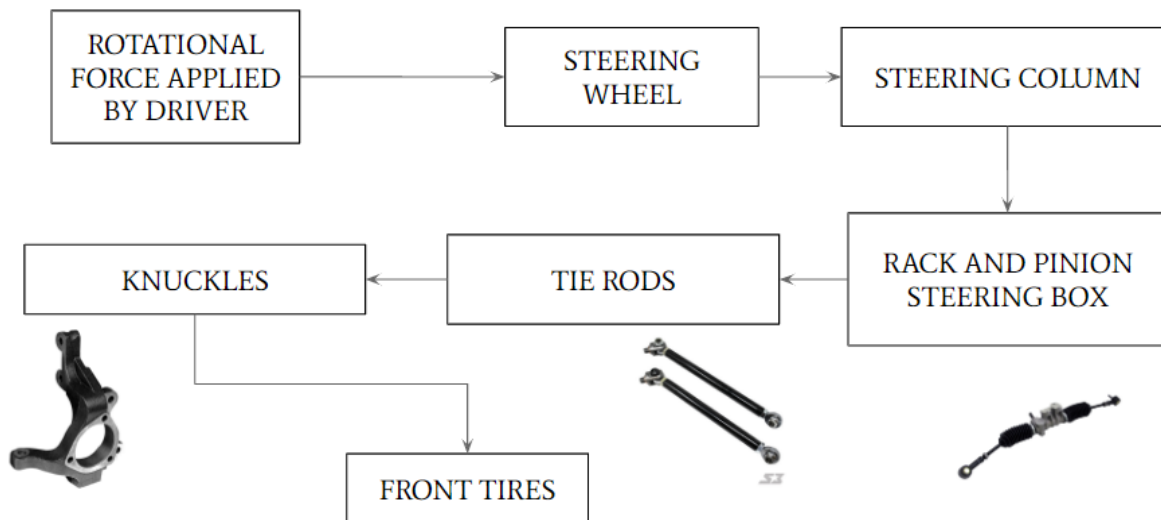


Figure 29: Bump Steer Diagram

Bump steer occurs when the toe angle changes during wheel travel. Wheel travel is when the suspension is bumping (upwards motion) or drooping (downwards motion). Causes of bump steer are the mounting points for the control arms and tie rods not falling along the same vertical plane. The upper control arm, lower control arm, and tie rod follow different arcs in a bump or droop scenario because of this. To correct bump steer draw lines from the outer ball joints of the upper and lower control arms and then extend these lines until they intersect at the Instantaneous Center. The tie rods should intersect with the Instantaneous center. Having inner ball joints of upper and lower control arms on the same vertical plane greatly reduces bump steer because the arms will follow the same path in a bump.

## *What is Steering?*

For an offroad vehicle such as the Baja, the goal of the steering is to give the driver enough feedback so that they have an adequate sense of where the vehicle is. Steering should also not require so much effort from the driver. Requirements for the steering are it should allow for great maneuverability, not take too much physical effort to operate, and should have minimal bump steer. The driver applies rotational force on the steering wheel, which spins the steering column, which then rotates the pinion. This pinion rides on a rack that will turn the tie rods which are attached to the knuckles. The knuckles are attached to the wheels, which turn the car.



*Figure 30: Steering Functional Diagram*

### **Rack and Pinion:**

Rotational input from the driver on the steering wheel is used to turn the wheels via a rack and pinion system in the case of the baja. The rotational movement from the driver spins the steering rack which has a pinion gear attached to the end of it. This pinion rides on top of the rack which has teeth on it which the pinion rides on. The rack is connected to tie rods which are then attached to the knuckles. Rack and pinion steering has a high mechanical efficiency, has a simple

construction, does not take up a lot of space, and is readily available. The components of the steering system must be designed so that they can withstand the forces acting on them in the baja competition. They should also be placed in a manner that allows for the desired vehicle dynamics to be achieved.

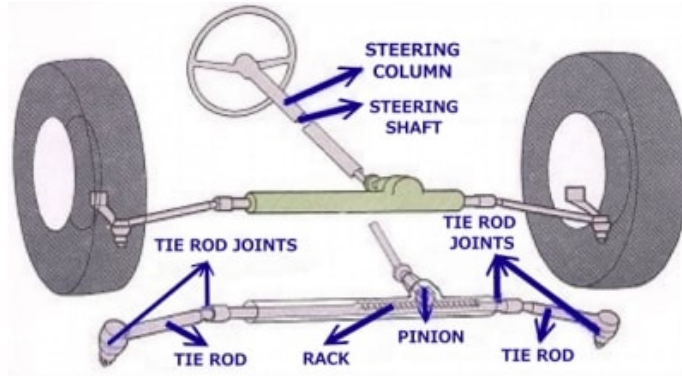


*Figure 31: Rack and Pinion*

### *Ackerman Steering*

When a car goes around a corner each wheel follows a path of different radii. If a car is turning left the right tires have to move faster than the left ones because they must cover a greater distance in the same amount of time and vice versa for a right turn. In all turns (left or right) the front tires move faster than the rear tires. This will lead to the wheels slipping and cause unnecessary and uneven tire wear. To combat this, Ackerman steering can be used. The front tire that's on the inside of the corner will rotate more than the outside tire. The angle between the wheels and the line from the center of the turning circle must be 90 degrees. This is done to compensate for the different distances each tires cover in a corner. This will prevent the tires from slipping. An ideal or 100% Ackerman set up would mean the inner and outer wheels form concentric circles when turning. When the ackerman percentage is less than 100% the inside tire is trying to push or slip out of the turn. It is not turning enough and will cause understeer. 100% ackerman means that the wheels form perfect concentric circles in the turn and there is no dragging or slipping at the front. When the ackerman percentage is greater than 100% the inside tires are turning more than they would need to and cause oversteer.

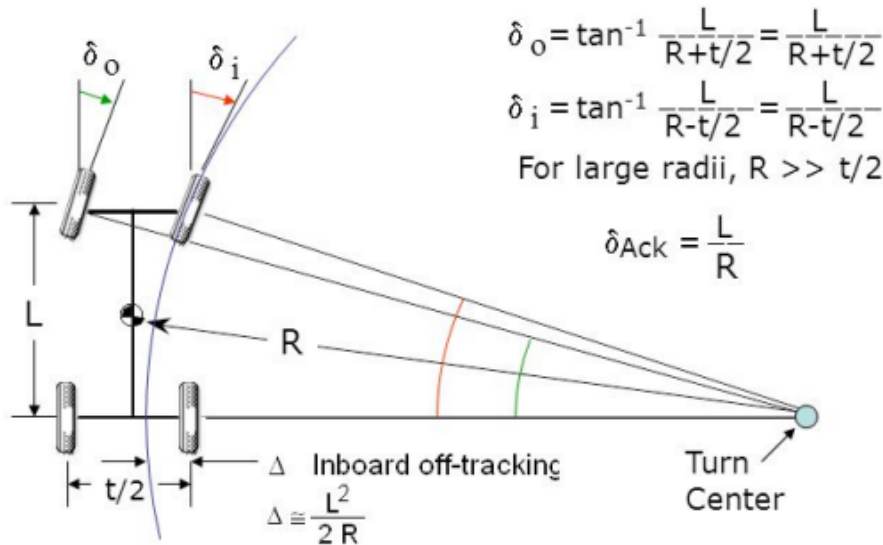


Figure 32: Ackerman Steering

## Suspension Customer Requirements

Overall, the main constraints for the suspension were that the widest point in the vehicle may not exceed 64 inches. In general, the wheels extend outside the chassis, so the distance between the wheel's outer walls should be less than 64 inches. There are no other restrictions for the suspension, but suspension theory is so vast and well collected that there are many guidelines for us to follow along with regardless of which suspension geometry we wish to use.

## *Components*

### *Knuckles:*

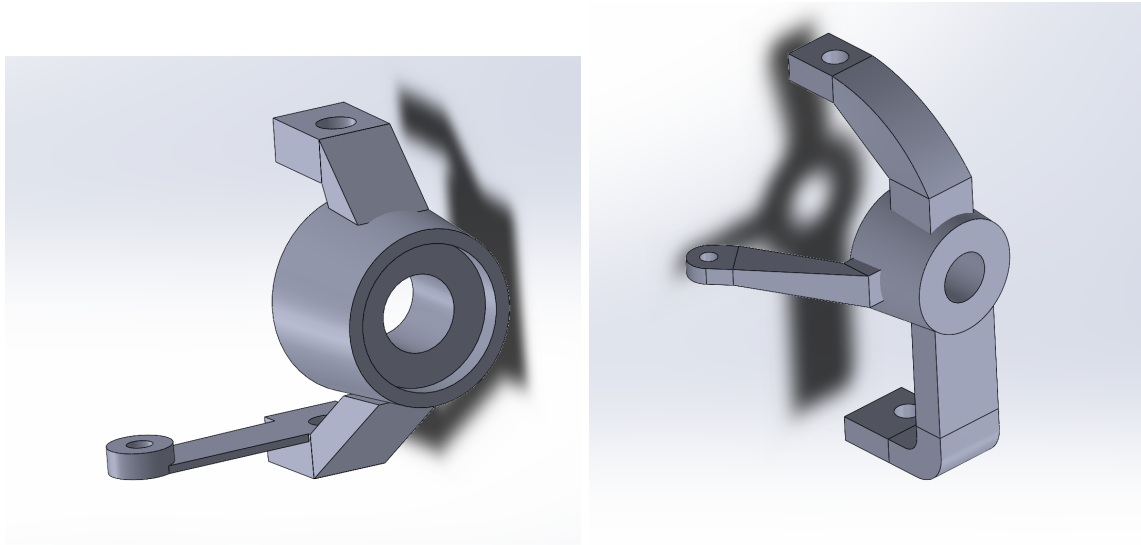


*Figure 33: Old (Left) and New (Right) Front Knuckle*



*Figure 34: Rear Knuckle (left), hub and rotor (right)*

Due to the COVID-19 pandemic, the previous year Baja team was unable to compete in the dynamic competition, so we decided to reuse their knuckles as a starting point for suspension geometry. Doing this would save cost considering our tight budget. The previous team ensured that these knuckles would be able to fit into

### *Shocks and Springs:*



*Figure 35: Rear Shocks*

Choosing the shocks for our rear suspension did not take too much thought because the previous year's team bought new King Off-Road Racing coil-over shocks to replace the old and fatigued Fox Podium X shocks from a 2008 Polaris Outlaw 525S ATV. Our goal was to choose shocks that could save cost and weight, and given that we had two brand new rear coil-overs from King, we thought it was best to work with what we had during this pandemic.

The decision we were now faced with was choosing the rear springs. The first step was deciding our suspension frequency, which is at a frequency of 1 Hz. The extended length of the rear shocks are 27.05 inches with a collapsed length of 17.05 inches, with a calculated adjustable spring rate of 135 Lbs/in and a recommended spring length of 10 inches from the manufacturer. The suspension is much softer than the previous year's springs by about, but implementing brand new shocks that were already previously bought allows us to allocate our budget towards other vehicle components.

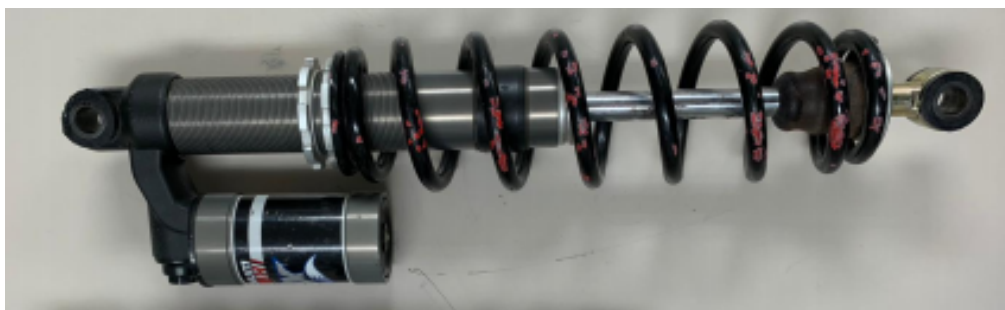


*Figure 36: Front Shock and Spring*

There was no real decision to be made when choosing the front shock and spring as the ones from the previous year would be used. These shocks are the Fox Podium X from a Polaris Outlaw 525S ATV. It has a spring rate of 149.1 lbs/in, is 10.5 in long, and weighs 4 lbs. We plan

on buying new springs, but for now we will work with the ones we have. This setup comes with a FOX Dual-Speed Compression (DSC) valve. It has 22 clicks of high speed adjustment and 24 clicks of low speed adjustment. This valve allows for the shock to be tuned for different terrain or personal preference by the driver. The factory setting is 12/12 which is an all-around setting that is adequate for low and high speeds.

### *Wheels:*



*Figure 37: SUNF A033 22" x 7" with a 12" rim size (left)  
Maxxis AT 22" x 7" with 12" rims (right)*

For the tires, unsprung weight was the biggest factor in choosing the wheels, including compatibility with the tires and knuckles. The front tires will be reused since its performance and compatibility with the front knuckles. The rear tires have been changed to the SUNF A033 22" x 7" with a 12" rim size. The rear tires are even more thin than last year's rear tires, in hopes to achieve more understeer by providing slightly less traction in the rear and better turn in with the rear limited slip differential. The front tires were reused, using the Maxxis AT 22" x 7" with 12" rims, due to its performance and wider tires to aid in oversteer efforts.

### *Ideal Spring Rate Calculations*

Wheel rate and motion ratio are important to understanding how the vehicle will behave over bumps, and in general determine how bumpy of a ride the user will feel in the vehicle. Wheel rate, or suspension frequency is the end goal of choosing a spring rate, and in general most street cars have suspension frequencies of ~1 Hz while race cars have frequencies of 3 Hz. For an off road vehicle, it is likely that in order to smooth out all the bumps, we would need a wheel rate that is less than 1. With a target suspension frequency of around 1 Hz, a suspension calculator to see what exact suspension frequency we might want for the front and rear in order to keep the

overall vehicle “flat” over bumps, and then used the formulas below in MATLAB to find a target spring rate for our vehicles front and rear suspension.

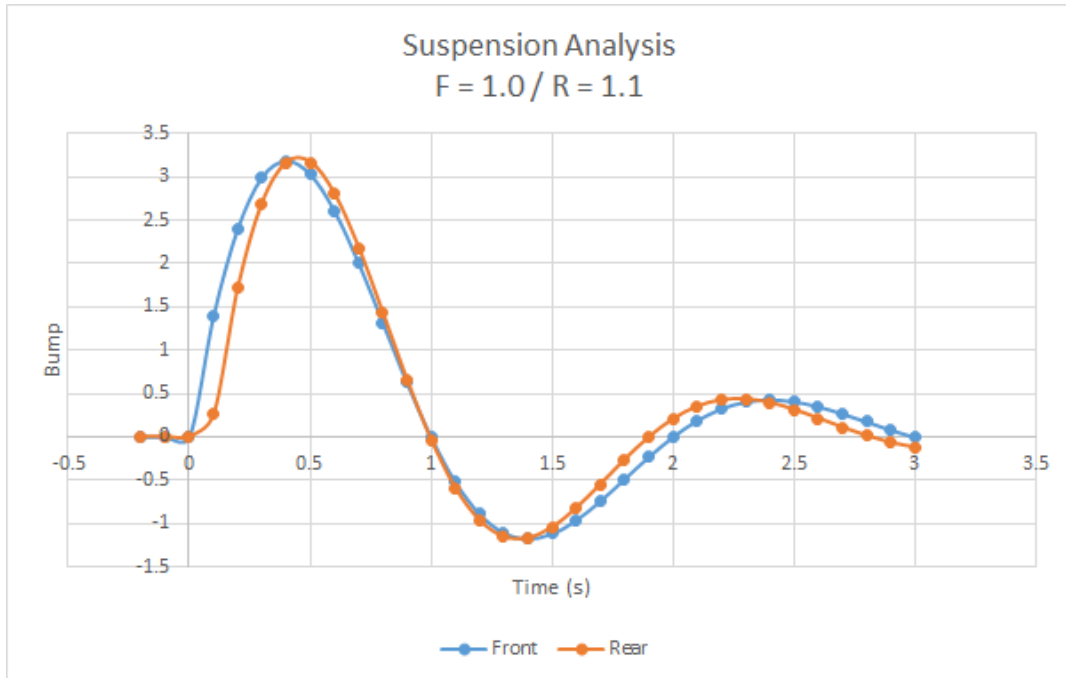


Figure 38: Suspension Frequency Analysis

$$WR = \left( \frac{SF}{187.8} \right)^2 (\text{sprung})$$

$$C = \frac{WR}{MR^2 \cdot ACF}$$

WR	Wheel Rate
SF	Suspension Frequency
MR	Motion Ratio
ACF	Angle Correction Factor
Sprung	Sprung Weight
Unsprung	Unsprung Weight

The ideal spring rates we found for the front and the rear were roughly 100 and 135 lb/in respectively.

### *Front Suspension and Steering*

The two suspension types considered for the front suspension were double wishbone and pushrod. Both these suspension types have their pros and cons. Double wishbone suspension allows for greater optimization of the geometry. Double wishbone suspension is known for allowing the wheels to maintain a constant camber angle when the chassis rolls in a corner. This setup is also commonly used in Baja SAE therefore there are a lot of resources available when conducting research. However double wishbone suspension is pretty complex and has many parts. Pushrod can be shaped to address the design needs, has a low unsprung weight due to many of the components being mounted inboard, and it has a lower profile thus leading to low drag. However, this suspension type is expensive and is not commonly used in Baja SAE so there are not many resources to use for researching the implementation of this suspension. Both of these positives and negatives of each suspension type were considered and a decision matrix was conducted. The double wishbone suspension better suited our needs and was more practical to implement, therefore it was the better choice.

	Cost	Manufacturing	Handling	Weight	Total	Weighted Total
Score Weight	1	0.6	0.8	1		
Double A - Arm	7	7	8	5	27	22.6
Push Rod	4	4	6	7	21	18.2

*Table 3: Front Suspension Decision Matrix*

Another critical decision that had to be made was whether or not to use the current knuckle or design a new one. The existing hard points on the old knuckle made it difficult to obtain optimal bump steer and ackerman characteristics. A decision matrix was made to determine whether or not the additional cost and time required to make a new knuckle was worth the anticipated benefits with respect to handling and weight. As a result of the decision matrix creating a new knuckle was the path that was chosen.

	Cost	Manufacturing	Handling	Weight	Total	Weighted Total
Score Weight	0.8	0.8	1	1		
Current Knuckle	9	9	4	4	26	22.4
New Knuckle	5	5	9	9	28	26

Table 4: Front Knuckle Decision Matrix

## Design

The front suspension was redesigned using last year's Lotus file. This file contained the hard points that, initially, could not be modified during the redesign. This ensured that key components could not be changed, or changed very little throughout the process. The chassis mounting points are points 1, 2, 5, 6 in the figure below. Points 5 and 6 connect to point 7. These connections create the upper wishbone. Points 1 and 2 connect to point 3. These connections create the lower wishbone. Points 3 and 7 represent the points where the wishbones are attached to the knuckle. Point 12 is where the tie rod is attached to the steering rack and point 11 is where the tie rod is attached to the knuckle. The previous year's geometry was scrutinized for factors that could be improved. Points in Lotus were moved around in order to see how they affected the vehicle's dynamics. Throughout the course of the design process it was realized that some of these hard points would have to be moved in order to achieve the goals set for this design.

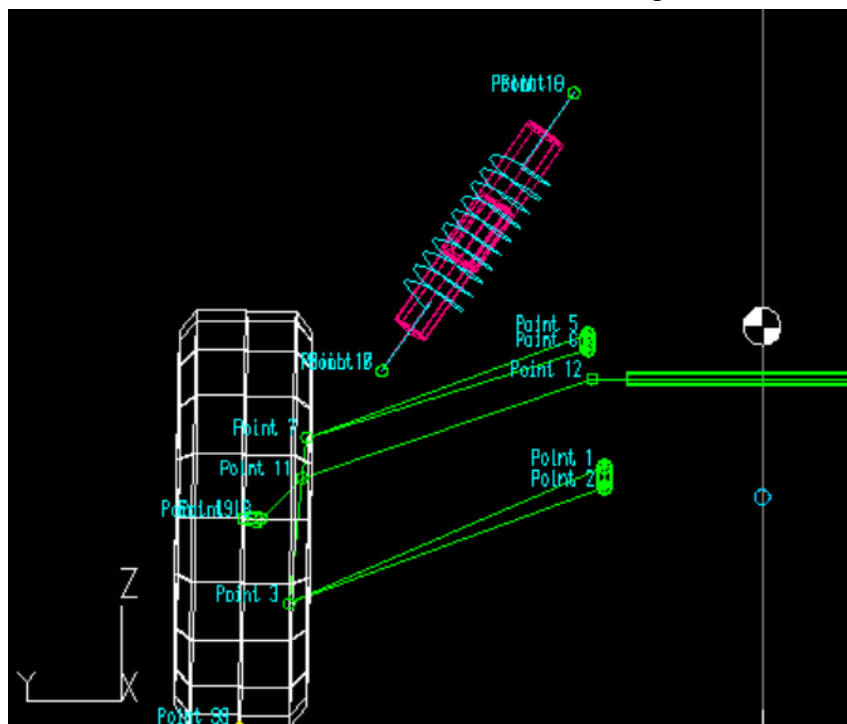


Figure 39: Front suspension points in Lotus

Research was conducted on how the configuration of the components would positively or adversely affect the desired vehicle dynamics. For the baja the desired characteristics were a vehicle that was prone to oversteering in corners, straight line stability, and a linearized, low amount of bump steer when the suspension was bumping or drooping. Oversteer characteristics were desired because this year the baja would have been all wheel drive. Having some power going to the wheels now would leave the baja being prone to understeering in corners which would decrease the speed at which the baja could take a corner. Creating a geometry that would be prone to oversteering would help in combating the negative cornering affects the all wheel drive system would have on the baja. To increase the oversteer characteristics a camber angle of -1 degrees was added to the geometry. This will ensure that the contact patch the front tires have will be larger when cornering, thus increasing front end grip in a corner, thus leading to oversteer. To give the baja more straight line stability the toe and caster angles were modified. The toe angle was changed to +0.25 degrees inward. This slight inward toe angle will allow the car to maintain straight line stability on the uneven surfaces present at the competition. Having the tires point slightly inwards will make them want to maintain a straight path. If there was a slight outward toe angle the baja's front end would be prone to getting pulled from side to side off its straight path by the uneven surfaces of the terrain. The toe angle selected is large enough to ensure straight line stability while not negatively affecting the cornering abilities of the baja. The castor angle used was 4.85 degrees. Having a slight positive castor angle will also ensure that the baja has straight line stability. This is a similar approach used when designing the front suspension forks on a downhill mountain bike. The front fork is typically angled so that there is a positive castor so that the bike can be stable at high speeds. Negative castor would make the baja unstable at high speeds. Negative castor can be found on a shopping cart, which never "wants" to point straight.



*Figure 40: Mountain Bike castor angle (left), Shopping cart castor (right)*

STATIC VALUES		
CAMBER ANGLE	(deg):	-1.00
TOE ANGLE (SAE) (+ve TOE IN)	(deg):	0.25
TOE ANGLE (PLANE OF WHEEL)	(deg):	0.25
CASTOR ANGLE	(deg):	4.85
CASTOR TRAIL (HUB TRAIL)	(mm):	1.07
CASTOR OFFSET	(mm):	22.60
KINGPIN ANGLE	(deg):	6.13
KINGPIN OFFSET (AT WHEEL)	(mm):	73.91
KINGPIN OFFSET (AT GROUND)	(mm):	48.78
MECHANICAL TRAIL	(mm):	22.52
ROLL CENTRE HEIGHT	(mm):	282.72

Figure 41: Lotus Static Values

The first way in which the goal of increasing the oversteer characteristics of the vehicle was addressed was by ensuring that throughout the design process the front track remained wider than the rear track. This increases the oversteer characteristics because the side that is wider generally has more grip. Adding more grip to the front will make it more oversteer prone. As a result the track width in the front is 10 in wider than in the rear.

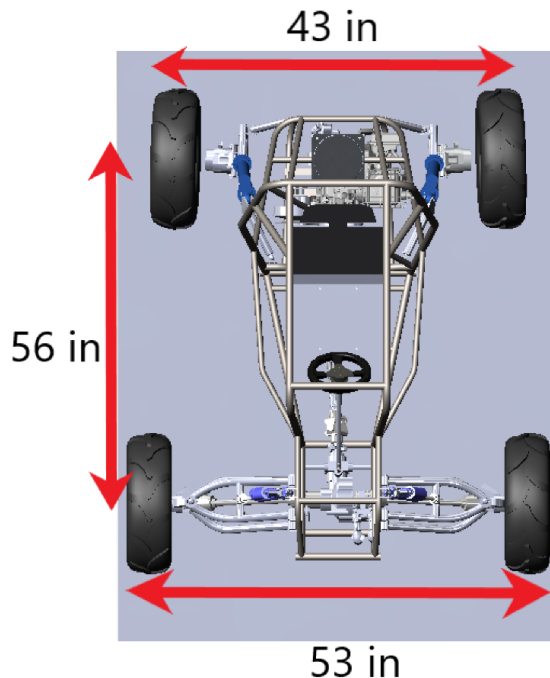


Figure 42: Track Width

The previous front suspension geometry had a high amount of bump steer. This bump steer was also not linearized. Bump steer is when the toe angle changes when the suspension bumps or droops. This makes it harder for the driver to control the baja when driving over bumps, which are present during the competition. Having non linear bump steer makes the effects of bump

steer feel harsher. Bump steer can be caused by the upper and lower control arms as well as the tie rod following different arcs when bumping or drooping. Bump steer is corrected by finding the instantaneous center where the lines from the upper and lower control arms meet. A line is drawn from the instantaneous center to the tie rod mounting point on the knuckle. The tie rod should follow this path to the steering rack. Having the chassis mounting points for the upper and lower control arms directly above each other will linearize bump steer. When they are at an angle in relation to each other the bumpsteer will be non linear.

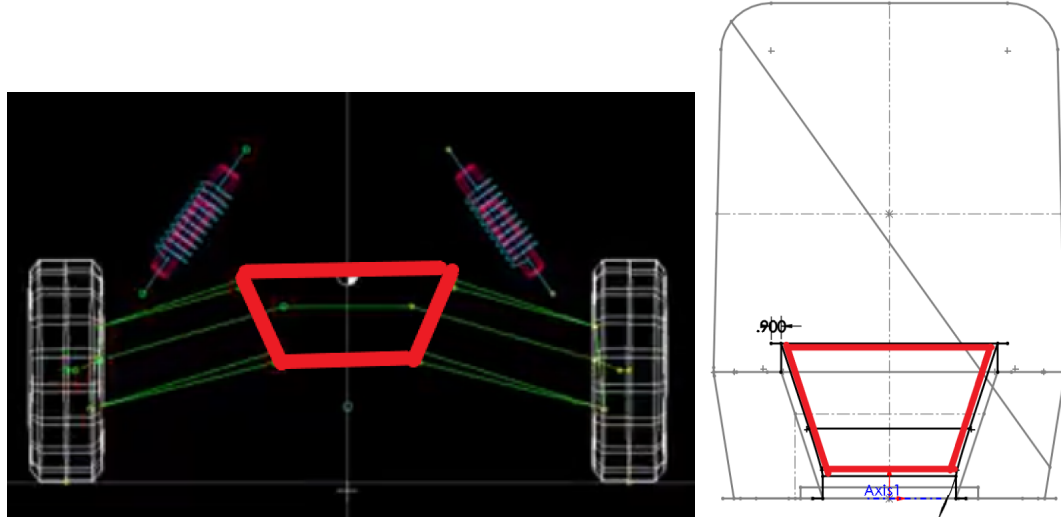


Figure 43: 2020 Front Profile Lotus (Left), 2020 Front Profile SolidWorks (Right)

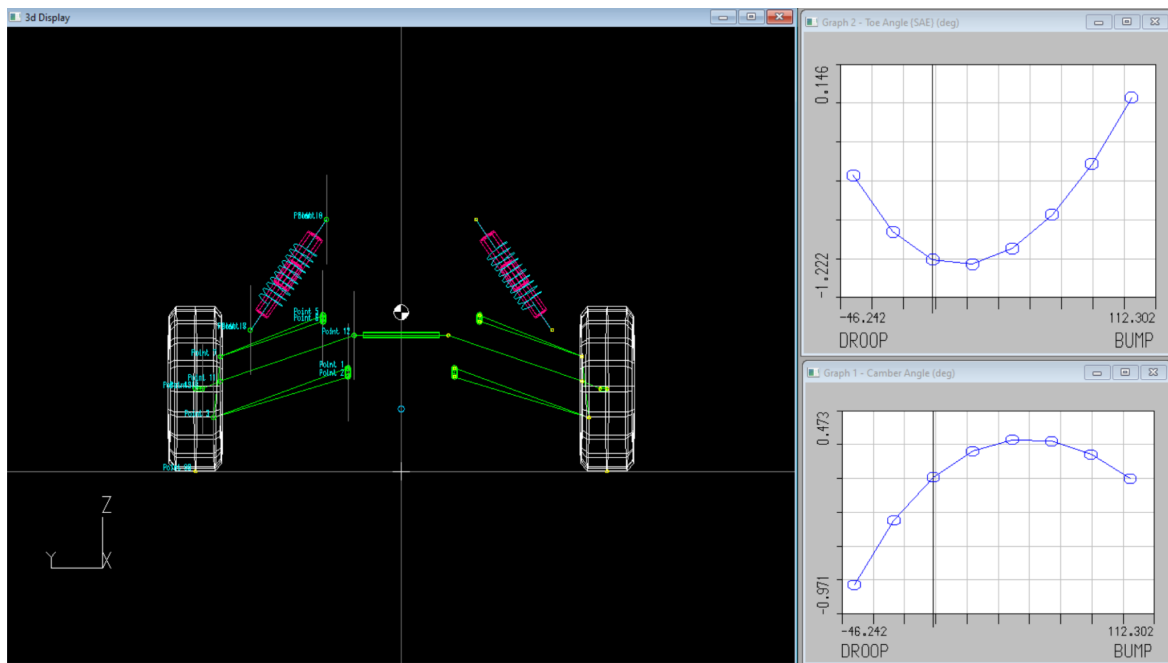


Figure 44: 2020 Geometry (left), Toe with respect to droop and bump (top right), Camber with respect to droop and bump (bottom right).

These critiques are backed up by the data from Lotus. Toe Angle and Camber Angle both change in a nonlinear fashion. Having curves like these as the profile for toe and camber angles create an unpredictable and potentially dangerous vehicle to operate. To put this in context, the bump or droop of the suspension in competition settings would occur on a jump. So when the baja lands, having a high and non linear toe angle profile could make the baja veer off to one side upon landing. This is not ideal because it could put the driver and spectators at risk. Minimizing and linearizing the angle changes makes the vehicle safer. To summarize, a linear profile is a safe profile.

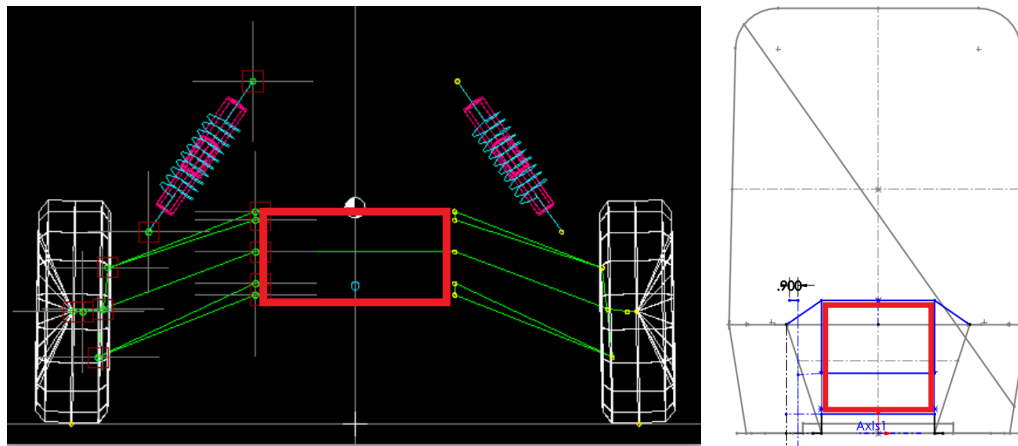


Figure 45: 2021 Front Profile Lotus (Left), 2021 Front Profile SolidWorks (Right)

Modifying the front of the chassis so that the control arm mounting points would lie on the same vertical plane resulted in linearized bump steer characteristics. However the Ackerman rating was terrible. The hard points that the 2020 knuckle had made it hard to find a “sweet spot” where the desired ackerman rating and bump steer rating was satisfied. Changing the soft points to get a good ackerman rating would sacrifice the bump steer rating and vice versa. New Knuckle points were then created in order to satisfy these conditions.

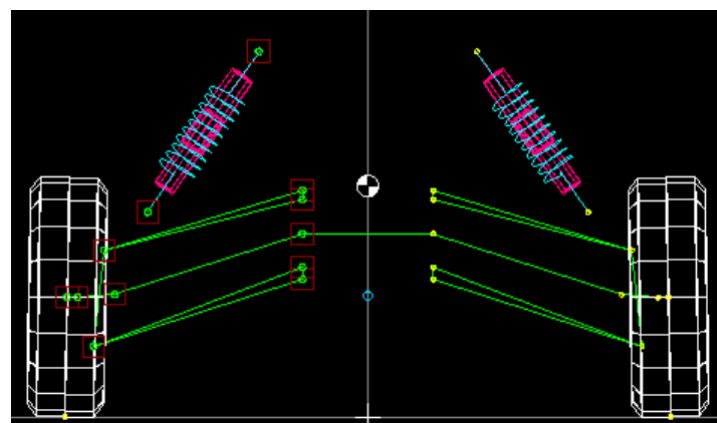


Figure 46: 2021 Lotus File

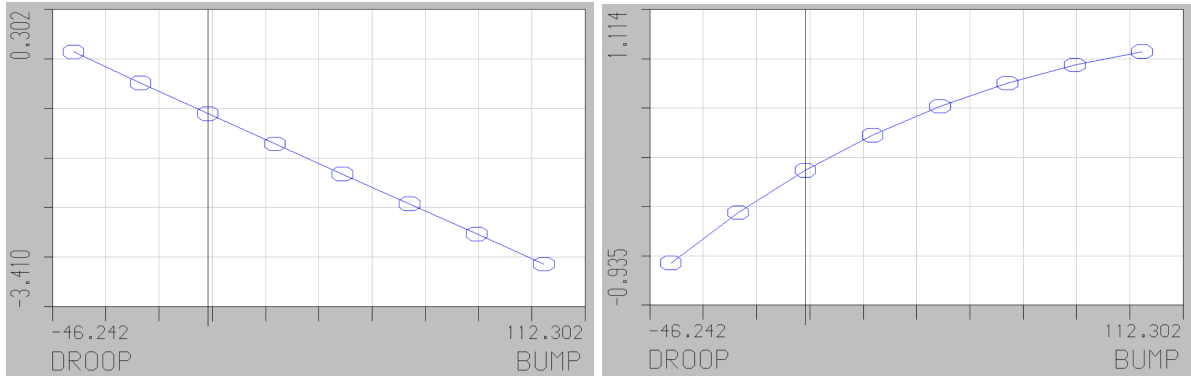


Figure 47: Toe Angle w.r.t Bump & Droop (Left), Camber Angle w.r.t Bump & Droop (Right)

RACK TRAVEL (mm)	TOE ANGLE RHS (deg)	TOE ANGLE LHS (deg)	CAMBER ANGLE RHS (deg)	CAMBER ANGLE LHS (deg)	ACKERMANN (%)	TURNING CIRCLE RADIUS (mm)
-63.50	-59.73	41.80	20.58	-3.53	52.46	1246.40
-58.62	-58.01	38.54	15.61	-3.38	62.96	1376.60
-53.73	-57.03	35.33	13.79	-3.23	77.51	1507.97
-48.85	-56.23	32.15	11.46	-3.07	95.45	1654.63
<b>-43.96</b>	<b>-48.48</b>	<b>28.99</b>	<b>6.98</b>	<b>-2.91</b>	<b>95.24</b>	<b>1969.58</b>
-39.08	-36.76	25.85	3.82	-2.74	74.70	2491.65
-34.19	-29.83	22.71	2.50	-2.56	66.49	3026.91
-29.31	-24.27	19.57	1.63	-2.37	61.48	3684.49
-24.42	-19.43	16.41	0.98	-2.18	58.08	4562.12
-19.54	-15.06	13.23	0.46	-1.97	55.69	5837.44
-14.65	-11.00	10.01	0.02	-1.76	54.04	7916.90
-9.77	-7.17	6.74	-0.36	-1.52	52.94	12014.29
-4.88	-3.52	3.41	-0.70	-1.27	52.32	24192.21
0.00	0.00	0.00	-1.00	-1.00	52.11	0.00
4.88	3.41	-3.52	-1.27	-0.70	52.32	24192.21
9.77	6.74	-7.17	-1.52	-0.36	52.94	12014.29
14.65	10.01	-11.00	-1.76	0.02	54.04	7916.90
19.54	13.23	-15.06	-1.97	0.46	55.69	5837.44
24.42	16.41	-19.43	-2.18	0.98	58.08	4562.12
29.31	19.57	-24.27	-2.37	1.63	61.48	3684.49
34.19	22.71	-29.83	-2.56	2.50	66.49	3026.91
39.08	25.85	-36.76	-2.74	3.82	74.70	2491.65
<b>43.96</b>	<b>28.99</b>	<b>-48.48</b>	<b>-2.91</b>	<b>6.98</b>	<b>95.24</b>	<b>1969.58</b>
48.85	32.15	-56.23	-3.07	11.46	95.45	1654.63
53.73	35.33	-57.03	-3.23	13.79	77.51	1507.97
58.62	38.54	-58.01	-3.38	15.61	62.96	1376.60
63.50	41.80	-59.73	-3.53	20.58	52.46	1246.43

Figure 48: Ackerman Rating (Percentage at full lock highlighted in red)

The combination of chassis mounting points that were on the same vertical place and new knuckle points allowed for the desired camber, toe, and ackerman ratings to be obtained. The camber angle in bump and droop is minimized and linearized. It ranges from  $-3.410^\circ$  in bump and  $0.302^\circ$  in droop. The toe angle change is close to linear and ranges from  $1.114^\circ$  in bump and  $-0.935^\circ$  in droop. The Ackerman rating at full lock, when the steering rack is at maximum travel, is 95.42% at 43.96mm. This is close to a perfect Ackerman rating when the wheels are fully turned. Looking at Figure\_ shows that the ackerman rating progressively increases as the wheels go from pointing straight to fully turned.

Once the Lotus file was finalized the new knuckle, new A-arms, and suspension mounting points had to be made in SolidWorks. The SolidWorks files were created using the points from Lotus.

Point	x (mm)	y (mm)	z (mm)	
1	3992.877	152.4	348.955	Lower-Arm
2	4194.1	152.4	320.675	Lower-Arm
3	4083.87	638.378	165	knuckle/low-A
4				
5	4040.019	152.4	528.13	
6	4190.935	152.4	506.92	Upper-Arm
7	4102.83	614.378	388.525	Knuckle/Up-A
8	4115.478	512.778	478.044	Bottom Shock
9	4115.478	254	852.551	Top Shock
10				
11	4180.12	590	285.432	k
12	4218.484	152.4	427.938	
13				
14				
15				
16				
17				
18	4092.5	675.977	278.981	Knuckle
19	4092.5	700	279.4	Knuckle

Figure 49: Lotus Points of Interest

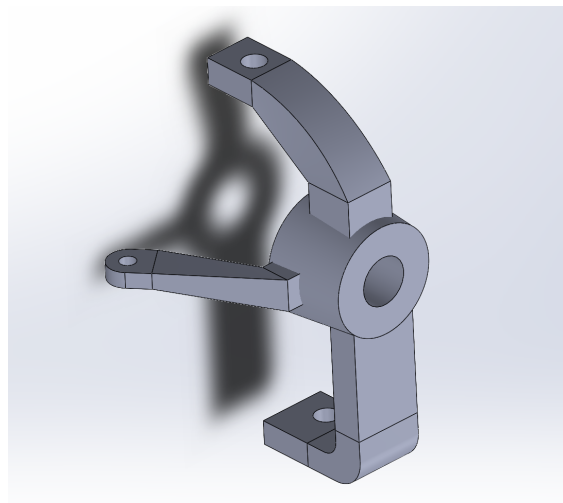
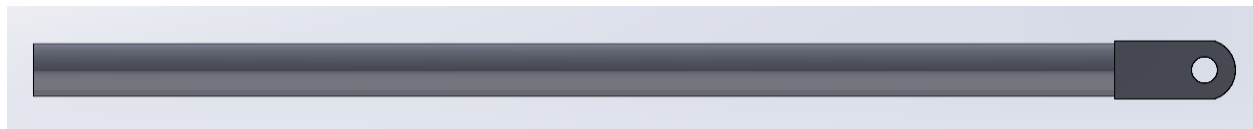


Figure 50: 2021 Knuckle



*Figure 51: Lower A - Arm (Left), Upper A - Arm (Right)*



*Figure 52: Tie Rod*

This year's vehicle will be four wheel drive. As a result there is an axle shaft running above the lower A-Arm and below the upper A-Arm. This eliminates the option of having the shocks mounted onto the lower A-Arm. Now that the shock needs to be mounted to the upper A-Arm the chassis mounting point for the top of the shock is also raised. A new section of tubing was added to the front of the chassis for the shock to mount to.

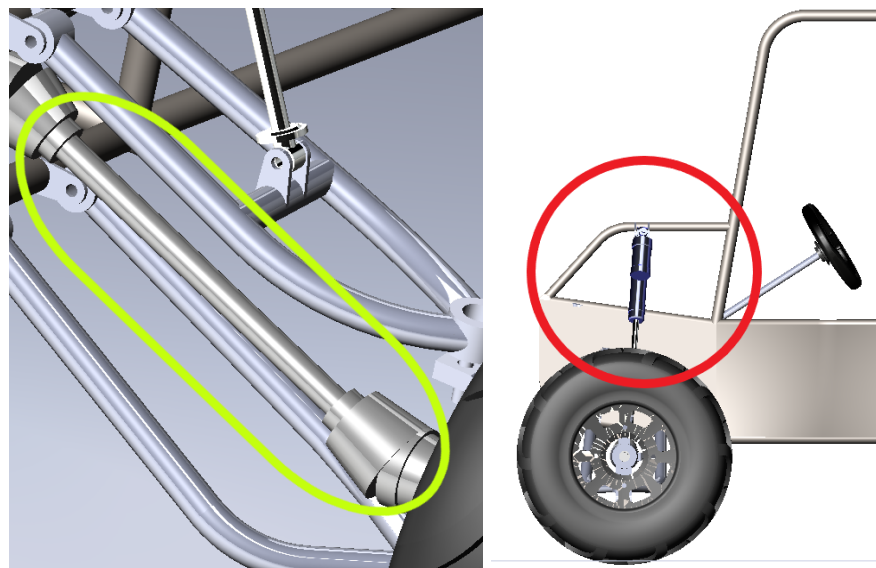


*Figure 53: Axle shaft circled in green (left), New shock mounting circled in red (right)*

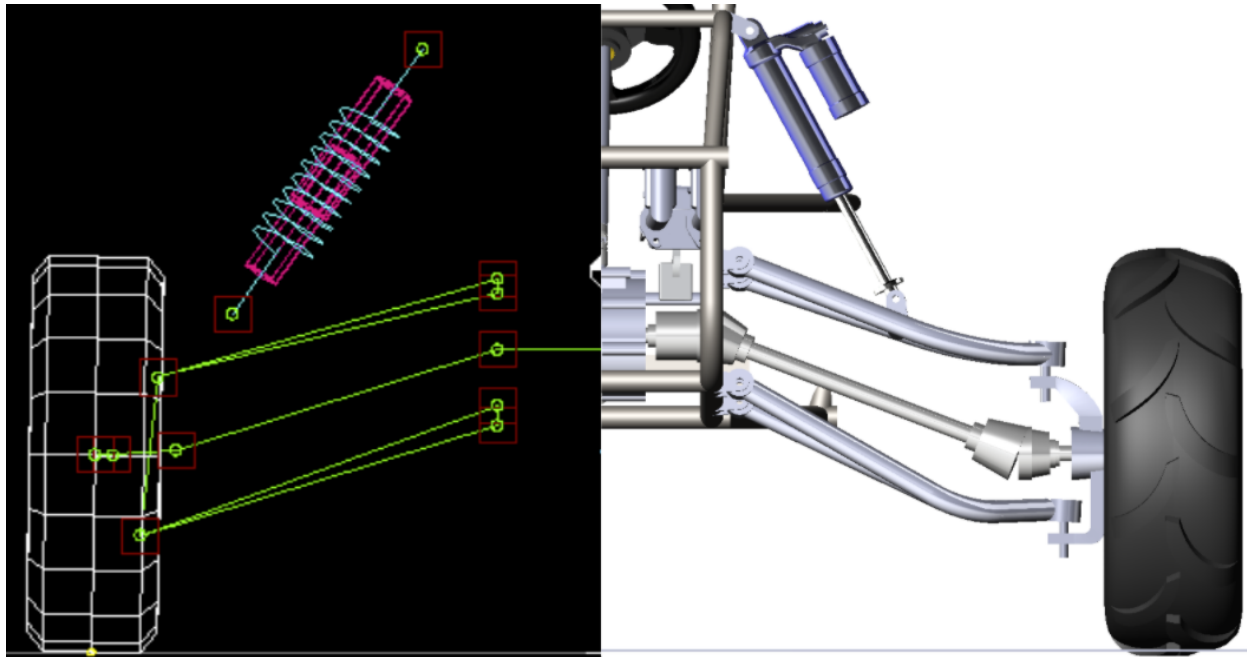


Figure 54:Front Suspension Assembly Lotus(left), SolidWorks(Right)

All the new suspension and steering components then had FEA conducted on them.

**Drop Test:**

$$\begin{aligned} \frac{1}{2}mgh_1 + \frac{1}{2}mgv_1^2 &= mgh_2 + \frac{1}{2}mgv_2^2 \\ \frac{1}{2}mgh_1 &= \frac{1}{2}mgv_2^2 \rightarrow v_2 = \sqrt{2gh} \\ F_{avg} &= \frac{m\Delta v}{\Delta t} = \frac{(270kg)(7.62\text{ m/s})}{0.5s} = 4.115\text{ kN} \end{aligned}$$

This force would be used as a worst case scenario, and a model of both a-arms were created to import into ANSYS for analysis. A simple “knuckle” was made to connect the upper and lower a-arms as they are positioned in the assembly. On top of our hand calculations, an impact force calculator was used in order to see if there were any instantaneous forces that would be found after a drop of 10 feet onto 1 suspension component. The impact calculator gave us an instantaneous force of 8.220 kN, and we upped this number to **10 kN** to give some sort of safety factor on top of this for all our simulations (e.g. the chassis, knuckle, and rear suspension).

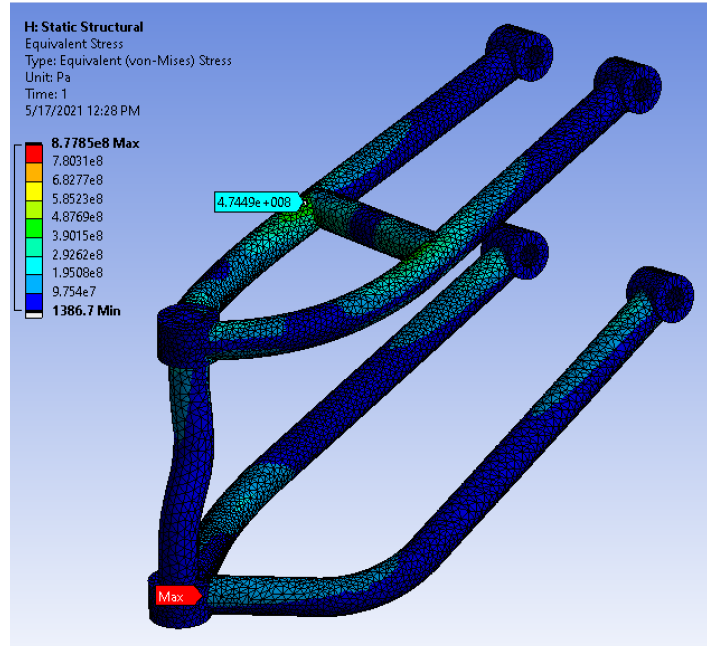


Figure 55: Drop Test FEM on Upper A - Arm done by last year's team

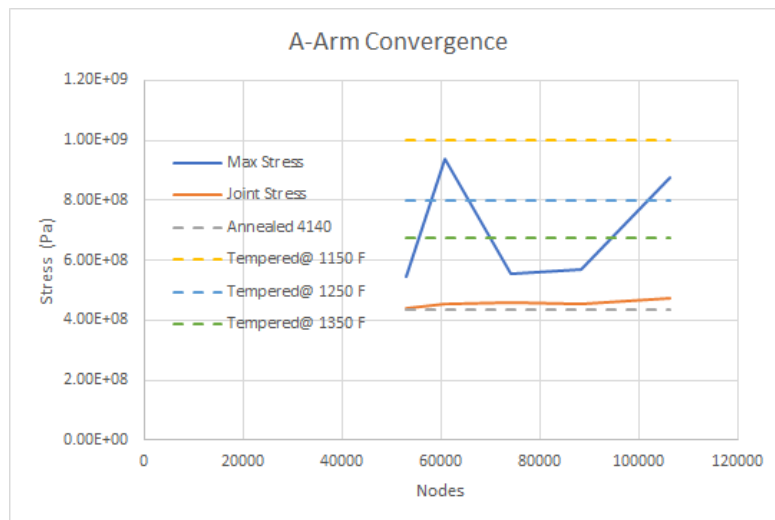


Figure 56: Convergence Study done by last year's team

In this simulation the maximum stress was 878 MPa which was located at the boundary conditions. Because the maximum stress diverged, we decided to ignore it because it was at the boundary condition due to St. Venant's Principle, where if the stress decays quickly from a singularity, it can be ignored as long as the overall stress distribution looks accurate. The A-arm was probed at the second highest stress location which was near the piping where the shock mounts to. This stress location converged to 475 MPa, which is a bit higher than the yield

strength of annealed 4140. However, 4140 steel can be tempered in order to increase the yield strength at the cost of lower ductility.

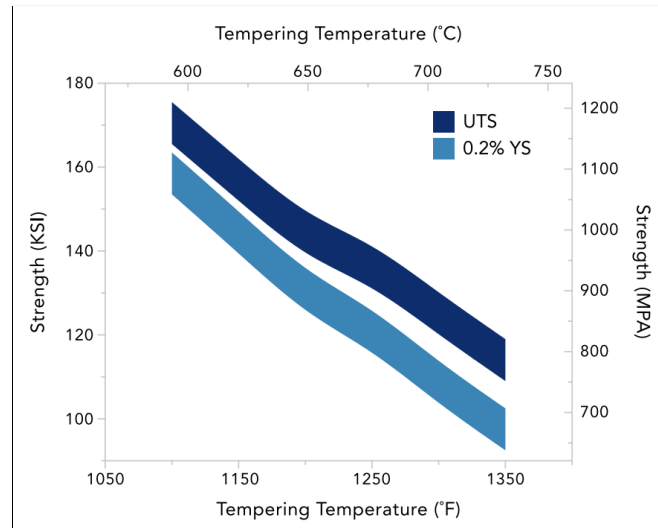


Figure 57: 4140 Steel Tempering Temp vs. Yield Strength

The new knuckle needed to be stress tested to ensure it would handle the stresses of an impact equaling 10 kN of force. With a yield stress of 276 MPa, 6160 Aluminum Alloy was chosen as the material because of its machinability and cost. A max stress of 96 MPa was found near the fillets of the knuckle giving our knuckle an effective safety factor of 2.875

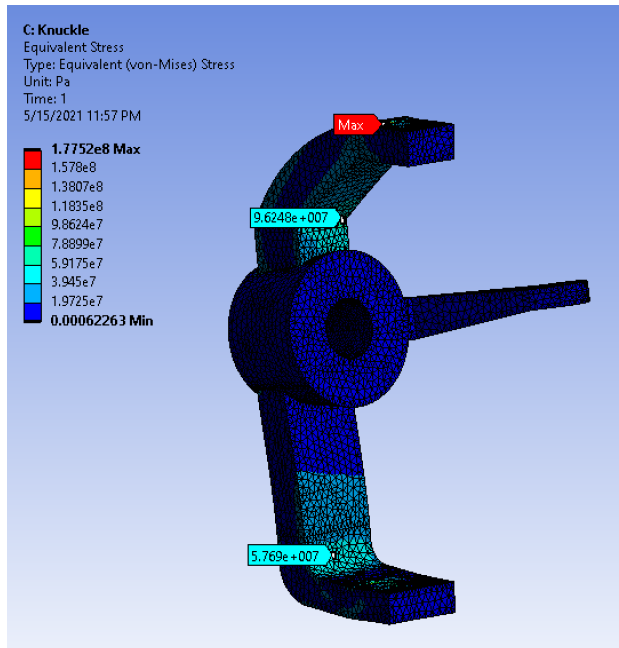


Figure 58: Knuckle FEA Results

The divergence seen can be ignored because it is on a bolt constraint, which generally isn't a place where knuckles would fail. On top of this, the stress is located directly on the boundary constraint meaning that St. Venant's Principle can be used to ignore the stresses in the area.

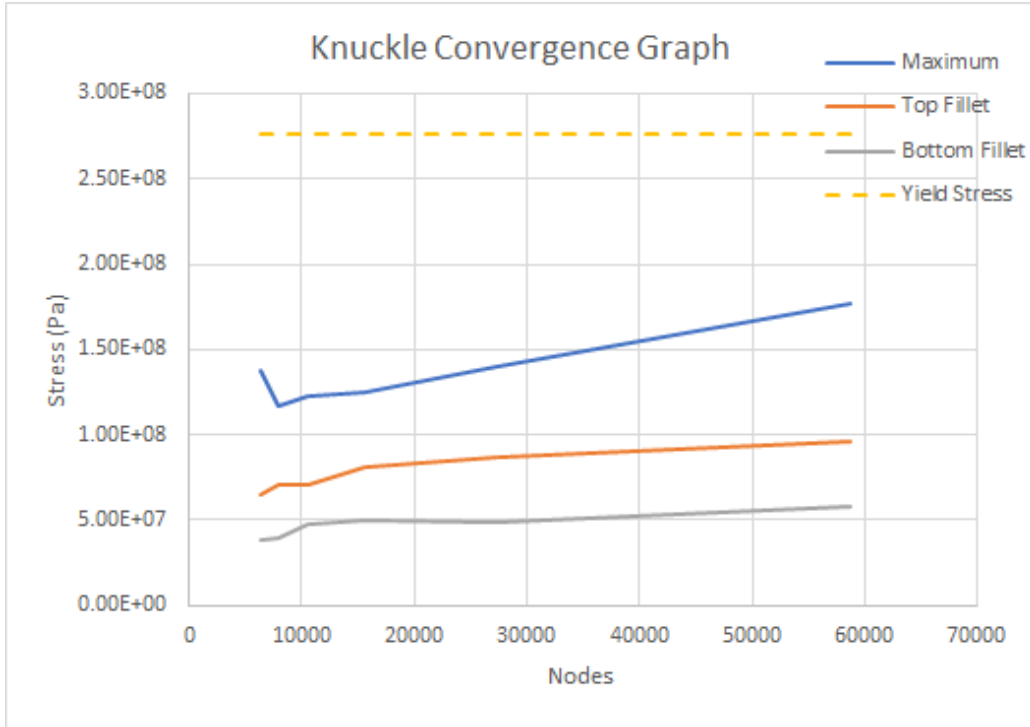


Figure 59: Knuckle Convergence Plot

The tie rod mounting point on the knuckle was moved to be higher up and closer to the chassis. This allowed for the tie rod to be shortened. The tie rod length was shortened to 430 mm. Now the length of the tie rod was determined the appropriate diameter had to be obtained. A free body diagram of the wheel going over a rock with the tie rod present is drawn. The force acting on the tie rod and moment of inertia were calculated. Using these values, the required tie rod diameter was obtained. The required diameter is 0.39 in (9.6 mm), but 0.75 in (19.05 mm) will be used.

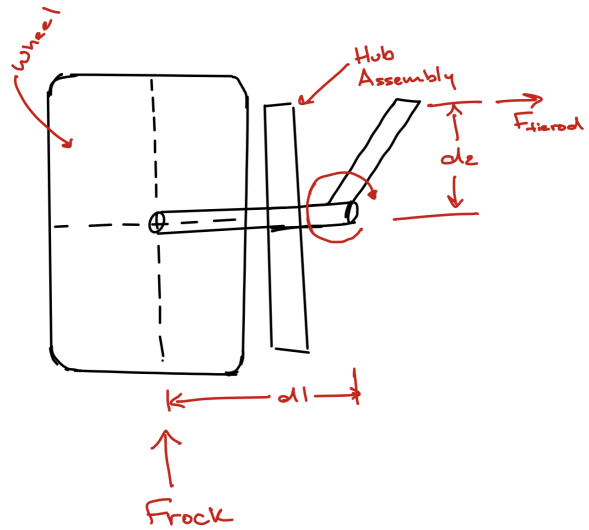


Figure 60: Tie rod Free body Diagram

$$F_{rock} = M_{baja} * a = (291\text{kg}) \left( \frac{15.65 \frac{m}{s}}{0.5s} \right) = 9108.3 \text{ N}$$

$$M_{kingpin} = F_{rock} * d_1 = 9108.3 \text{ N} * 0.114 \text{ m} = 1038.35 \text{ N}$$

$$F_{tierod} = \frac{M_{kingpin}}{d_2} = \frac{1038.35 \text{ N}}{0.142506 \text{ m}} = 7286.33 \text{ N} = 1638.032 \text{ lbf}$$

$$F_{tierod} = \frac{\pi^2 E L}{(kL)^2} \rightarrow I = \frac{(1638.032 \text{ lbf})(16.929 \text{ in})^2}{\pi^2 (27.56 * 10^6 \text{ Pa})} = 0.001094 \text{ in}^4$$

$$D = \sqrt[4]{\frac{64I}{\pi}} = \sqrt[4]{\frac{64(0.001094 \text{ in}^4)}{\pi}} = 0.39 \text{ in}$$

Figure 61: Tie rod calculations

The tie rod was then modeled in solidworks and FEA was conducted. Tie rods will be made of 4140 Steel and undergo compressive and tensile forces when in use, therefore these types of simulations were conducted. The calculated force on the tie rod was 1638 lbf or 7286 N. A compressive force then a tensile force of 7500 N, to leave room for a factor of safety, was applied in the axial direction.

Element Size (mm)	No. Nodes	No. Elements	No. DOF	Simulation Time (s)	Maximum Stress (MPa)	Maximum Displacement (mm)
12	3502	1775	10443	0	3.827*10^1	6.108*10^-2
10	3877	1949	11550	0	3.634*10^1	6.118*10^-2
8	4645	2301	13842	0	3.751*10^1	6.134*10^-2
6	7292	3611	21723	0	3.687*10^1	6.115*10^-2
5	14246	8187	42531	1	3.689*10^1	6.113*10^-2
4	21940	12743	65529	1	3.836*10^1	6.113*10^-2
3	52918	32869	158355	2	4.02*10^1	6.115*10^-2
2	125551	79832	37586	10	4.412*10^1	6.118*10^-2

Table 5: Compression Test on tie rod data

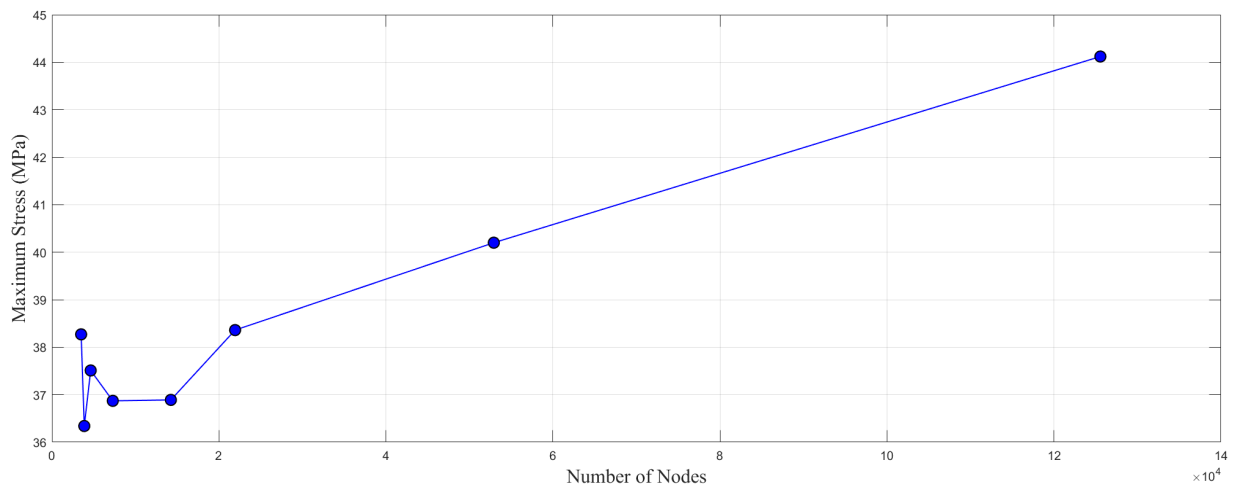


Figure 62: Convergence graph for stress in compression

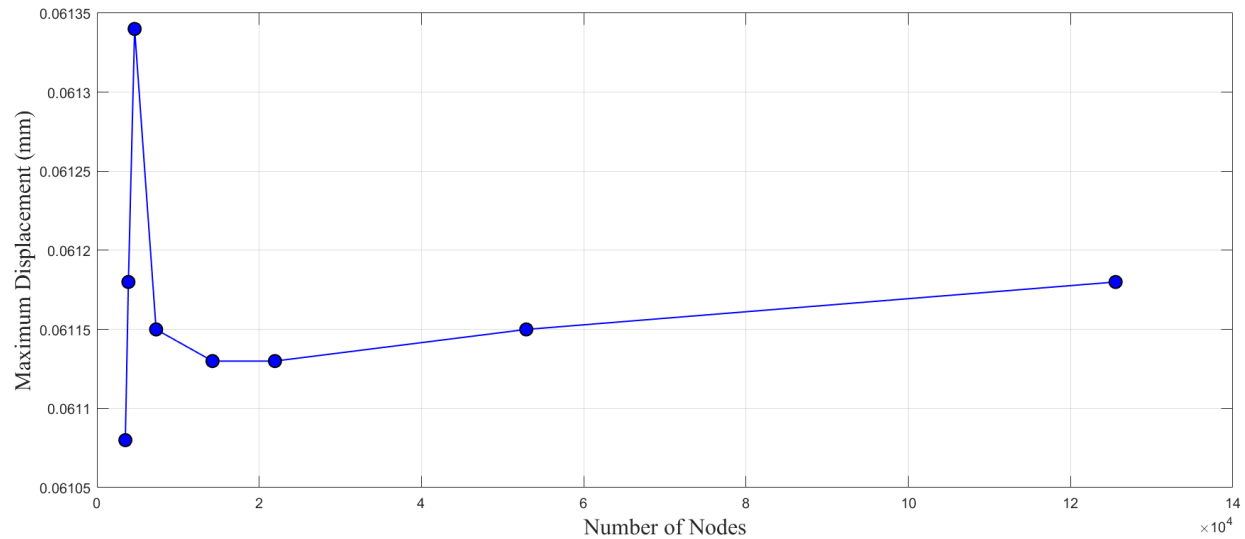


Figure 63: Convergence graph for displacement in compression

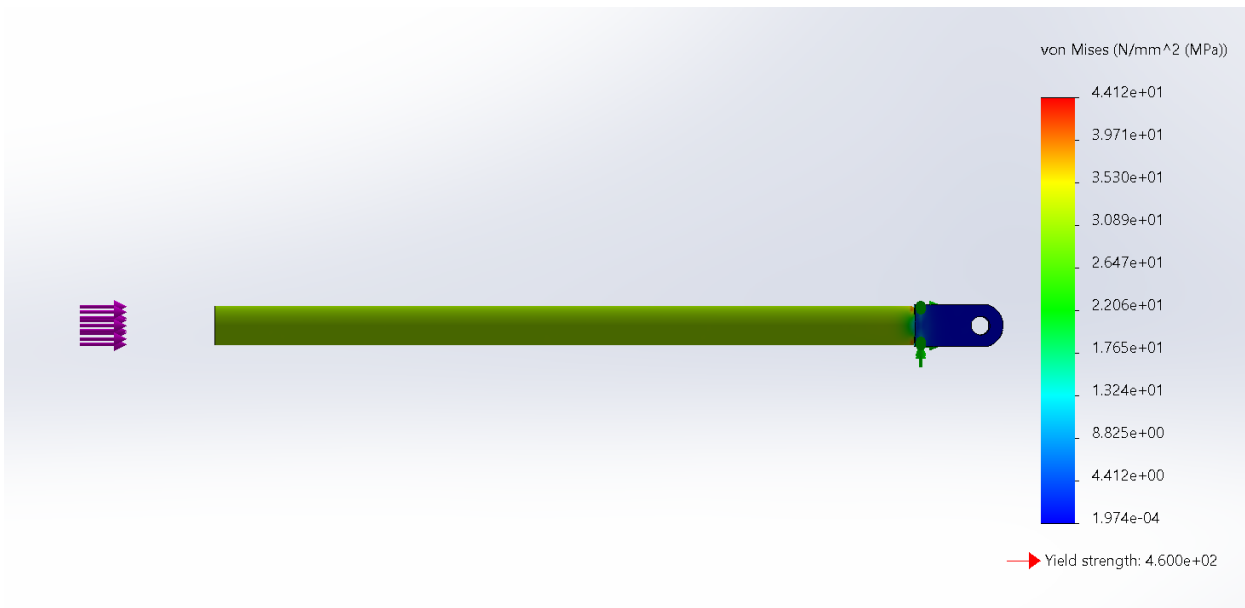


Figure 64: Stress of tie rod in compression



Figure 65: Displacement of tie rod in compression

Element Size (mm)	No. Nodes	No. Elements	No. DOF	Simulation Time (s)	Maximum Stress (MPa)	imum Displace (mm)
12	3502	1775	10443	0	3.827*10^1	-6.108*10^-2
10	3877	1949	11550	0	3.634*10^1	-6.118*10^-2
8	4645	2301	13842	0	3.751*10^1	-6.134*10^-2
6	7292	3611	21723	0	3.687*10^1	-6.115*10^-2
5	14246	8187	42531	1	3.689*10^1	-6.113*10^-2
4	21940	12743	65529	1	3.836*10^1	-6.113*10^-2
3	52918	32869	158355	2	4.02*10^1	-6.115*10^-2
2	125551	79832	37586	10	4.412*10^1	-6.118*10^-2

Table 6: Tension test on tie rod data

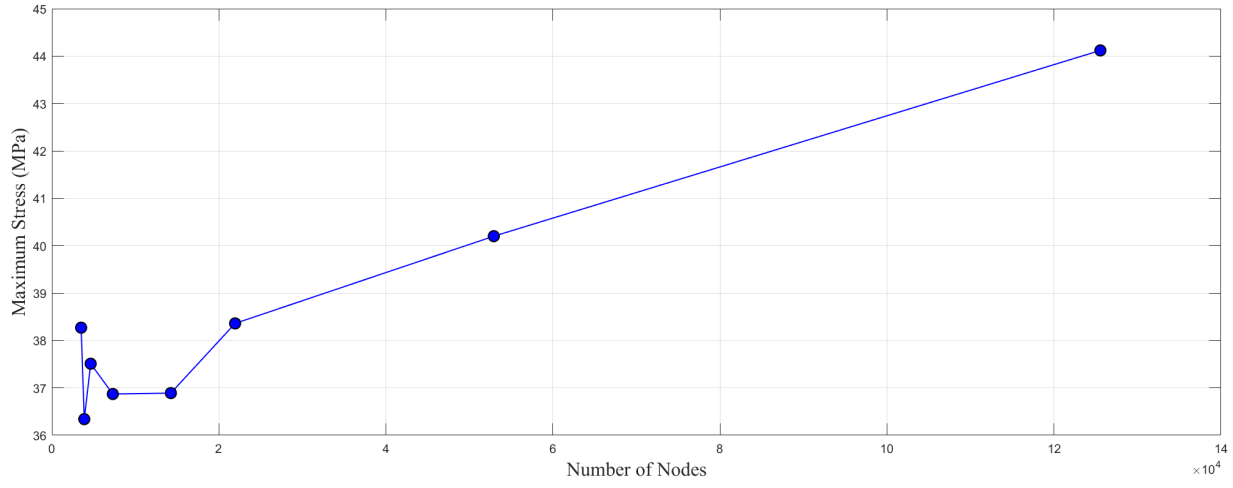


Figure 66: Convergence graph for stress in tension

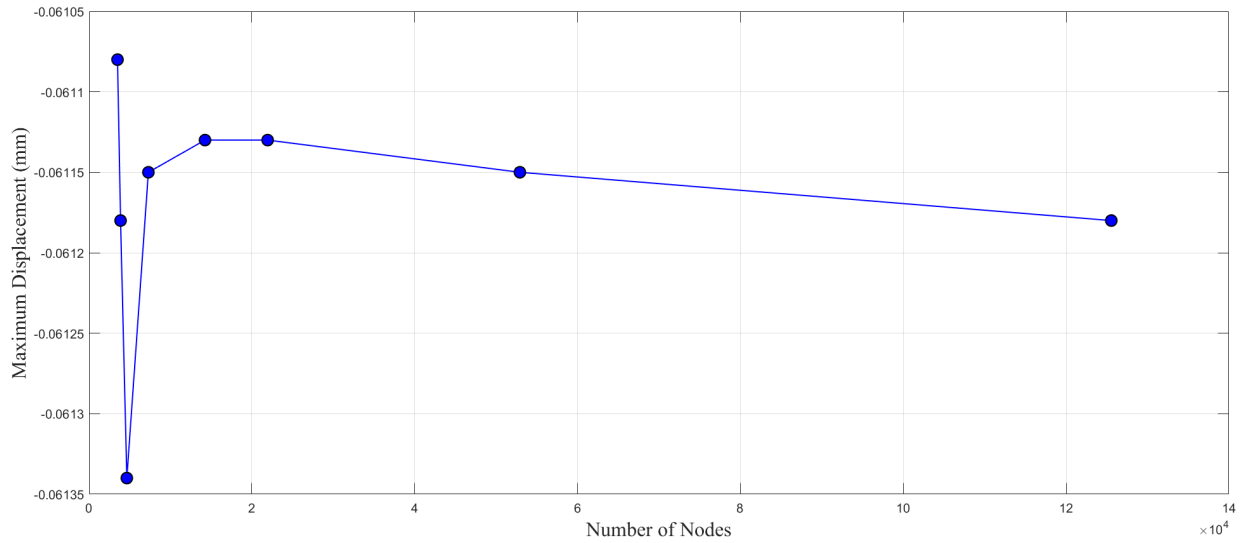


Figure 67: Convergence graph for displacement in tension

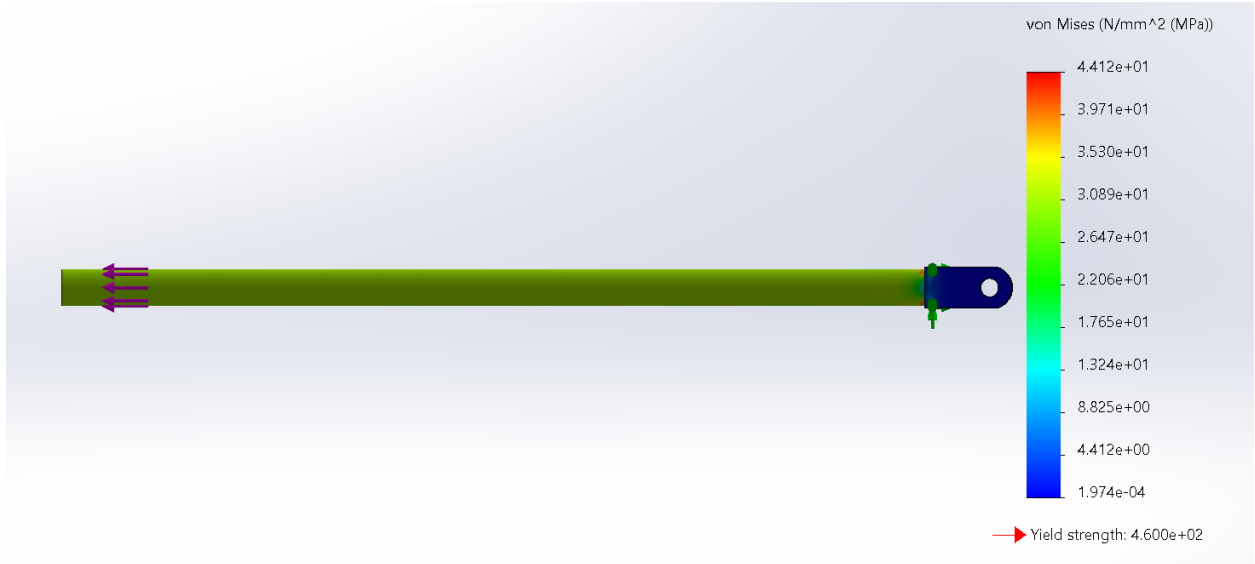


Figure 68: Stress on tie rod in tension

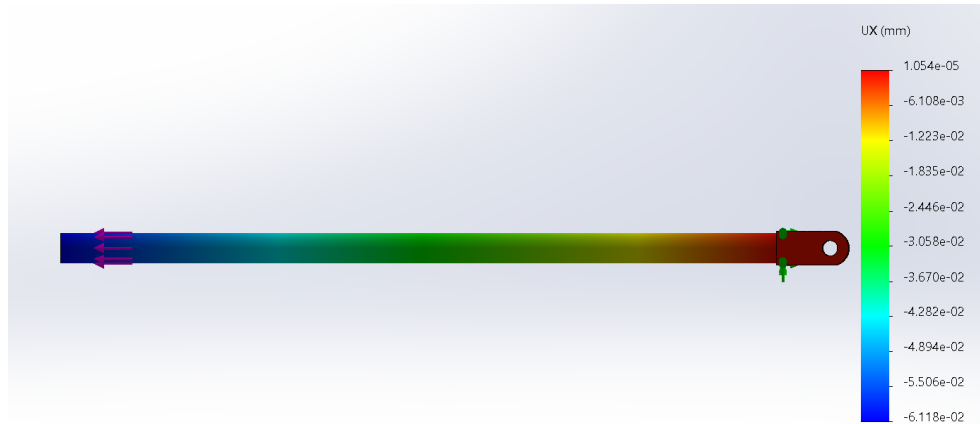


Figure 69: Displacement of tie rod in tension

The tie rod experienced the same amount of Von Mises stress when in tension or compression. It experienced 44.12 MPa. The displacement values for compression and tension were the same, except the tension values were negative. The tie rod experienced, in the x direction, 0.06118 mm of deformation under compression and -0.06118 mm of deformation under tension. These results indicate that the tie rod design will be able to handle the forces it will experience during the competition.

## Rear Suspension

For the rear suspension, there was a lot more freedom with the rear chassis, so there were many more options to pursue for the suspension geometry. The three options chosen were double

wishbones, multilink trailing arms (with camber links), and semi-trailing arms. The decision matrix for choosing which geometry to pursue is shown below.

	Score Weight (Max 1)	Multi Link Trailing Arm		Semi-Trailing Arm		Double Wishbone	
		Score Weight (Max 10)	Total Weight Score	Score Weight (Max 10)	Total Weight Score	Score Weight (Max 10)	Total Weight Score
Cost	1.0	9	9	8	8	4	4
Manufacturability	0.6	8	4.8	7	4.2	4	2.4
Handling	0.8	5	4	5	4	9	7.2
Weight	1.0	9	9	8	8	5	5
Weight Total		26.8		24.2		18.6	

Table 7: Decision Matrix for Rear Suspension

After deciding to go with a multi-link trailing arm, the next plan of action was to decide on whether to use a heim joint or a bushing for the trailing arm pivot point. Since a heim joint accounts for better load handling and provided larger rotational degrees of freedom over the bushing, the heim joint was chosen for our trailing arm pivot point. Figure 70 below shows a close up of the heim joint pivot point.

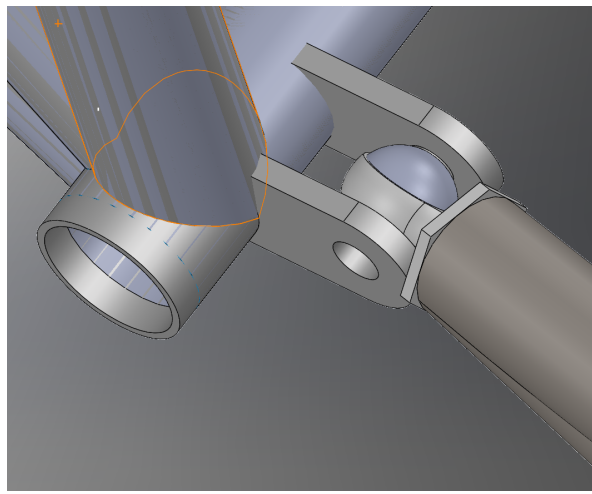


Figure 70: Heim point pivot point, rear trailing arm

Now that a multi-link trailing arm suspension and pivot point fixture is chosen, the following step was to configure the geometry on LOTUS. Luckily, the previous year's BAJA team also

chose a multi-link suspension. In this case, the previous year's suspension geometry was modified to account for our design philosophy.

The ultimate goal of the rear suspension team was to create a vehicle that had a shorter wheelbase and similar track width compared to the previous semester to have a lighter and more nimble vehicle to aid in the front suspension's cornering capabilities. On another note, the 2020 model had some issues with acceleration due to traction, therefore prioritizing traction in the rear was important.

Due to this, the rear suspension geometry was optimized in anti squat values, roll center movement, and camber changes in roll. The reasoning for optimizing anti squat is so that upon landing on the ground from a jump, the rear suspension has some sort of safety against bottoming out. Figure 71 below shows a comparison of the 2020 and 2021 rear suspension hard points

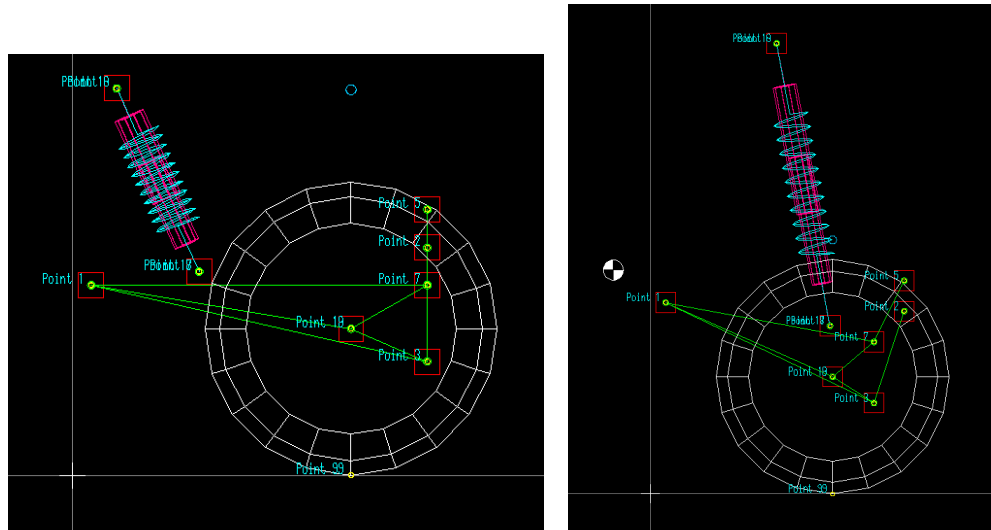


*Figure 71: LOTUS side view of 2020 rear suspension hard points (left)  
LOTUS side view of 2021 rear suspension hard points (right)*

To decrease negative anti-squat, the main hard points that were changed was the front pivot point of the trailing arm, as well as the vertical positions of the upper and lower camber link that mount to the chassis. By doing this, the anti squat values for the rear suspension stayed above 0, which is what we wanted. Specifically, an anti-squat value of between 24% and 5%, as shown in Figure 73 below. Roll center movement was also minimized as it also got closer to the center of gravity. Although we attempted to optimize for camber changes in roll, this affected the suspension geometry in a way that wouldn't be advantageous for our setup. An effect we didn't plan on optimizing when raising the front pivot point was that the toe change in bump was decreased (although the rear suspension does not have a steering setup associated with it, the possibility of the rear wheels toeing out in bumps would not be a good thing for vehicle stability).

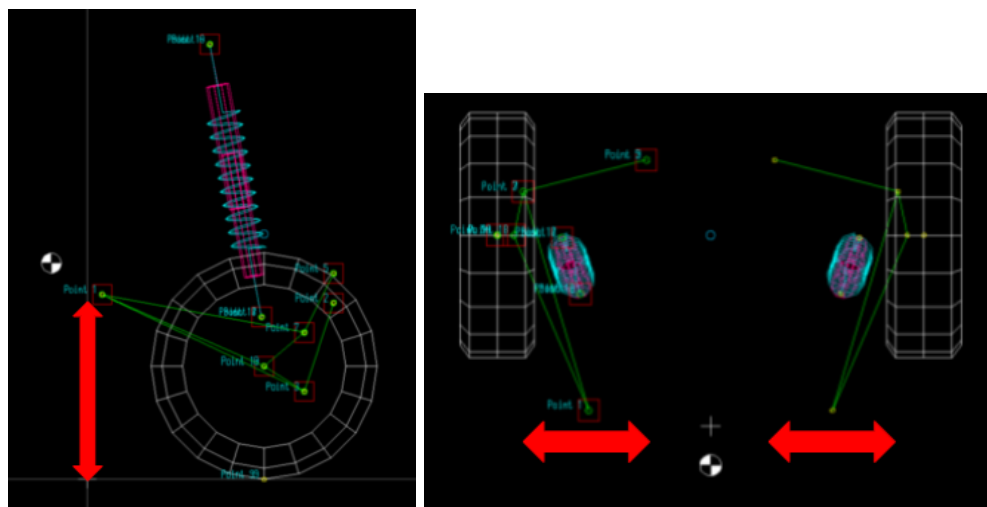


Figure 72: Hard points representing the direction of movement of hard points to minimize negative anti-squat

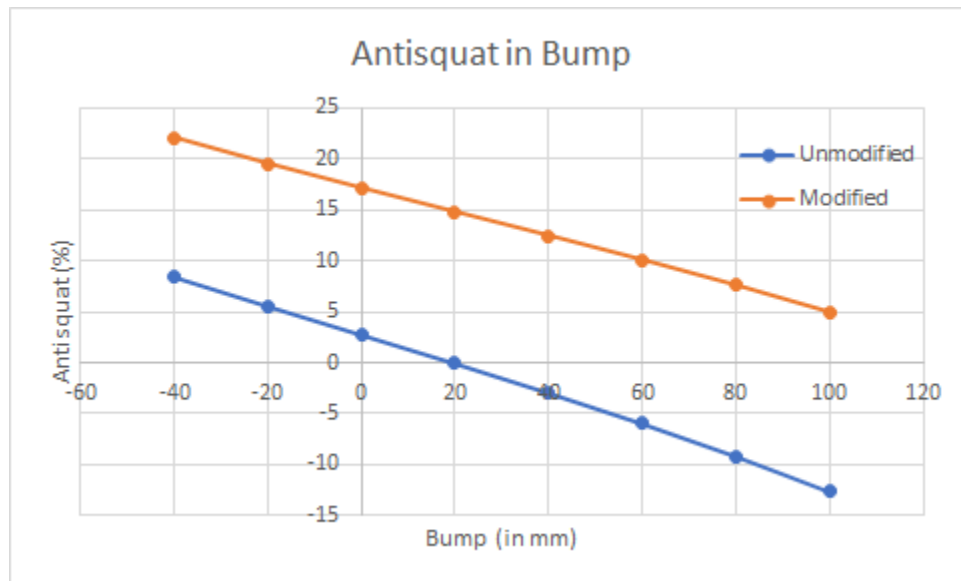
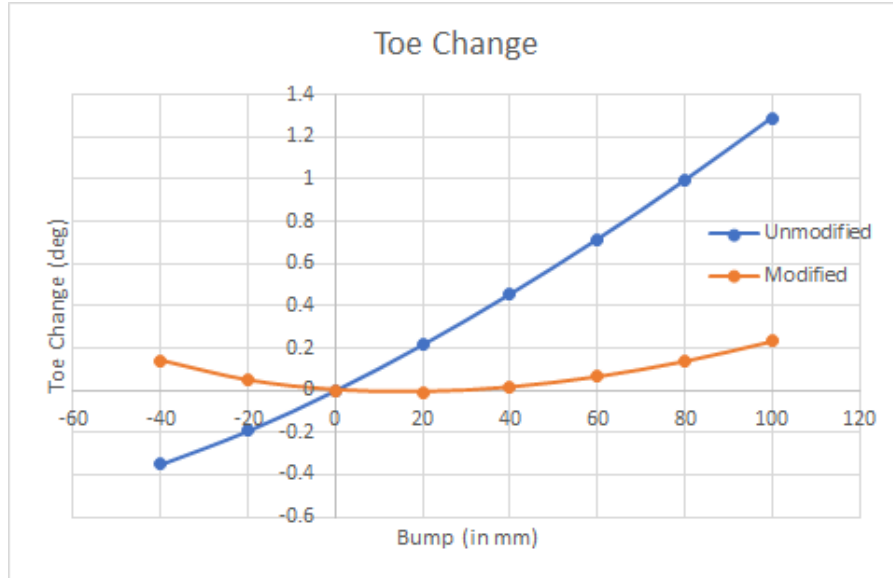


Figure 73: Anti Squat percentage in Bump



*Figure 74: Toe change in Bump*

Modifying the hard points also allowed for a maximum toe angle of about 0.2 degrees which is not exactly ideal, compared to the modified 1.3 degrees in toe. However, the benefit of having less toe is that it aids in slight oversteer. This is ideal since it is easier to control a vehicle during oversteer rather than understeer.

## FEA

For now the most important suspension component that needed to be validated was the rear trailing arm as trailing arms generally undergo more loading than A-arms, and in general fail more frequently than A-arm suspensions do. A compression support was placed at the lower shock mount and a frictionless support was placed at the heim joint. A 10kN force was placed onto where tabs would be located on the trailing arm according to the calculations done for the front suspension impact forces.

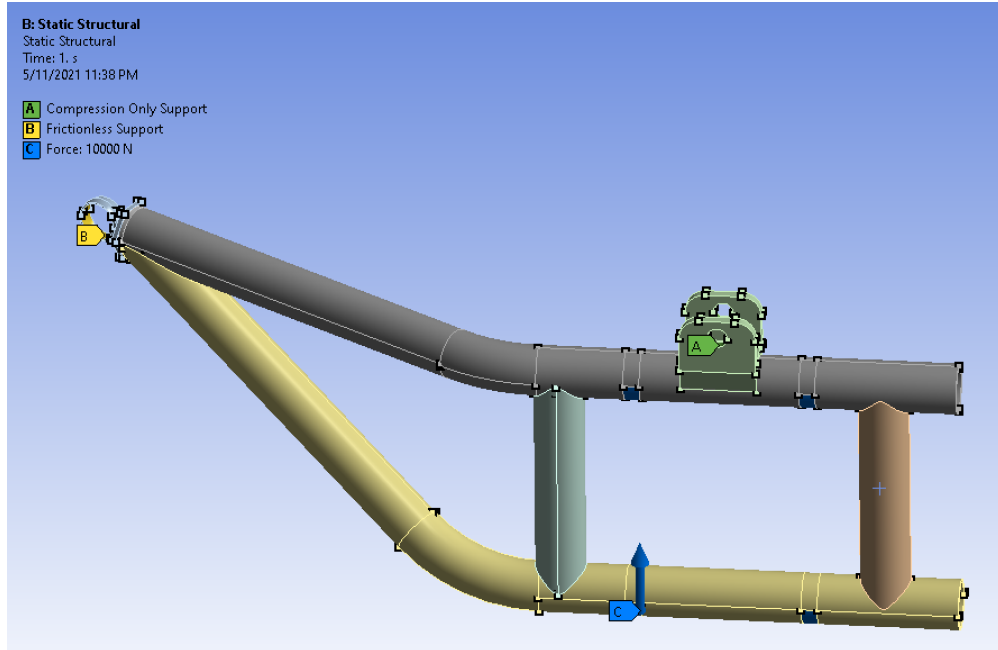


Figure 75: Boundary Conditions on the Trailing Arm

The trailing arm experiences approximately 216 MPa of stress near the shock mounting point with no sign of divergence in the convergence graph. This gives us a factor of safety of 1.89 if we use 4140 Steel for the trailing arm. Both the front and rear suspensions can make use of more robust impact studies using an explicit dynamics study as these are overengineered impact studies done on static structural studies which won't take into account the overall movement of the control arms.

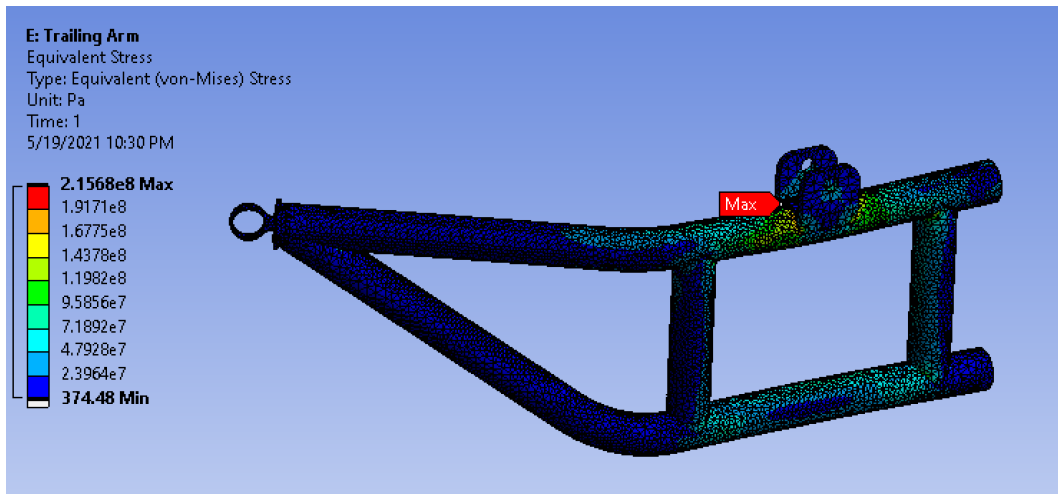
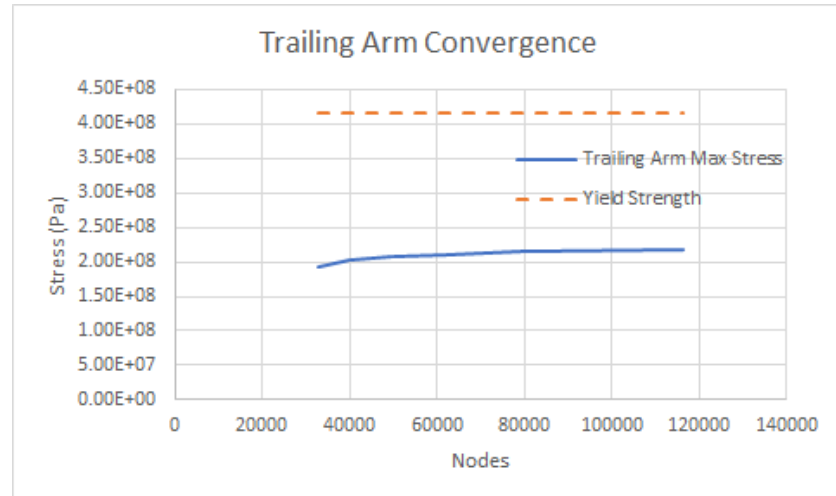
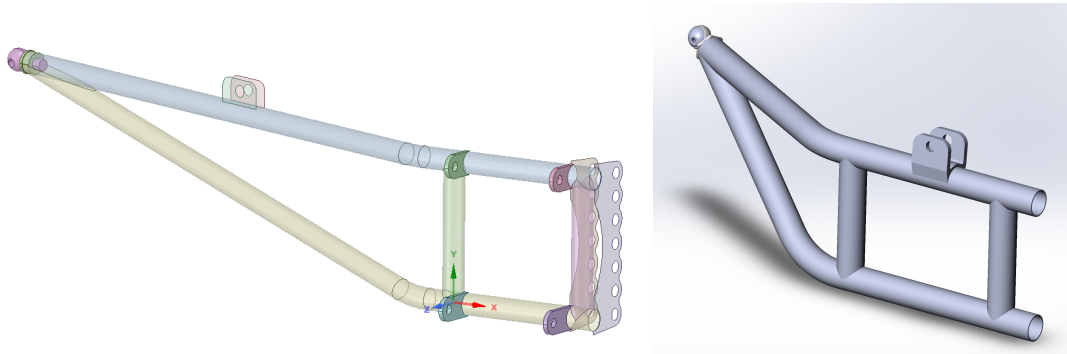


Figure 76: Stress Distribution on Trailing Arm



*Figure 77: Trailing Arm Convergence Graph*

### *Final Design Comparison*



*Figure 78: Old Trailing Arm (left), Finalized Trailing arm (right)*

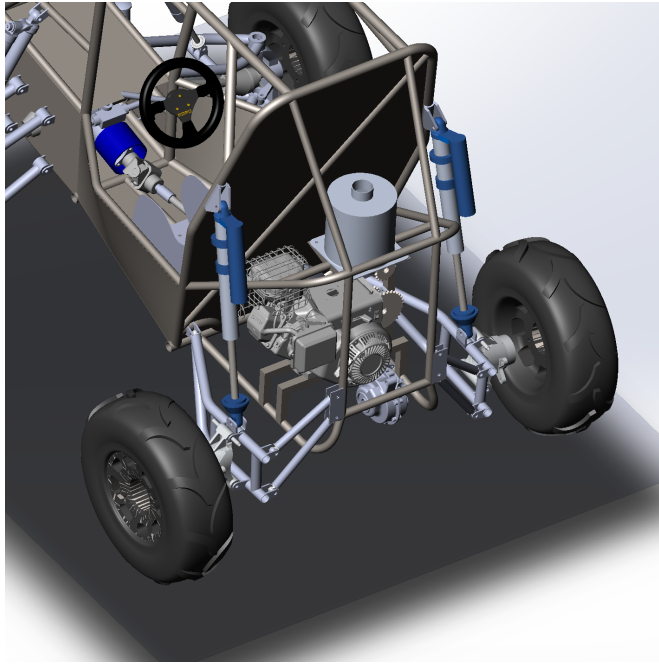


*Figure 79: 2021 BAJA rear suspension setup*

After finalizing the rear suspension setup, it is apparent to note that the new trailing arm is much shorter to aid in providing a shorter wheelbase, less material to satisfy a strict budget, all while maintaining a factor of safety of 1.89. Negative anti-squat was mitigated in the rear, while traction was maintained to aid in acceleration of the rear tires, and ultimately, the rear trailing arm worked to create a smaller and agile vehicle to assist in the front suspension's tight cornering.

## Powertrain

### *What is the Powertrain?*

The powertrain in the vehicle is the driving force of the vehicle. When talking about the powertrain, this deals with between the engine and wheels, inclusive. Specifically, the powertrain's main job is to deliver power from the engine to the wheels. There have been many variations to sending power to the wheels. However, modern technology deals with varying power, not just distributing it to the wheels. This is especially true with all wheel drive (AWD) and 4 wheel drive (4WD) systems. This year, although it was optional, the team still planned on going with the AWD system. On top of the extra points it gives the team, this is also a way to break the traditional rear wheel drive (RWD) or forward wheel drive (FWD) that has been in the SAE BAJA competition for a while.

Following *figure 80*, the powertrain starts off at the engine. After the engine, there are two choices, automatic or manual transmission. In this case, it would be an automatic transmission, specifically a continuously variable transmission (CVT). After the CVT, which can increase or decrease the gear ratio, there is a gearbox. This gearbox has a set gear ratio, so it reduces or increases the torque from the engine. Since our vehicle is going with the AWD system, the power is divided between the two drive shafts; one going to the front and the other going to the rear. In the rear side, the power goes to the rear propeller shaft and then to the rear differential. The differential usually has a gear reduction as well. Then, the power splits again to the wheels. In the front side, the process is the same, except for one key factor; it has to go through the clutch pack. If this clutch pack is not actuated, as governed by the electronics system, the front propeller shaft and the shaft coming out the gearbox is mechanically disconnected, therefore all the power goes to the rear. However, if it is actuated, then the process is the same as that of the rear side.

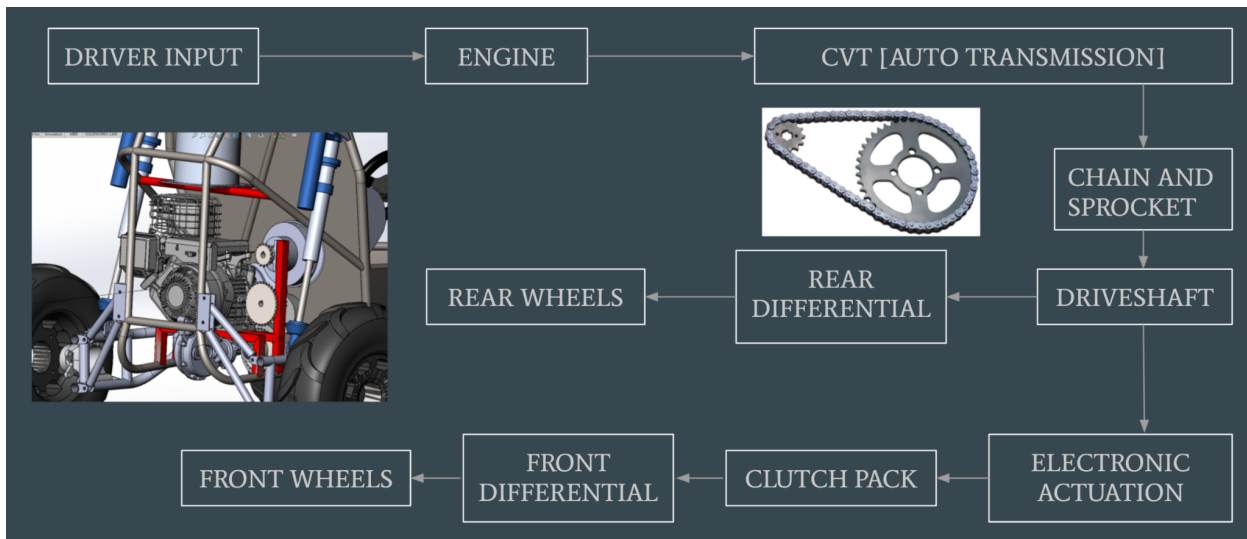


*Figure 80: Functional diagram of the powertrain*

### *Overview of current setup*

This year, the powertrain has gone with the AWD system. Not only does this better suit the future of BAJA members within CCNY, since the rules state that by 2021, all vehicles must be AWD or 4WD, this gives the team some extra points.

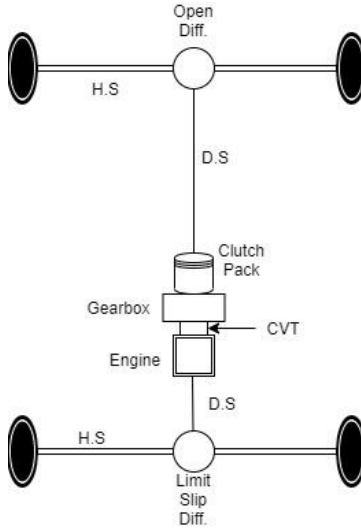


*Figure 81: A diagram of how the AWD powertrain is laid out*

Following *figure 81*, the powertrain will start off at the engine. Then, the power and torque from the engine is delivered out to the CVT. This CVT is connected to the gearbox. Once the gear reduction occurs, the power and torque is transferred to the front and rear of the gearbox. The rear side shows the rear propeller shaft connecting to the limited slip differential. This limited slip differential does another gear reduction, and then the power is transferred to the rear wheels. On the front side, the front of the gearbox is connected to the clutch pack. In the front side, the process is the same, except for two key factors. First, it has to go through the clutch pack. If this clutch pack is not actuated, as governed by the electronics system, the front propeller shaft and the shaft coming out the gearbox is mechanically disconnected, therefore all the power goes to the rear. However, if it is actuated, then the process is the same as that of the rear side. The second key factor is that the front differential is an open differential. Therefore, the way to actuate the power on the wheels is different from that from the back.

## *Customer Requirements*

The requirements for the powertrain is heavily governed by the rulebook. One of the restrictions SAE BAJA participants have for the powertrain is that the engine that must be used is the 4-cycle, air cooled Briggs & Stratton 10 HP OHV Vanguard Model 19 engine. This engine can't be modified in any way. This is to provide a fair standing for all vehicles in terms of input power. However, this is the main restriction powertrain has in terms of component usage. Another requirement that is for powertrain, that is heavily needed for design, is the guarding of rotating components. The main reason this is needed is because of the hazard it has on the driver. This seems to be the main restriction on the design of the powertrain. We still have the liberty of using a AWD, FWD, RWD, or 4WD system. Moreover, the components in the powertrain can be oriented and designed in any way that suits our needs.

## *Component Specifications*

### *Engine*

The engine is the input for the whole powertrain. This feeds the power and torque into the powertrain. The engine is the 4-cycle, air cooled Briggs & Stratton 10 HP OHV Vanguard Model 19 engine. This engine is the same as last year's engine for two reasons. First, it will save money for the BAJA, since the money is definitely a restriction on the powertrain. Moreover, since the engine requirement is the same, the same engine can be utilized.

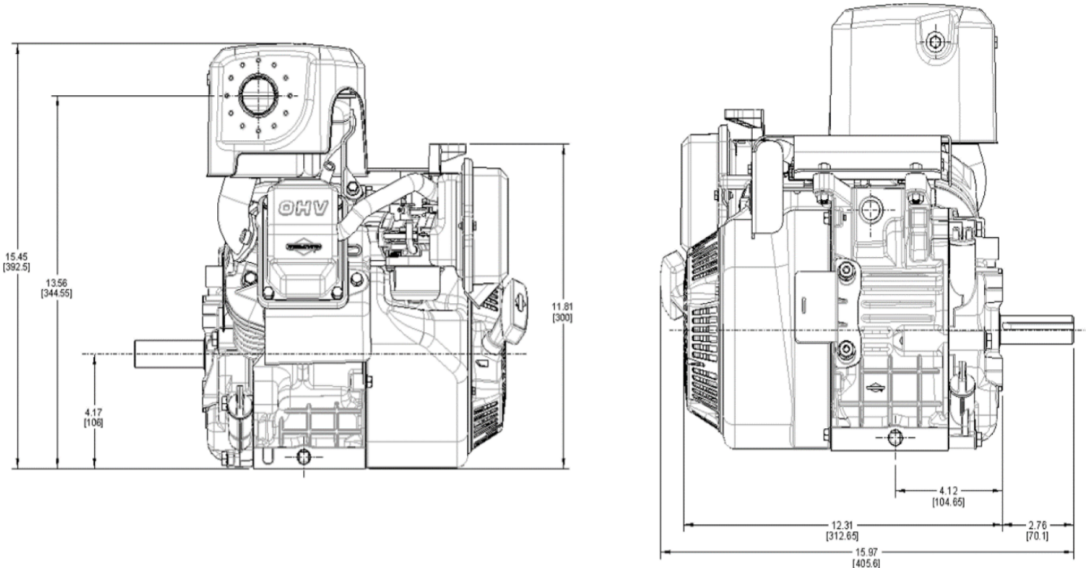


Figure 82: Briggs & Stratton 10 HP OHV Vanguard Model 19 engine engineering drawing

Engine Specification	
Model	19L232-0054 G1
Compression Ratio	8.1:1
Displacement	305 cc
Bore/Stroke	3.12"/2.44"
Horsepower	10 hp
Oil Capacity	24 Ounces
RPM	3,800 RPM
Fuel	87 Octane
Weight	69lbs

Table 8: Briggs & Stratton 10 HP OHV Vanguard Model 19 engine specifications

### *Continuously Variable Transmission (CVT)*

The CVT is a form of an automatic transmission. The CVT, as the name suggests, continuously varies the torque output of the engine. This does so by having two pulleys connected by a belt. As the pulleys are rotating, the pulleys are varying their radii. Since they are connected by the belt, and their radii are varying, the “effective gear ratio” is changing. The reason this is in quotations is because there are no actual gears, however, the torque output is varying based on their radii, hence it is the effective gear ratio. This can be seen in *figure 83*.

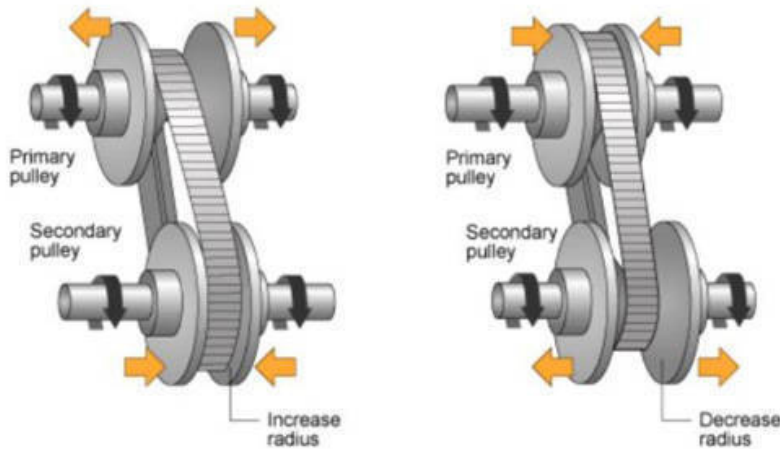


*Figure 83: Simple diagram of how CVT varies gear ratio (<https://www.overdrive.in>)*

The CVT that we are using for the powertrain is the CVTech AAB Pulley Series 0600 and 5600. Similar to the engine, the same CVT is used from last year’s team. The main reason for this is due to budget restraints. Since less money is used on CVT, that money can be used to buy and manufacture stock material or other components, if necessary. The specifications for the CVT is shown in *table 9*

CVT Specifications		
Brand	CVTech AAB	
Model	Pulley Series 0600	
Ratio	Min	0.43
	Max	3.00
Power	5-10hp	

*Table 9: CVTech AAB Pulley Series 0600 and 5600 specifications*

### Old Gearbox

To start off, there is a decision to be made for a 2 stage vs 3 stage gearbox. Even though a 2 stage gearbox is lighter, the 3 stage gearbox has less concentrated stresses. Therefore, *table 10* shows the decision matrix for the 2 stage vs 3 stage gearbox. A higher value means a more favorable decision. There was no weight to the criteria since every criteria is valuable in its own way.

*Table 10: Decision matrix for a 2 stage vs 3 stage gearbox*

Gearbox Decision Matrix		
Criteria	2 Stage	3 Stage
Weight	8	4
Preliminary Stresses (overall)	6	4
Output Torque	5	8
Output Speed	6	4
Maneuverability	6	4
Material Cost	7	5
Manufacturing complexity	3	3
Total	41	32

As it can be seen, the 2 stage was the better choice. Therefore, a decision of a 2 stage gearbox was used.

Gearbox Input		Gearbox			Torque Characteristics			
Input Torque	Stage	Teeth	Ratio	ft-lbs	N-m			
42	ft-lbs	30	2.666667	42	56.94	Driver		
56.94		80		112	151.84	Driven		
		40	1.75	112	151.84	Driver		
		70		196	265.72	Driven		
Final Ratio		4.666667						

*Table 11: Torque transfer throughout gear reduction*

Next, a new gearbox design was created. Since we are taking out a stage from the previous gearbox design, a shaft will be removed as well. This means that the gearbox has to be changed as well. *Figure 84* shows the new gearbox design. This will be a lighter, stronger, and tinner gearbox that will, overall, cost less to manufacture than the previous gearbox designs.

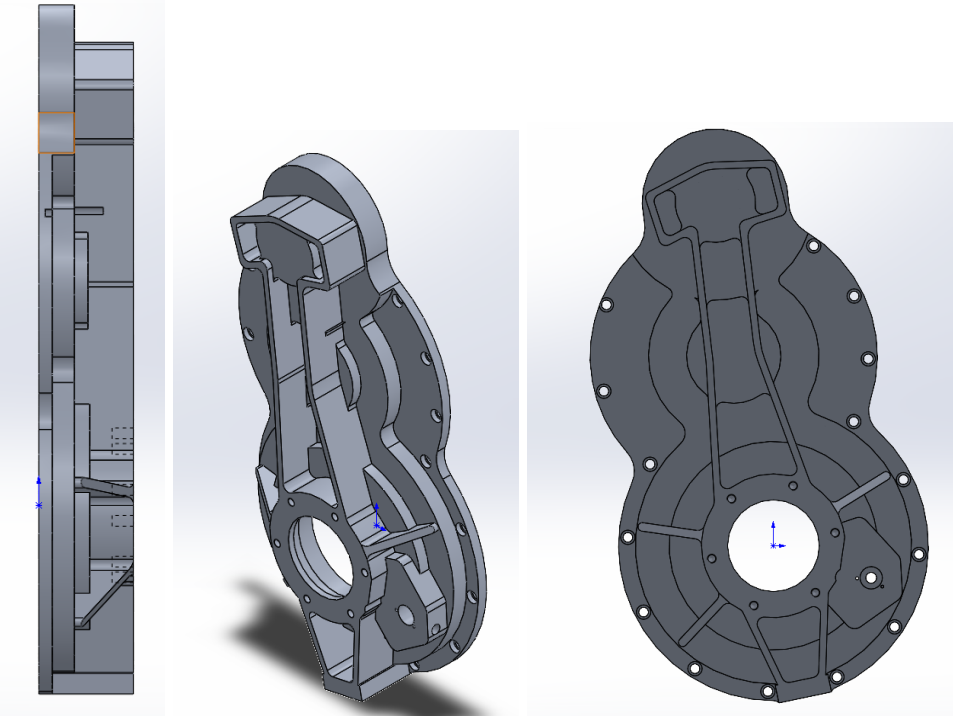


*Figure 84: New preliminary gearbox design.*

Due to the new gearbox design, the input shaft is on top of the gearbox, giving it a vertical orientation, as shown in *figure 85*. In a powertrain standpoint, this is ideal. Since the gearbox is completely vertical, the stresses applied to the gearbox will be completely compressive or tensile. The oblique orientation that it was in last year introduces shear stresses on the shaft and gearbox, which makes it prone to more different types of failure. However, this has its own drawbacks on the other teams. Therefore, this is only a preliminary design, and will be iterated to reflect the concerns for the chassis and suspension team (which is shown on the section “New Gearbox”). Once these new designs are done, the mounting points will be established when collaborating with the chassis team, and a stress analysis will be conducted. After all this optimizing, a bill of material (BOM) will be created to look at the costs, as well as order the stock material to CNC the gearbox.

## New Gearbox

The gearbox is the heart of the powertrain. This is where the majority of the gear reduction occurs. A gear reduction reduces the speed of the gears, while increasing the torque. This is especially useful for traction, such as turning and going up an incline.

Since the gearbox got iterated to a new design, there have been more thought on that design. Since the focus for the powertrain is for reliability, there are also large goals, such as cost and weight. Therefore, a new design was proposed to make a chain and sprocket system. We chose the chain and sprocket system based on the decision matrix shown below. Although the gearbox has better reliability, it wasn't the cost, adaptability, and weight were far more advantageous to the BAJA.

	Sprocket and Chain	Gearbox	Weight
<b>Cost</b>	9	6	1
<b>Reliability</b>	6	9	0.8
<b>Manufacturability</b>	8	9	0.8
<b>Adaptability</b>	9	6	0.7
<b>Weight</b>	8	7	0.8
<b>Weighted Total</b>	32.9	30.2	

*Table 12: Decision matrix between 3 stage gearbox and chain and sprocket.*

Now, the concept of a chain and sprocket system is very similar to a regular gearbox design. In terms of torque and angular velocity, the chain and sprocket system is the same as gears teeth physically mating. Therefore, the calculations for the new gearbox design will be similar for the gear ratio needed from the chain and sprocket system. Below is the free body diagram of the vehicle.

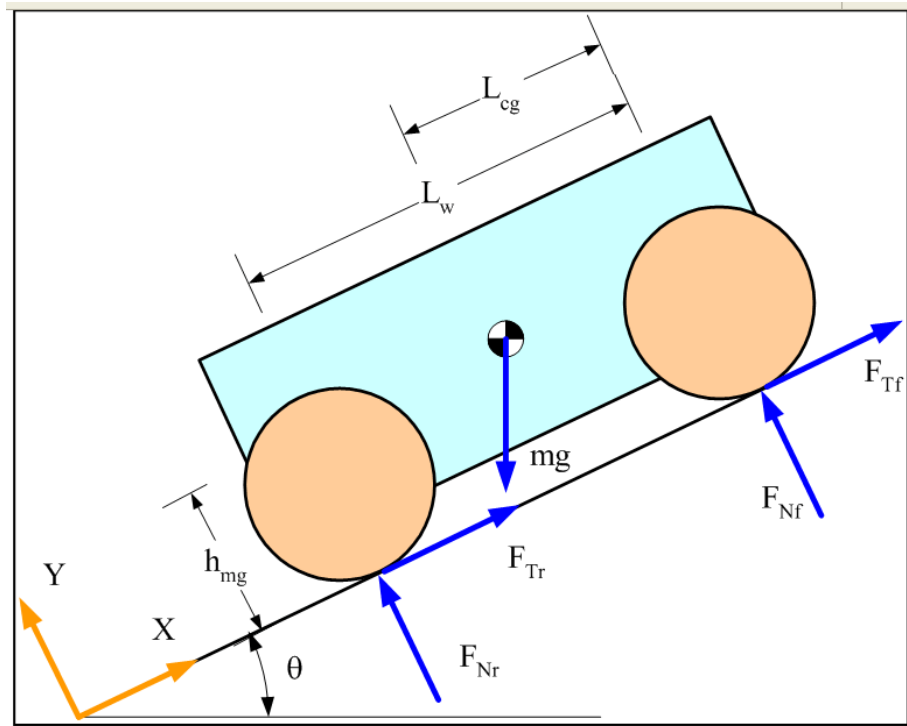


Figure 85: Free body diagram of a vehicle going up an incline, as per  
<https://www.engineersedge.com>

$$\sum F_x = 0 = \mu \gamma_r F_{Nr} + \mu \gamma_f F_{Nf} - mg \sin \theta$$

$$\sum F_y = 0 = F_{Nr} + F_{Nf} - mg \cos \theta$$

$$\sum M = 0 = F_{Nr} L_w - mg (L_{cg} \cos \theta + h_{mg} \sin \theta)$$

$$F_{Nr} = \frac{mg (L_{cg} \cos \theta + h_{mg} \sin \theta)}{L_w}$$

$$F_{Nf} = \frac{mg ((L_w - L_{cg}) \cos \theta - h_{mg} \sin \theta)}{L_w}$$

$$\mu \geq \frac{L_w \sin \theta}{(\gamma_r - \gamma_f)(h_{mg} \sin \theta + L_{cg} \cos \theta) + \gamma_f L_w \cos \theta}$$

tipping over backwards:

$$\theta = \tan^{-1} \left( \frac{L_w - L_{cg}}{h_{mg}} \right)$$

Where  $\theta$  is the angle of the slope,  $h_{mg}$  is the center of mass of the vehicle in the y direction,  $F_N$  are the normal forces on the wheel,  $F_T$  are the traction forces on the wheel,  $L_w$  is the wheelbase,  $L_{CG}$  is the distance between the center of mass and the front wheels in the x direction, and  $\mu$  is the coefficient of friction between the wheels and ground. Plugging in for all these variables, we get that the torque needed to climb up an incline of 30 degrees is approximately 660Nm (~487 ft lbf).

Next, to find the gear ratio needed, we need to find the overall gear ratio.

$$\frac{T_o}{T_i} = n$$

Where  $T_o$  is the output torque,  $T_i$  is the input torque, and  $n$  is the gear ratio.

$$\frac{487 \text{ ft lbf}}{14.5 \text{ ft lbf}} = n$$

$$n \approx 33.6$$

With the known ratios of the front and rear differentials, we can divide that out.

$$\frac{n}{n_{df} n_{dr}} = n_g$$

Where df and dr means front and rear differential gear ratios, and  $n_g$  is the gear ratio of the gearbox.

$$\frac{33.6}{(3)(3)} = n_g$$

$$n_g = 3.73$$

So now, we have the gear ratio we need to climb up the incline. Next, an iterative process was done to find the gear ratio of the combinations of sprockets. In the end, when combined with the available sprockets in the catalogue (shown in the BOM), we decided on going with a 2 stage chain and sprocket design. A final gear ratio of 3.77 was done

BAJA 2021 Powertrain Specs							
Engine			CVT	CVT			
Power	10.00	hp		Ratio	min	max	
	14.50	ft-lbs			0.43	3.00	
Torque	19.66 N-m			Torque [ft-lbs (N-m)]			
Speed [rpm]	Idle	Redline		14.50			
	1750	3800		(19.66)			
				6.235	43.5		
				(8.45)	(58.99)		
Gearbox							
				Torque			
Input Torque		# Teeth	Ratio	[ft-lbs]	[N-m]		
43.50	ft-lbs	Stage 1	17	43.50	58.99		
58.99	N-m		33	84.44	114.50		
		Stage 2	17	84.44	114.50		
			33	163.92	222.27		
Final				3.77			
Vehicle Speed							
Tire Size [in]		20	21	22	23	24	
Max Speed [mph]		46.51	48.84	51.16	53.49	55.82	

Table 13: Calculations of torque from gears and torque input.

For calculating the gear ratio needed from the chain and sprocket system, the torque needed at the wheels need to be known. In terms of designing, we used a 30 degree incline slope in our analysis, since there is a portion in the competition for hill climbing. This is also when the wheels have the least amount of traction.

Now for the part that is most important in terms of failure, selecting the chain. The loading on the chain would be the following,

Chain Size	Weight (Per Ft)	Working Load (lbs)
<b>RS 25</b>	0.09 LBS	140
<b>RS 35</b>	0.22 LBS	480
<b>RS 41</b>	0.42 LBS	500
<b>RS 40</b>	0.28 LBS	810
<b>RS 50</b>	0.68 LBS	1430
<b>RS 60</b>	0.97 LBS	1980

Table 14: Chain size catalogue

$$\begin{aligned} \text{Working load} &= \frac{T}{r_{\text{sprocket}}} \\ \text{Working load} &= \frac{164 \text{ ft-lbf}}{0.22 \text{ ft}} \\ \text{Working load} &\approx 748.3 \text{ lbf} \end{aligned}$$

With the working load, we looked at the higher rated loading chain, therefore, we chose **RS 40**.

### *Front Differential*

The main purpose of the differential is to allow the wheels to rotate at different speeds. Of course there are different methods to this. An open differential is on the front of the BAJA. An open differential essentially allows the wheels to rotate at any speed. This differential is from the Arctic Cat 500 4x4 all terrain vehicle (ATV). This is the same differential as last year, so that costs and manufacturing time for components that need to connect to the differential can be saved.



Figure 86: Arctic Cat 500 4x4 ATV differential that is on the front of the BAJA

Due to the differentials having their own gear reduction, *table 11* was made to find the torque on each wheel.

Front Diff		Torque		
Gear Ratio	3	ft-lbs	N-m	
		98	132.86	Driver
		147	199.29	Driven

*Table 15: Torque output of the front differential*

### *Rear Differential*

As stated in the Front Differential section of the report, the rear differential does the same thing. However, this time, instead of going for an open differential, the back consists of a limited slip differential. Similar to an open differential, a limited slip differential allows the wheel to rotate at different speeds. However, the key difference is that the limited slip limits the difference of power between the wheels. In other words, it allows the wheels to rotate at different speeds, but it has a maximum difference of how much the wheels can rotate in respect to each other. Since power is always being sent to the rear, this will ensure that the rear wheels can undergo cornering and acceleration without losing traction. The differential for the rear is from a Honda TRX-400FA 4.4 ATV.



*Figure 87: Honda TRX-400FA 4.4 ATV differential that will be mounted in the rear.*

This differential also has a gear ratio associated with it, as shown in *table 12*.

Rear Diff		Torque		
Gear Ratio	2.93	ft-lbs	N-m	
		98	132.86	Driver
		143.57	194.6399	Driven

*Table 16: Torque output of the rear differential per wheel*

The problem with the rear differential is that it comes with its internal clutch mechanism. In our case, it would not be useful. Therefore the encasing for the pinion has to be made. *Figure 88* shows a breakdown of the input of the differential. With the original encasement detached, the pinion gear is exposed to the environment, as well as lacks a way to connect the output propeller shaft. On top of a rotating component being exposed, which is not allowed for safety, there is also the fact that the oil for the differential will spill out. Of course, being exposed to the

environment, especially in an off-road environment, will put particles on the splines, which will inhibit and possibly damage the pinion gear.

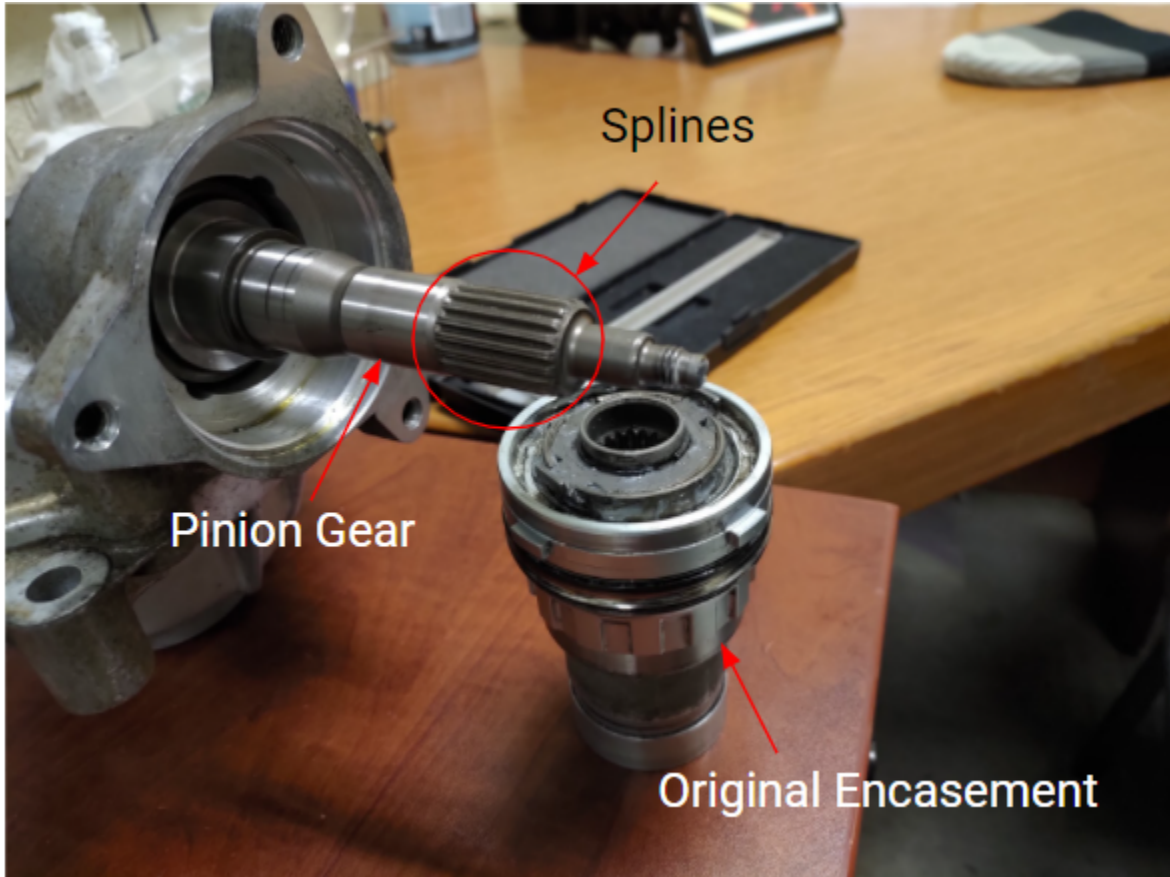


Figure 88: Picture of the input of the rear differential detached from the original encasement

So far, there are two concepts that are up for consideration. The first one, as shown in *figure 89*, is the idea of making a sleeve interface. This sleeve connects to the output propeller shaft and pinion gear by weldments. Then, there will be an encasing that has a lip seal and a bearing. One big advantage of this idea is that it has the actual encasement of the pinion gear baked into the design. However, after talking to our welder, it seems that it would be harder to weld, as compared to the second conceptual design in *figure 90*. The second conceptual design deals with cutting off the splines of the pinion gear and creating an adapter, one for the pinion gear and one for the propeller shaft. This adapter will be bolted and welded together. This seems like it would take up less space on the rear propeller shaft, therefore less costs. The biggest problem with this design deals with the fact that there is no true encasement of the pinion gear, it is only the interface. Therefore, a separate encasing has to be designed.

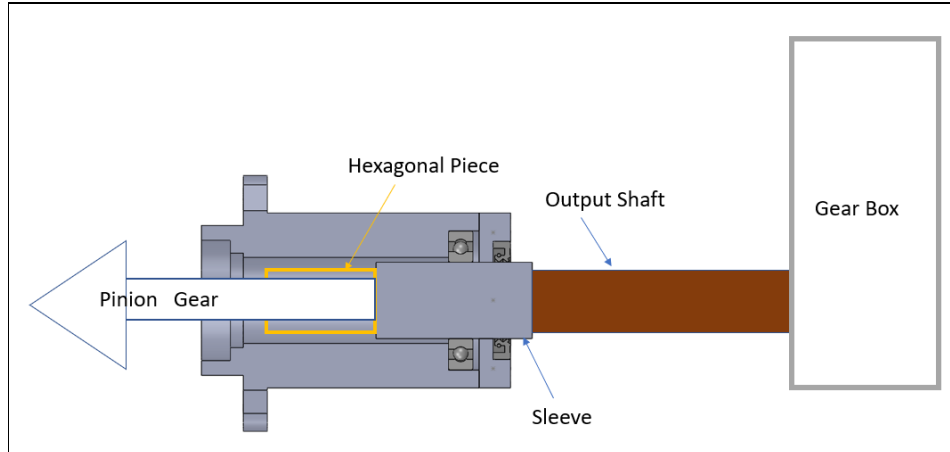


Figure 89: First conceptual design of the pinion gear interface with shaft.

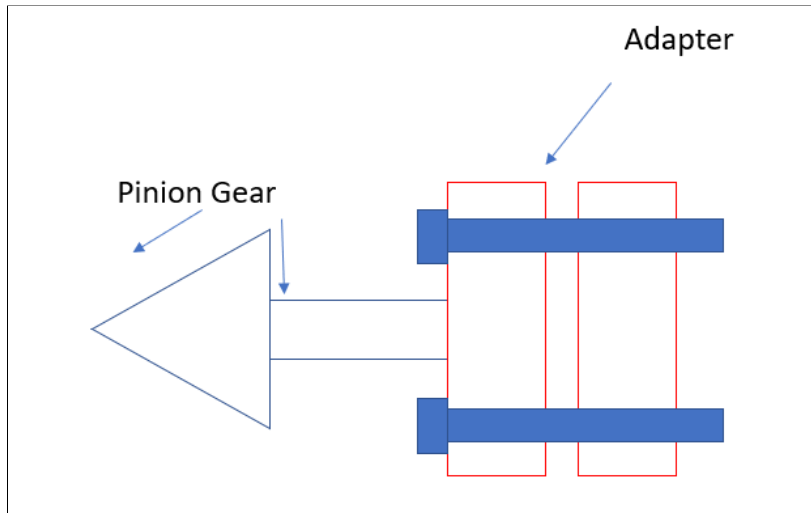


Figure 90: Second conceptual design of pinion gear interface with shaft.

In the end, this is one of the design problems that the powertrain team is solving. Once the designs are fully fleshed out, there will be a decision matrix to compare the two. Once those are done, FEA has to be done on them in order to make sure they do not fail. Then, a BOM must be created, so that we know what to order for manufacturing. Moreover, although we have a picture of the pinion gear, there is no CAD model of the pinion gear. If the team can get into the school, the pinion gear can be created in the CAD model.

### ***U Joints***

Next is the U joints in the car. From the figure below, the U joints are the ones shown in red. U joints allow the front and rear powertrain and suspension to move independently of each other. This is especially important for cars that need to go up a hill. Assume that the floor is perfectly flat (which it never is). Now imagine there is an incline approaching, and you are driving your

vehicle. When you approach the incline, the front wheels of the car will engage with the incline, while the back are still on the flat surface. Due to this, the car will want to rotate about the axis of the back wheels, since the whole vehicle is rigid. However, with U-joints, they allow the transmission of angular rotation while not being aligned without losing angular speed. This works by two arms connected by a centerpiece. These arms rotate about that centerpiece, one degree of freedom is along the axis of rotation, and the other is perpendicular to the axis of rotation, which allows the shaft to be misaligned with the rest of the vehicle.

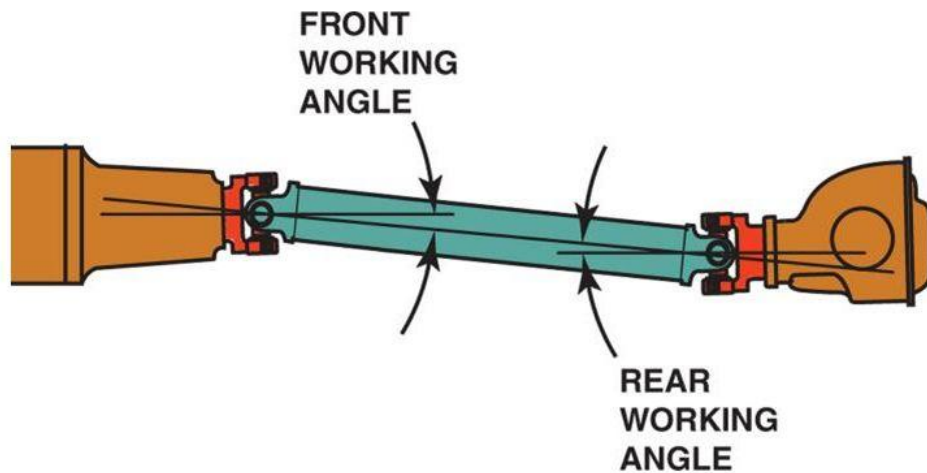


Figure 91: A side view of the U Joint connected to the shaft while not aligned.

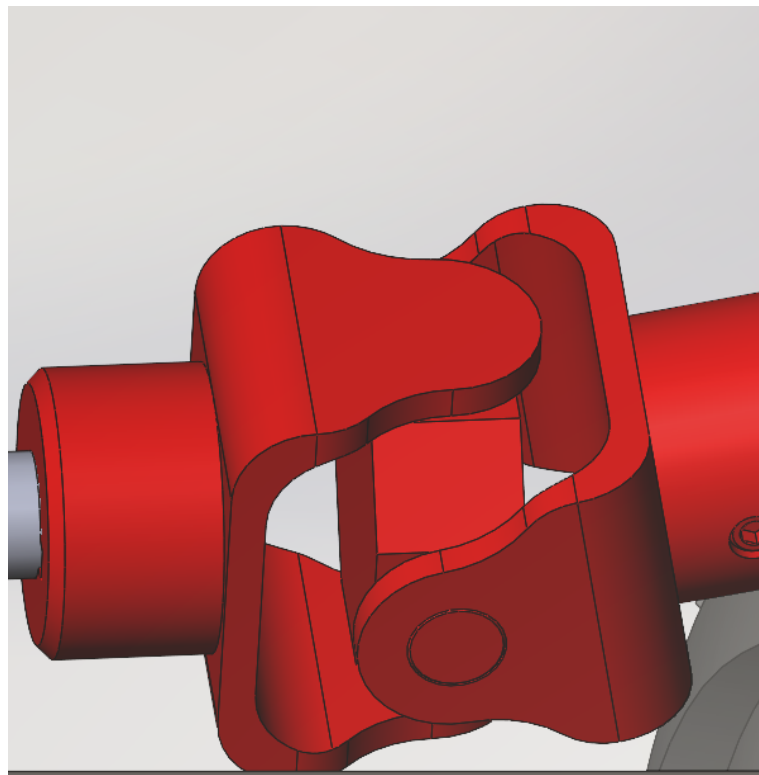
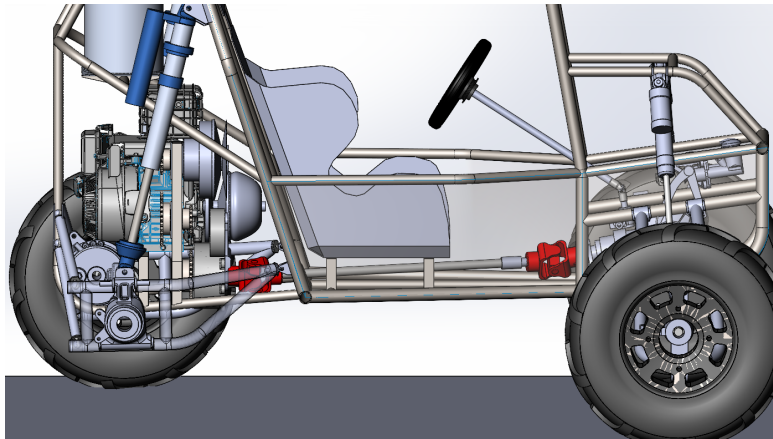


Figure 92: U joints within the BAJA



*Figure 93: Side view of BAJA. The U-joints within the picture are shown in red*

To validate the U-joint, the following was done. Since we know that the working angle is around 10 degrees, and we have a maximum RPM of 330 RPM, the steps are the following,

- 1) Multiply speed x working angle
- 2) Subtract the result from 10,000
- 3) Divide the answer into 10,000
- 4) Multiply this result by the application torque

$$330 * 11 = 3630$$

$$10000 - 3630 = 6370$$

$$10000 / 6370 = 1.57$$

$$1.57 * 165(1.5) = 388.58 \text{ ft-lbs} = 4662.96 \text{ in-lbs}$$

### ***Propeller shaft***

The propeller shaft is one of the most crucial parts in the transmission. This is what allows a car to be long while transferring power to the front and rear end. In our case, the propeller shaft is transferring torque to the front end of the car. To make sure this propeller shaft is properly sized, a stress analysis will be done on the propeller shaft, as shown in the figure below.

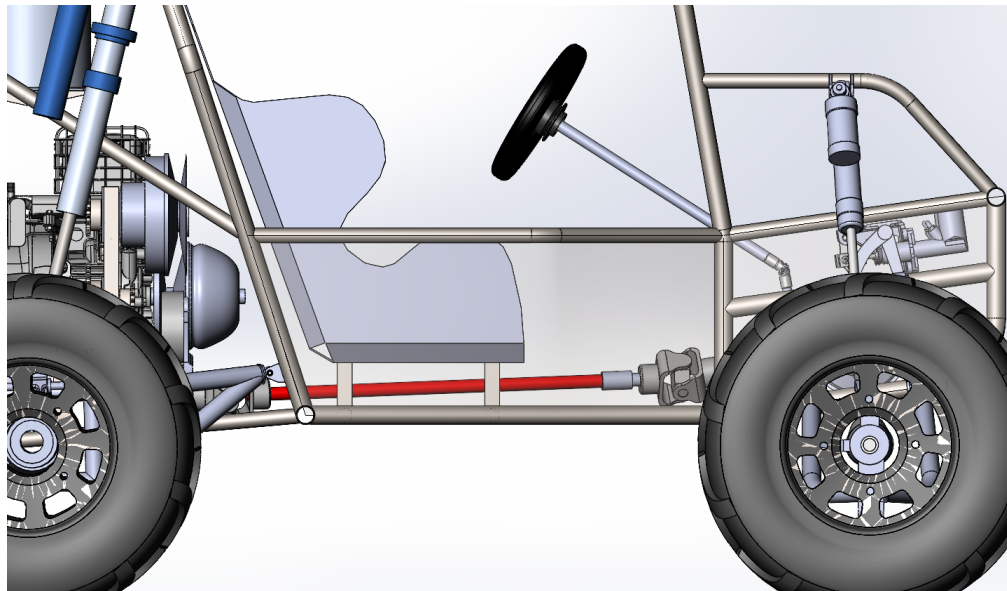


*Figure 94: Side view of BAJA. Propeller shaft is shown in red*

We will be using the same shaft size as last year. Given the diameter of the shaft, assume that the wheel gets stuck on the floor. One side of the shaft will be fixed while the other side experiences the torque from the gearbox. Therefore, the following model was made for the scenario.

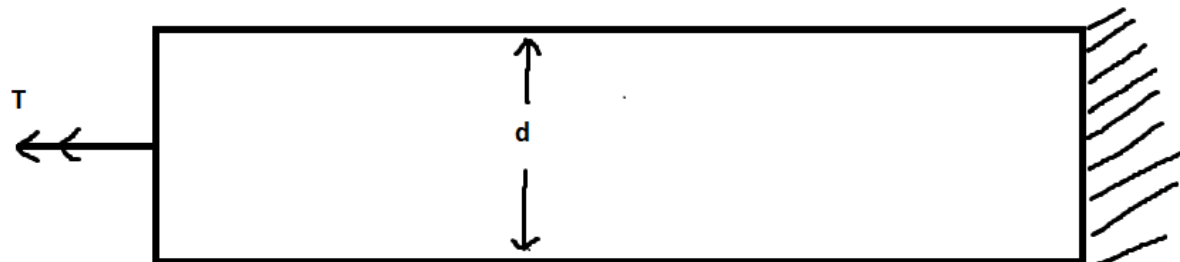


*Figure 95: Model of fixed shaft*

This was solved by finding the stress in the x and the shear stress. The stress in the y can be ignored, because it is insignificant compared to the other stresses. Starting off by taking a section of the shaft, and then finding the internal forces on the shaft.

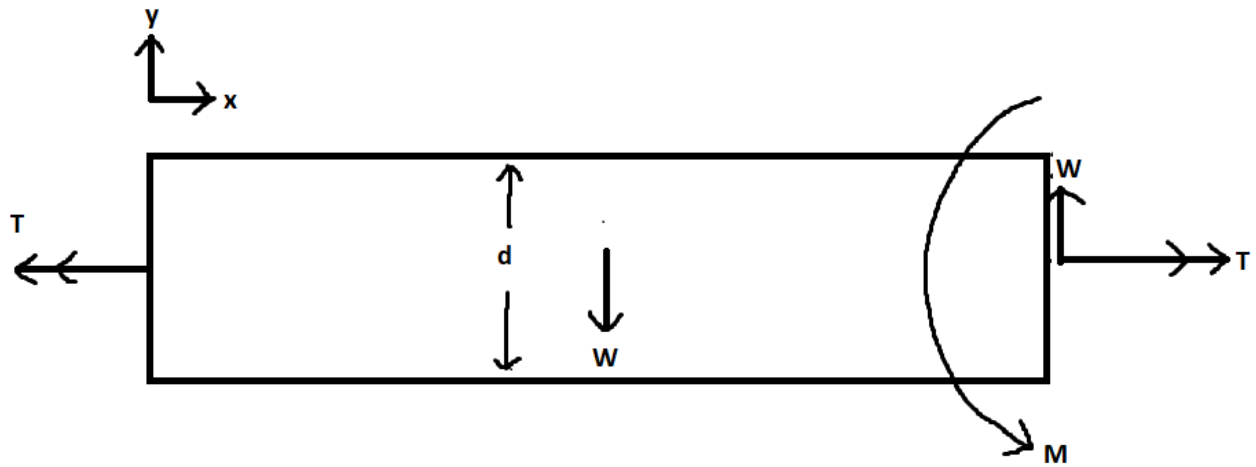


Figure 96: Free body diagram of the shaft under loading.

$$\sigma_x = \frac{Md}{2I}$$

$$\sigma_x = \frac{Md}{2 \left( \frac{\pi d^4}{64} \right)}$$

$$M = \frac{m_{shaft}gL}{2}$$

$$\sigma_x = \frac{32M}{\pi d^3}$$

$$\tau = \frac{Td}{2J}$$

$$\tau_{xy} = \frac{16T}{\pi d^3}$$

Finding the principal stresses on the shaft,

$$\sigma_{1,2} = \frac{\sigma_x + \sigma_y}{2} \pm \sqrt{\left(\frac{\sigma_x + \sigma_y}{2}\right)^2 + \tau_{xy}^2}$$

Once that is done, I use the Maximum Energy Distortion failure criterion to find if the shaft will fail. A safety factor of 2 was used.

$$\frac{n^2}{2} \left[ (\sigma_x - \sigma_y)^2 + (\sigma_y - \sigma_z)^2 + (\sigma_z - \sigma_x)^2 + 6(\tau_{xy}^2 + \tau_{xz}^2 + \tau_{yz}^2) \right] \leq \sigma_{yield}^2$$

Where n is the factor of safety. This equation can be simplified with the principles stresses instead

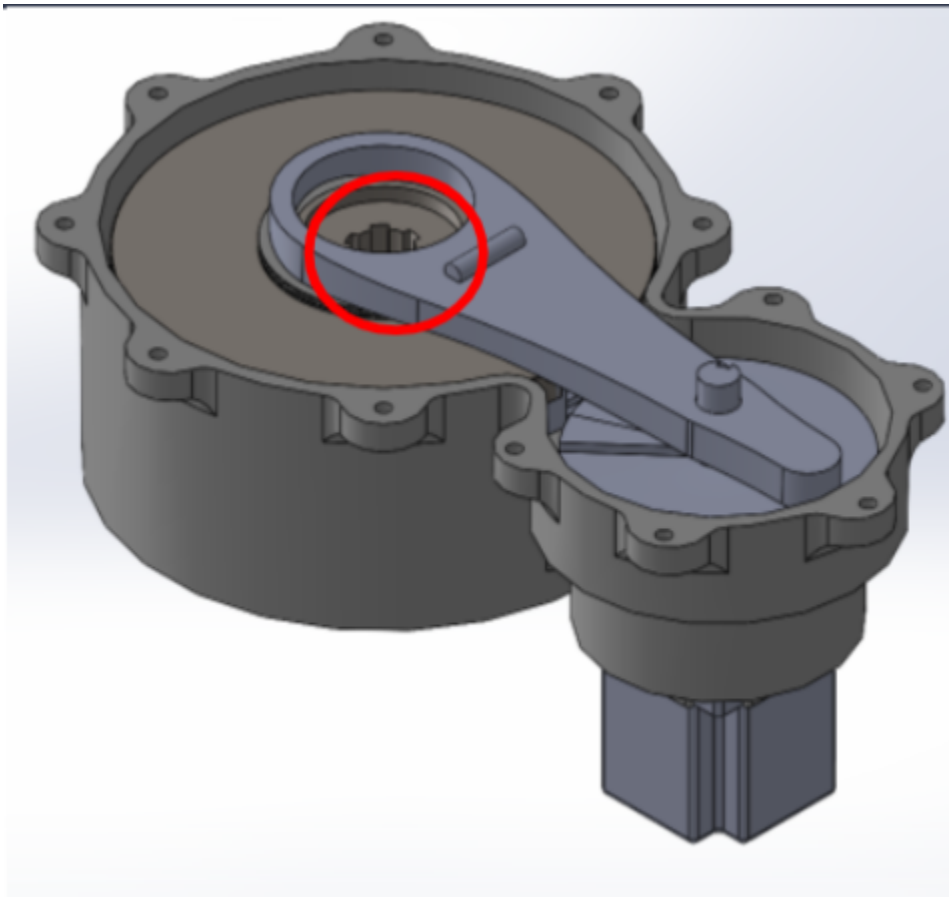
$$\frac{n^2}{2} [(\sigma_1 - \sigma_2)^2 + (\sigma_2 - \sigma_3)^2 + (\sigma_3 - \sigma_1)^2] \leq \sigma_{yield}^2$$

Using this failure criterion, the MATLAB code under the powertrain section was used to find the stresses within this criterion. In the end, the criterion is satisfied. Therefore, the shaft will not fail under extreme loading. Therefore, a **diameter of 0.875in.** was used as the shaft size.

$$360\text{MPa} \leq 415\text{MPa}$$

### **Shaft Spline**

To make sure the clutch pack connects with the shaft, a mate needs to be made. Therefore, a spline was chosen. There is a splined opening in the clutch pack, and this was determined from a spline selection catalogue.



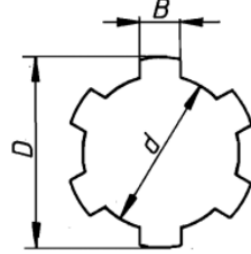
XDrive clutch mechanism. Notice the splined opening in red

There are two main types of splines. One is an involute spline, where the teeth of the spline is similar to that of a gear. The parallel key spline is a simple teeth that follow the shape of the outer circle. In terms of manufacturing, we chose the parallel key. The figure below shows an example of some splines.



Figure 97: Examples of different spline shafts.

We chose a spline size shown below ( $6 \times 18 \times 22$ mm). The diagram below shows the dimensions of the spline looking at the cross section.



d mm	Light series				Medium series			
	Designation	N	D mm	B mm	Designation	N	D mm	B mm
11					6 x 11 x 14	6	14	3
13					6 x 13 x 16	6	16	3,5
16					6 x 16 x 20	6	20	4
18					6 x 18 x 22	6	22	5
21					6 x 21 x 25	6	25	5
23	6 x 23 x 26	6	26	6	6 x 23 x 28	6	28	6
26	6 x 26 x 30	6	30	6	6 x 26 x 32	6	32	6
28	6 x 28 x 32	6	32	7	6 x 28 x 34	6	34	7

Figure 98: ISO Parallel Spline Chart

However, the closest inner diameter bearing size is 25.4mm. Due to this, a new modification of the spline was created. A shoulder was created with a shoulder fillet of 9mm

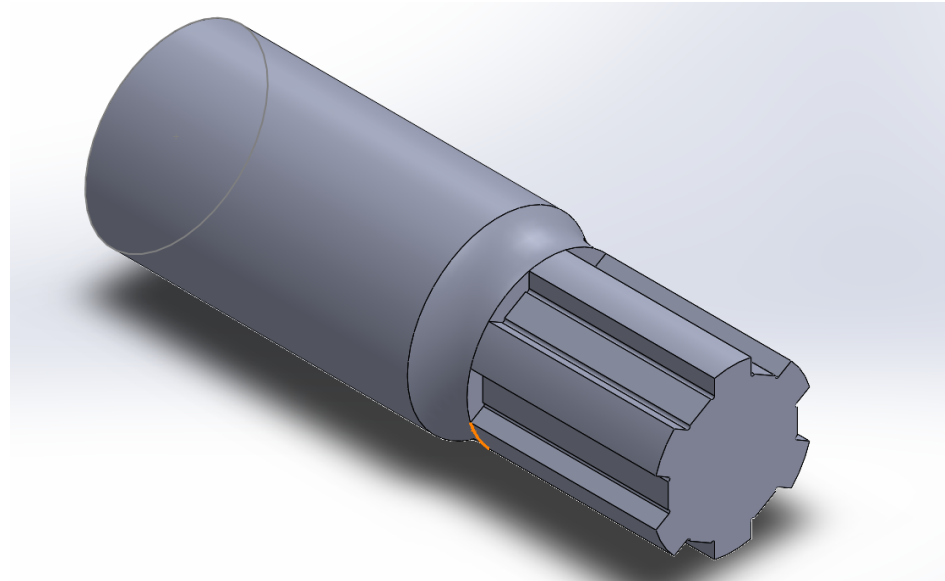


*Figure 99: Spline shaft with a shoulder fillet of 9mm.*

Since this a more complex geometry with very hard analysis by hand, FEA from ANSYS Mechanical was done. With a factor of safety of 1.25, the torque applied is 206.25 ft-lbf. The material for this shaft spline is 4140 Steel. Convergence was found around 382 MPa, which was less than the yield strength 435MPa. Therefore, **this spline shaft was chosen** for the mating of the XDrive.

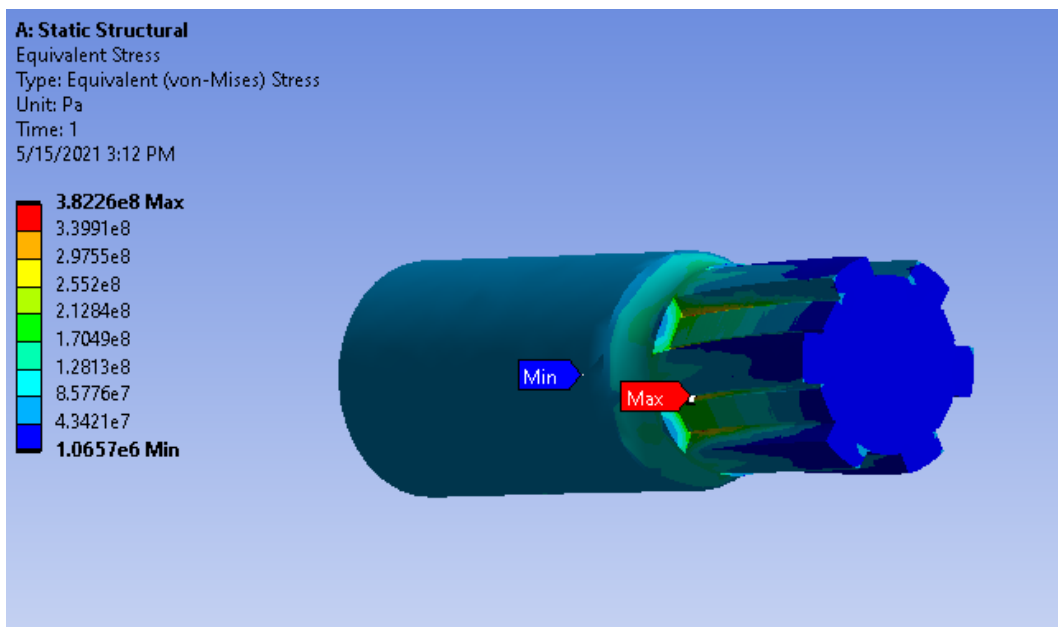


*Figure 100: FEA of spline shaft with a shoulder filler of 9mm*

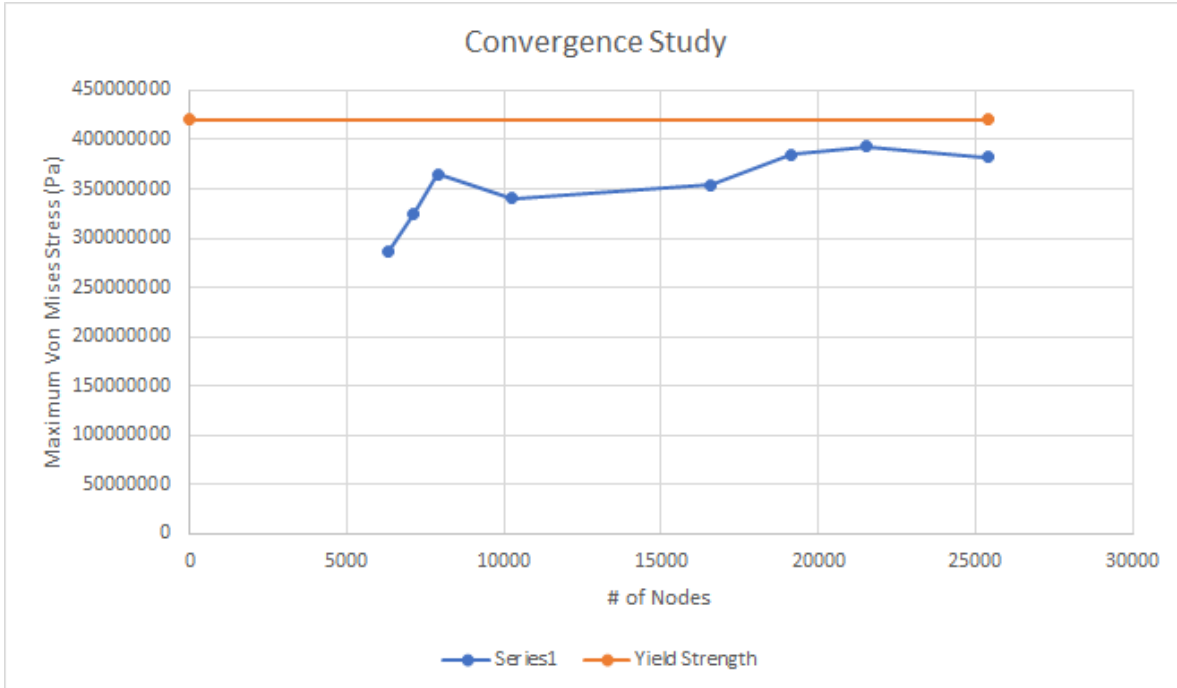


Figure 101: Convergence graph of spline fillet.

## Brakes

### What are Brakes?

A brake is a mechanical device that absorbs energy in a moving system to put the system at complete rest. It is used to slow and stop a moving vehicle, wheels or axle, and prevent moving motion by means of friction. Brakes also allow assistance to maneuvering vehicles through tight turns by decelerating the moving vehicle and applying force on select rotors to enable better cornering.

In the team's Mini Baja design, the brake that was used is the friction brake. This is known to be the most common type of brake used in the automotive industry. Friction brakes have a stationary pad, known as friction facing and a rotating wear surface. Some of the common configurations that are included in the friction brakes are drum brakes, caliper disc brakes and shaft mounted brakes with an integrated disc and rotor. This type of brake provides a controlled deceleration, stopping, holding, and tension control which are needed. In summary, this design will use a pad that is made with a material that can withstand a high friction coefficient and include a rotating surface which is the rotor. The way this essentially works is when there is friction applied against the rotor, kinetic energy is converted into thermal energy.

In order to build the brakes, the following guideline rules were met from the 2021 SAE Baja Regulations. Those customer requirements include:

- The brake pedal must withstand a maximum force of 450lbs – 2000N

- The brake pedal must be able to lock and slide all 4 wheels in both dynamic and static conditions.
- The system must utilize a minimum of 2 independent hydraulic circuits.
- The brake pedal must initiate operating brake lights when brakes are pressed.
- The brake pedal must withstand appropriate pressure and should be placed away from any visible sharp edges.
- The throttle pedal must be able to actuate the throttle arm from full throttle to idle
- 100% - 0% when released.
- The throttle cable needs to be jacketed.
- The throttle cable needs to return to idle stop in the event of any failure.

## *Braking System Function*

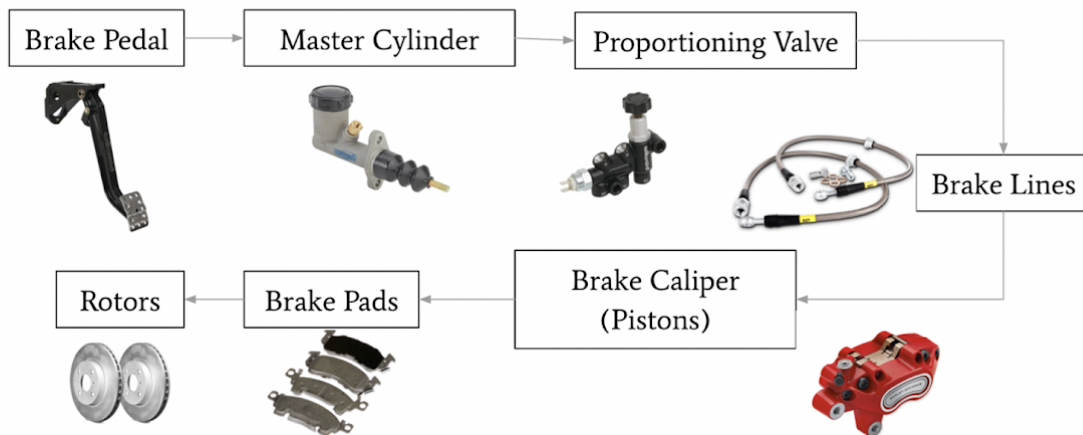


Figure 102: Functional Diagram of Braking System

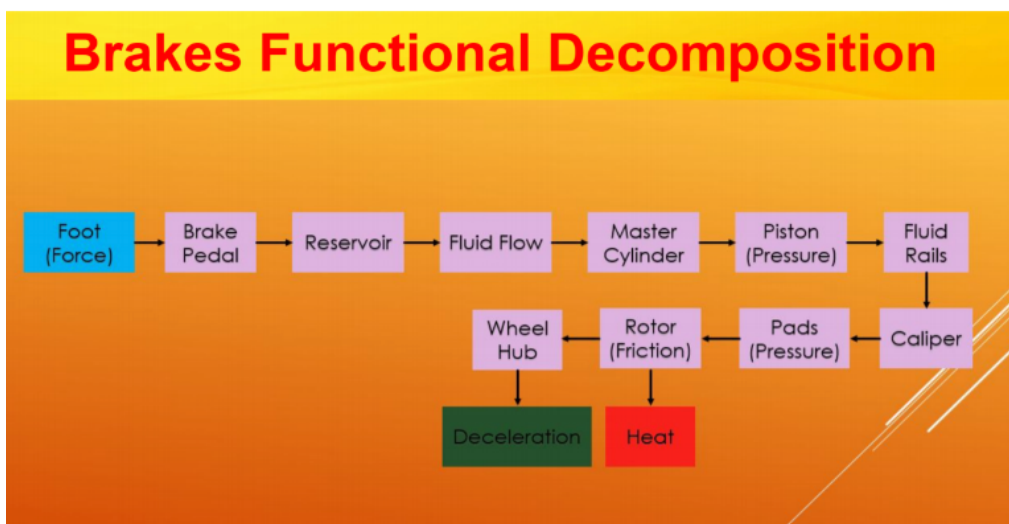


Figure 103: Brakes Functional Decomposition

When force is applied as soon as the foot pushes on the brake pedal, the input force generated by the person's leg is amplified by mechanical leverage. This further amplifies the force with the action of the brake booster which actuates the brake calipers to put a stop to the moving rotors making the moving vehicle come to a complete stop. When the driver applies that force, the driver essentially causes it to rotate about a pivot point. After the pedal is moved, there is pressure applied to the pushrods which are connected to the pistons that are located inside the master cylinder assembly. The pushrods move horizontally, and it compresses the brake fluid in the two master cylinders. The master cylinder is a control device that converts force from the driver's foot into hydraulic pressure and it includes 2 brake circuits. The reason for having 2 circuits is so that if one circuit fails, the brakes will continue to function but will just require more pressure. When a piston moves into the cylinder, it squeezes hydraulic brake fluid out of the other end forcing the fluid to flow around the entire braking system within a network of brake lines all with an equal pressure. This process is then sent to the proportioning valve. The proportioning valve is a safety valve that restricts the flow to the rear brakes during a 'panic stop' and prevents the rear wheels from locking up before the front wheels by engaging the rear brakes first allowing more pressure to be sent to the front brakes. The reason for more brake fluid to be distributed to the front brakes than the rear is to account for the shift in weight during braking. After the braking fluid exits the valves through the brake lines, it then reaches the brake caliper assembly. The brake calipers serve as a piston cup where the fluid is pushed into, this allows the calipers to press onto the brake pads and the brake pads are then pressed onto the spinning rotors. After continuous pressure is applied to the rotors, the entire brake caliper assembly is driven backwards so that the second, outer brake pad pushes onto the rotor. Pressure is applied onto both brake pads until the rotors lock making the vehicle in motion come to a full stop.

## *Brake System Philosophy*

After examining the earlier production of the brakes in the 2019 Mini Baja Brake Assembly, it was visible that there were a few issues that needed to be changed and improved therefore a new design was proposed. Last year's design consisted of having the braking setup mounted to the ground, even though it is a simple concept the position of the brakes would make it very awkward for the driver to use. The brake pedal was extended to a point where the driver would have to use his or her ankle to push the pedal the rest of the way which overtime can potentially strain the ankle, and this does not best fit the driver's ability to use this type of braking system with comfort. In brighter light, older parts were reused to create the new brake assembly and those old parts include the master cylinders, the brake calipers, the clevis joints, the triangle bracket and the brake pedal. The 2019 Braking Assembly is shown in *Figure 92* below.

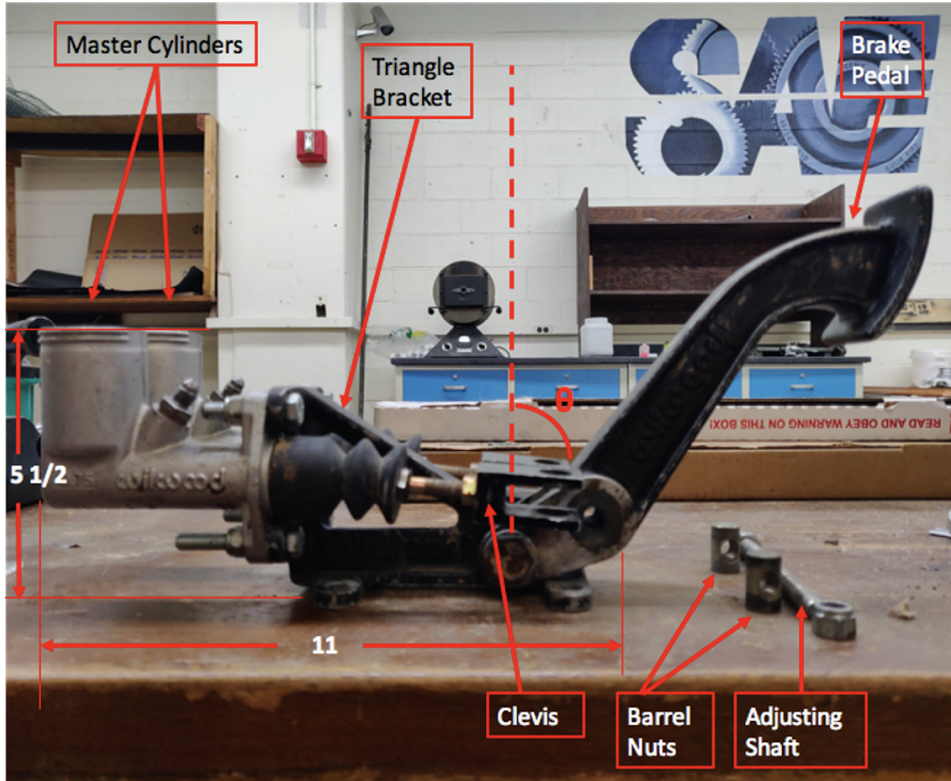
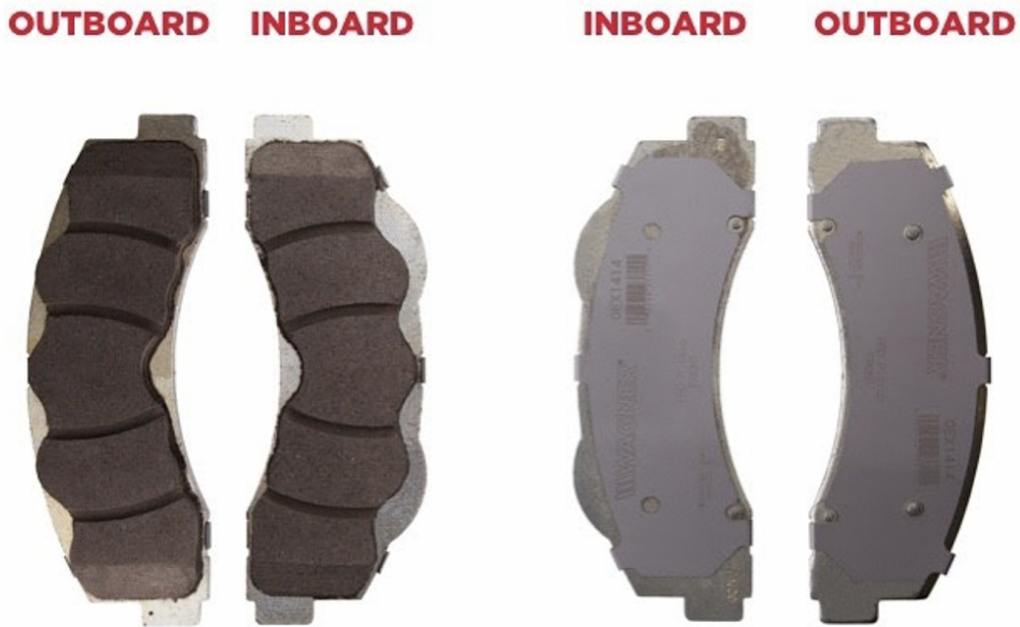


Figure 104: 2019 Baja Brake Assembly [Floor Mounted]

Some of the improvements that were implemented was choosing the outboard brakes over inboard brakes. Previously mentioned it was decided to use the proportioning valve, but the adjusting shaft design was used.. Another change that was implemented was using the floating caliper over the fixed and rum caliper. After reviewing different types of assemblies such as the vertical brake assembly and the traction assister cornering assembly, the decision to create the upside down brake assembly was finalized.

### *Inboard Brakes vs Outboard Brakes*



*Figure 105: Visuals of outboard vs inboard brakes*

The team decided to go with outboard brakes over the inboard brakes due to its easy access and it is inexpensive. Inboard and outboard brakes in relation to the location of the brake calipers and pads on the vehicle. In *Figure 106* shown below, the inboard brakes are mounted onto the chassis of the vehicle whereas outboard brakes are located on the wheel hubs. Due to this placement, the inboard brakes possess a lower unsprung weight and it applies braking torque directly to the chassis allowing the vehicle to have a lighter suspension if need be. Inboard brakes can utilize a larger braking disc without increasing the rotating mass. This allows a larger surface area to be exposed for the brake pads to apply force on and results in an increase of braking power and overall braking assembly. Another factor of the inboard brakes is that it allows improved roll centers which can lead to an improvement of the overall handling of the vehicle as well as an improved cooling system for the front inboard brakes. This particular setup can withstand higher temperatures since the rotors are located away from the wheels, but this also means that the rear inboard brakes have a poor cooling performance due to the lack of air reaching the rotors that are mounted near the rear of the chassis in a confined space. If there is no way to provide a better cooling performance to the rear brakes than there the rate of the brake pads fading will increase. The location of the inboard brakes allows torque to be applied to the chassis directly which is farther away from the wheels/tires. This results in more torque being applied to the driveshafts which extend from the brake motors to the tires and in order to withstand this a new driveshaft would have to be designed. Inboard brakes also require a braking shaft to be in place for the non-driven wheels. The rotors also have to be designed and placed to the differential which is

located in a confined space towards the bottom of the chassis. This makes the whole brake system complex and during a regular maintenance, this can make the brakes difficult to access. For instance, to perform a single rotor or brake pad change, the entire vehicle would be required to be raised and the differential would have to be removed and result in the whole system of the driveshaft to be changed and modified. This is not the design the team intended to work with.

Outboard brakes as mentioned previously are mounted onto the wheel hubs which are directly behind the tires. These types of brakes are most commonly used in off-road vehicles. They are much easier to maintain, easy to access and cost effective. In order to access the outboard brakes all that needs to be done is removing the tires. They do not typically suffer from overheating and this requires low maintenance. Outboard brakes possess a good cooling system and because of its exposure to the environment, the air is allowed to disperse the heat that is generated. The downside of having the brakes exposed to the environment, they are more prone to wear from water, dust, and other elements causing the brakes pads to fade faster and brake calipers to have accidental damage. Although this may be an issue, it is not something that the team was worried about as this can only happen over time with constant usage. One downside about these brakes is that because it increases the unsprung weight of the car, it can negatively affect the roll center of the vehicle as well as the handling. The team came to a final decision of using the outboard brakes for the vehicle since the focus is on accessibility and cost. The endurance race is four hours long, since the brake caliper is easily accessible to perform any needed repairs and clean any collected dirt, this will give the team a big time advantage when racing. The team has direct access to outboard brakes as opposed to inboard brakes which are difficult and more expensive to get. Most ATVs and UTVs utilize outboard brakes providing us a wide array of options to choose from.



*Figure 106: Visual of rear set of Inboard Brakes mounted directly onto chassis on CAD (sourced from 2016 BearCat Baja Design)*

A decisions matrix was implemented for the decision of outboard brakes.

Decision Factors		Outboard Brakes	Inboard Brakes
Criteria	Wt.		
Used with differential	2.0	2	0
Less Sprung Weight	2.0	1	2
Braking Control	2.0	3	1
Cooling	2.0	2	0
Safety	2.0	2	1
Cost	1.0	1	1
Ease of Repair	1.0	1	1
Weighted Scores		22.0	10.0

Figure 107: Decision Matrix for Outboard vs Inboard brakes

### Adjusting Shaft (Bias Bar) vs Proportioning Valve

The proportioning valves and the bias bars both regulate how much pressure each brake caliper intakes. Proportioning valves require a sensor to work that regulates the pressure being applied onto the different calipers and when they are engaged. It is required on vehicles that contain disc brakes in the front and drum brakes in the rear, and in this configuration the rear drum brakes rear drum brakes have to engage first since they are not initially coming in contact with the rotors whereas front disc brakes do. One advantage of the proportioning valve is that the process of which it is mounted, after the master cylinder it allows for flexibility on how the master cylinders can be manipulated. The most ideal setup for a hydraulic circuit would be to have one master cylinder connected to the front right and rear left brake while the other cylinder is connected to the front left and rear right brake. The reason for this is because if one circuit fails, the active circuit would still be able to output braking force to at least on the front and rear caliper. This prevents torque being applied to the vehicle preventing it to spin out of control.

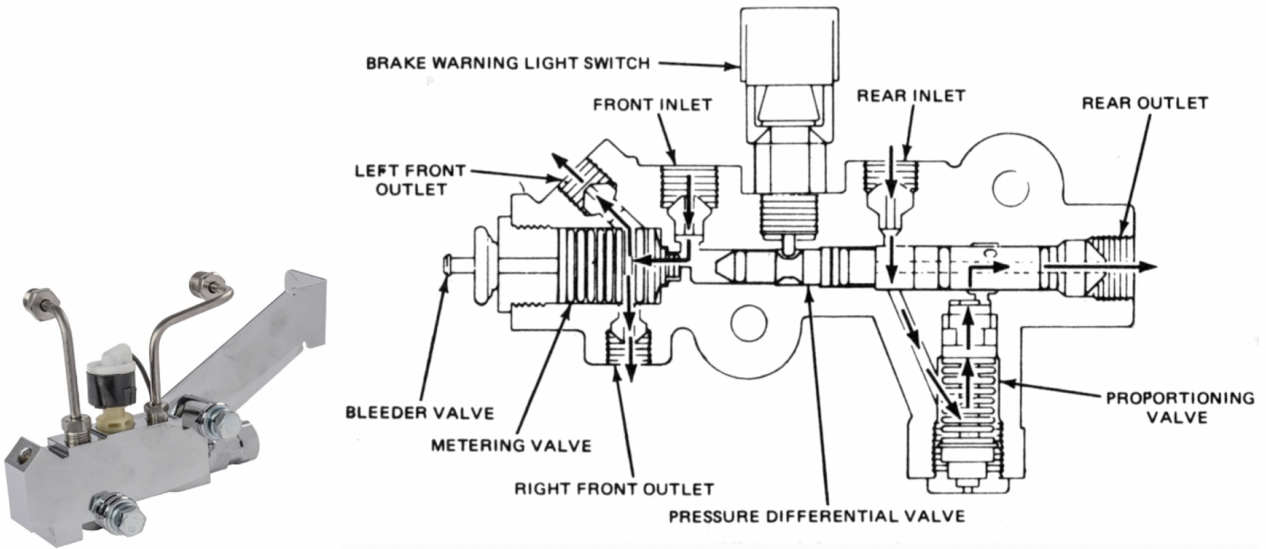


*Figure 108: Proportioning Valve (left) Configuration (right)*

Choosing the bias bar, the team eliminated the need for a proportioning valve. The main advantage of using the bias bar not only is it cheap but it usually comes included with a braking assembly kit. Using the bias bar, the system has the best hydraulic circuit setup which includes one master cylinder to control the front two brakes and the other cylinder controlling the rear two brakes. If the same master cylinder setup was used in the proportioning valve setup, there would be torque applied to the vehicle which can potentially cause it to spin out of control. There will be greater input force towards the front when braking because it is crucial that the rear brakes engage with less power than the front brakes. It is also important that they do not engage first on the vehicle that uses disc brakes on all four wheels so that the rear does not slide out while a turn is being made. The bias bar is located at the pivot of the brake pedal. It includes a threaded rod that can be manipulated to move closer to the right or left which will cause a slight tilt in position. If the bias bar was moved to one side, the master cylinder that is connected to that side will receive more pressure as well as the two brakes that are connected to that circuit. Even if having each master cylinder control the two front and rear brakes respectively is not ideal as the configuration used with the proportioning valve, it is still safe to use.

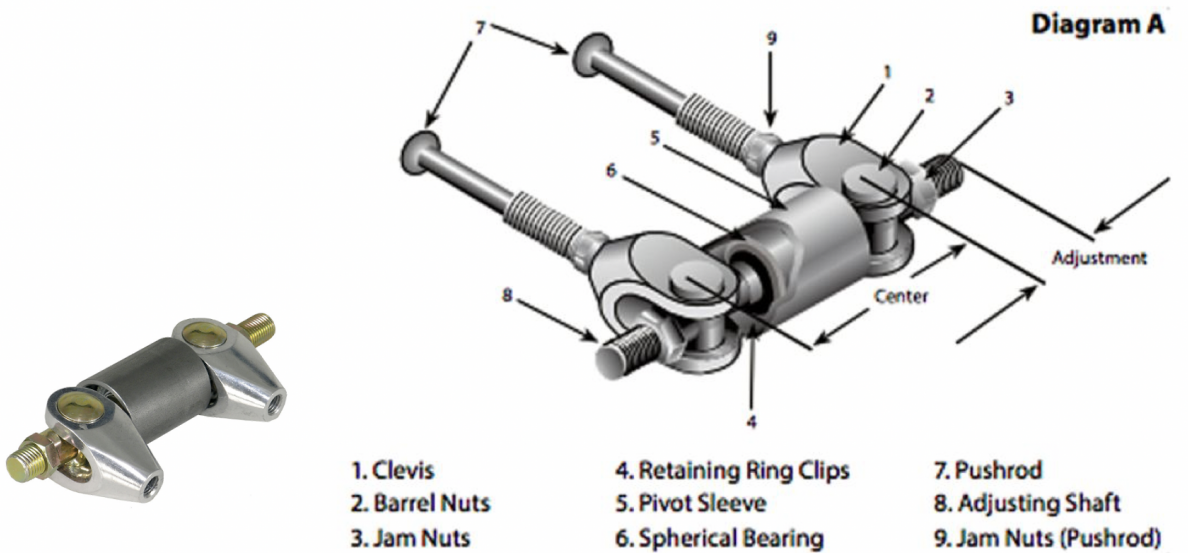


Figure 109: Bias Bar (left) Configuration (right)

### Fixed Calipers vs Floating Calipers

Fixed calipers have two opposite positions that create an equal stopping force on both sides of the rotor when the brake fluid is provided. They always contain an even number of positions, in this case it included two or four pistons. One of the advantages of using a fixed caliper is that they apply great braking force with no delay. In comparison to the floating caliper of the same size, it can do the same because of its increased piston area. They essentially collect less dust and debris and are not likely to exhibit rattling. This means that the fixed calipers do require less maintenance. Although, they are much more expensive than the floating calipers due to the design requiring more moving parts. This makes them less reliable as opposed to the design of the floating calipers. The fixed calipers also have a worse brake pedal feel, because more fluid is required to be supplied to the pistons, the driver has to press down further down on the pedal and that causes discomfort for the person operating the vehicle.

## FIXED CALIPER OPERATION

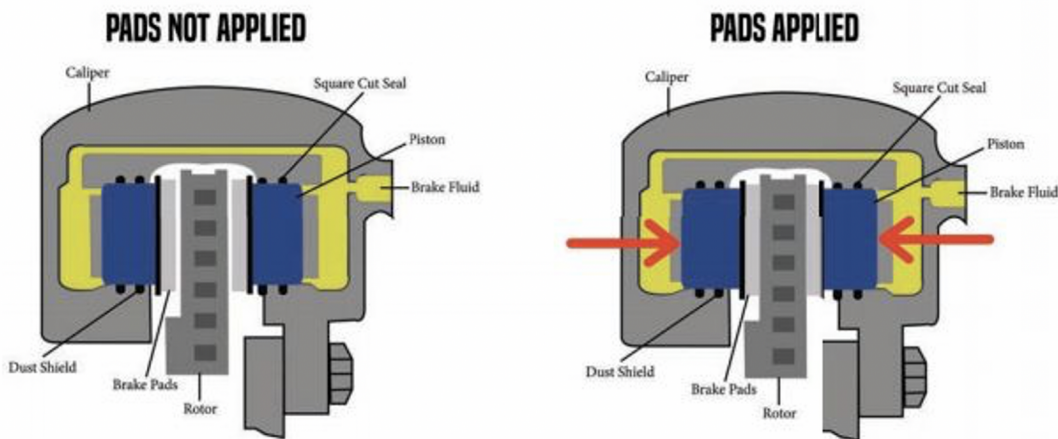


Figure 110: Fixed Caliper Configuration

Floating calipers on the other hand only use one piston to stop the rotor. The piston is in continuous motion until the inner brake pad comes in contact with the inner face of the rotor. It will continue to apply pressure to the rotor, and this causes the entire caliper assembly to move towards the car. The second brake pad comes in contact with the outer face of the rotor where both pads will continue to apply pressure until the rotors have come to a complete stop. Floating calipers contain fewer moving parts, and it is much more compact than their fixed counterparts. Not only does that make them more reliable but they are also cheaper. The only disadvantage is that the pad can wear unevenly between the inner and outer brake pads and they can also output a reduced braking force.

## FLOATING CALIPER PISTON OPERATION

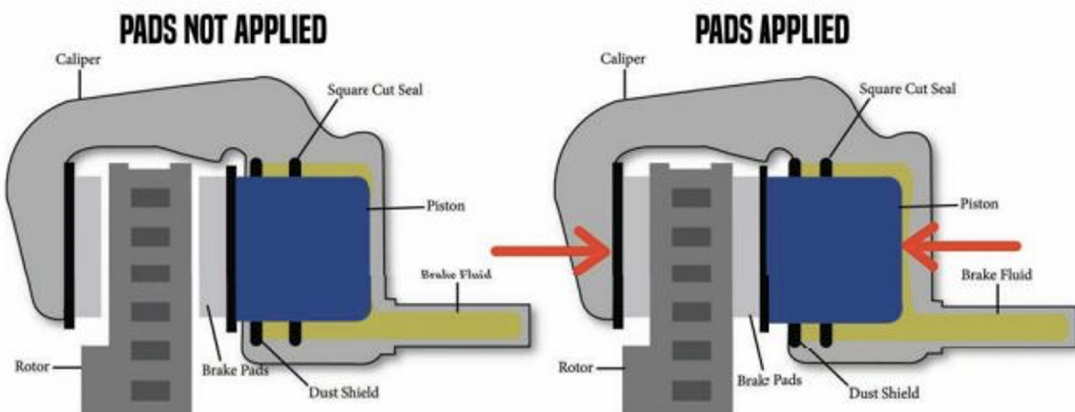
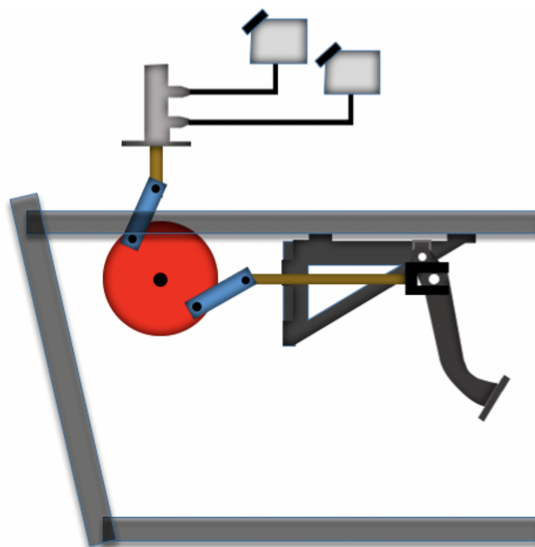


Figure 111: Floating Caliper Configuration

The team decided to choose the floating brake caliper due to the wide range of options accessible to us and low cost. The uneven wear that may happen will only be a result of intense and continuous usage of the brakes but since the team is competing in one long race, this is not something to worry about.

### *Vertical Brake Assembly*

In this assembly that was previously proposed, the master cylinders are shown to be separate with the mounted reservoirs. This is to ensure that they're mounted correctly upright to prevent air bubbles from entering the system. The main advantage of this design was that this would take up more vertical space than horizontal space. The way in which this design works is that the disc or cam being used would be able to convert the horizontal motion of the first pushrod to a vertical motion of the second pushrod. The second pushrod is then initiated by the master cylinder which requires the brake fluid reservoirs to be mounted separately from the master cylinder. The team did not want to go with this design because of the assembly's mechanical complexity involved with manufacturing it and the height limit between the two members of the chassis. The lower and upper pipe members of the front section of the chassis are only allowed to have a maximum distance of 13.5" and the disc required for this design is too big and would cause the pipe member to overextend its limit. The vertical distance ended up being more important than the horizontal distance because of the location of the front differential and steering rack. The overall design of this assembly can jam easily as there is already enough space being occupied by other mechanical components in the front chassis and it is too expensive, and it requires much more time to manufacture and establish so the team decided to not proceed with this assembly.



*Figure 112: Vertically Mounted Master Cylinder Concept Design*

## *Traction Assisted Cornering*

The traction assisted cornering design was proposed in the 2012 Mini Baja design. The master cylinder in this assembly was located on the left where connected to the front and rear left calipers and the master cylinder located on the right was connected to the front and rear right calipers. This applies more pressure to the inner wheels during a turn which assists in cornering. The reason for this assembly was so that they could change the position of the bias bar to the position of the steering wheel. The design was considered but the team had chosen to not go with this assembly due to its mechanical complexity and space that it would require in the front of the chassis which is already occupied with other mechanical components. Designing and building the traction assisted cornering would require extra external resources, time and money. It is also possible that adding this system, the vehicle can encounter an oversteer issue potentially causing the Baja to crash.

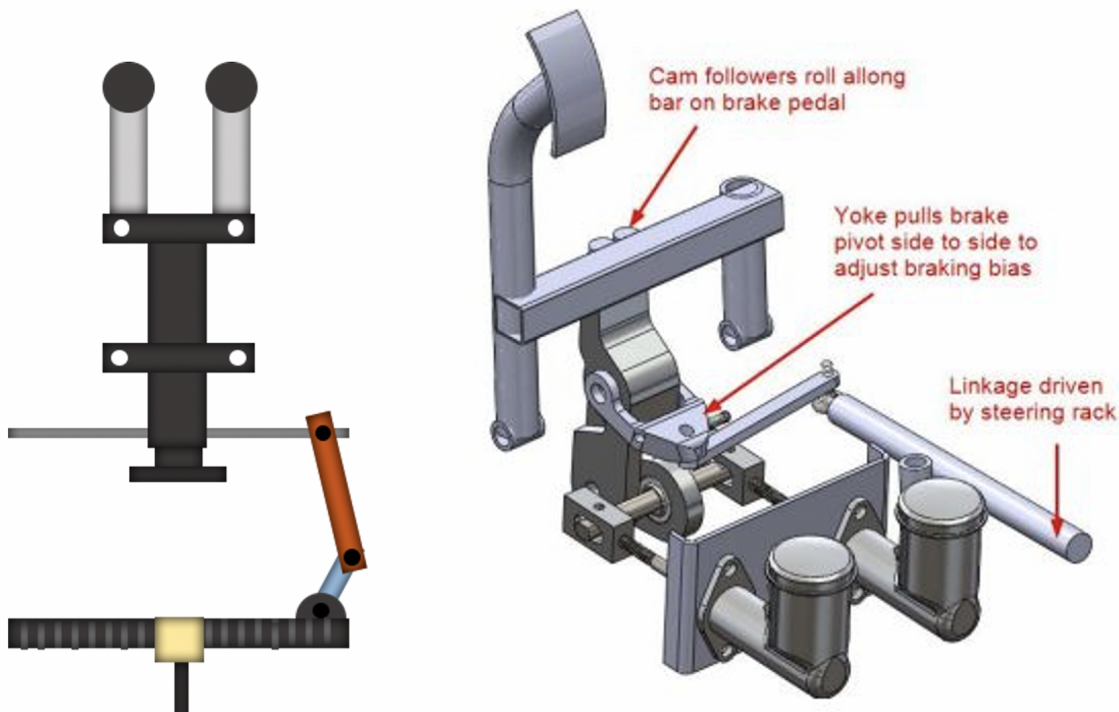


*Figure 113: Traction Assisted Cornering Concept Design*

## *Upside-down Brake Assembly*

For the final brake design, the upside down brake assembly was used instead of going with the original floor mounted brake design configuration used in the 2019 Baja brake assembly. The purpose of this decision was to improve the driver's overall driving comfort and feel as well as creating a more compact design. The hanging brake pedal design promoted the “heel-toe”

approach when pressure is applied to them using the sides of the driver's foot. This allowed and easier feel of control and it is not as sensitive as the floor mounted pedals from last year's design. The hanging brake pedal assembly did have a heavier weight than the floor mounted assembly, but it turned out to be the same weight when it was later implemented on the Baja. Reason being the front differential and steering rack that occupied the space in the front section of the chassis required an additional elevated floor mount to be manufactured in addition to the brake assembly itself making it about the same weight anyways. The hanging brake pedal design increased the overall center gravity of the vehicle, but it did not weigh much compared to the other components of the Baja, so the effect was negligible.

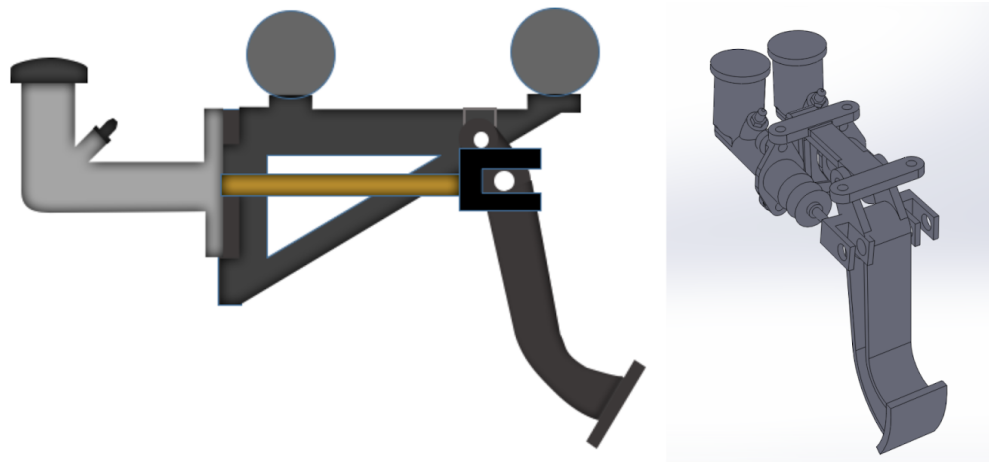


*Figure 114: Upside down hanging brake pedal assembly (left) on CAD (right)*

### *Final Brake Design*

For the final design, the braking assembly required the hanging brake pedal setup but utilized a new brake pedal and triangle bracket design. The new brake pedal is smaller and lighter than the older brake pedal which can lead to a slight disadvantage in the weight of the brake, but it allowed for a more compact design. The new brake has ridges that allow for a better grip of the driver's foot and it fits best with the hanging brake pedal assembly. The triangle bracket will be manufactured using aluminum stock. The pushrods are aligned with the mounting hole on the pedal more efficiently and it will have minimal deflection when compression is applied to the brake pedal. The bracket is mounted under the two secondary member pipes that were used by the four holes on the undersurface.

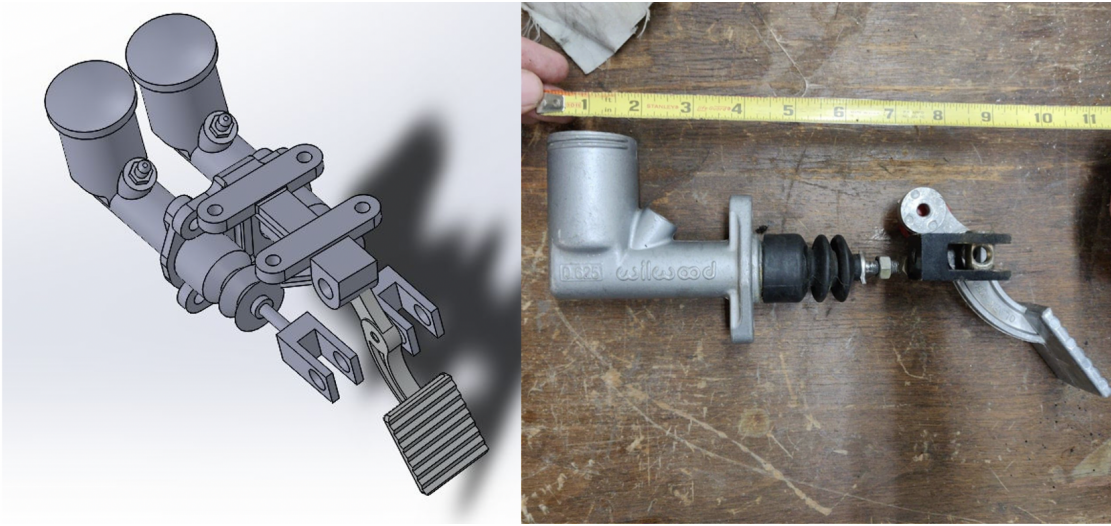


*Figure 115: Final Brake Assembly using CAD (left) and Preliminary Assembly (right)*

In order to create more space for the brake assembly, we modified the front of the chassis to create space for both braking and steering. As mentioned earlier in steering, the most current iteration of our chassis is shown in the Figure below. It implements a more rectangular square shape so the mounting of the brake assembly is much more compact.

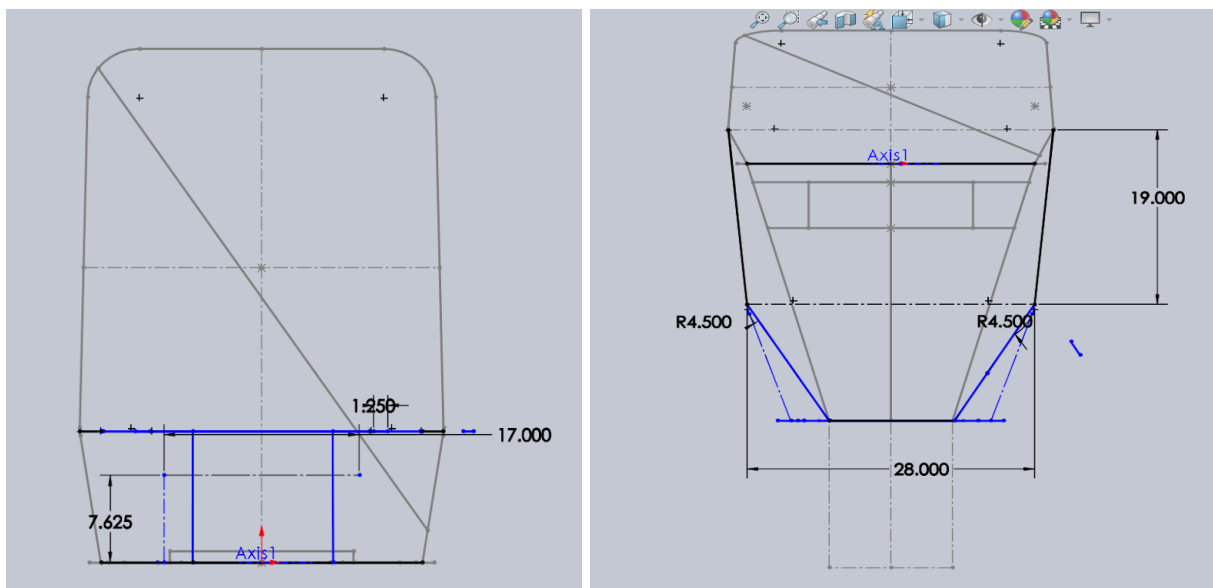


*Figure 116: Final chassis design front view (left) top view (right)*

In addition to the new brake design, the Arctic Cat 500 which the team has in stock was used. The front brake calipers were already purchased to replace the previous Polaris 500 Brake Calipers from the previous year. The hubs and rotors come from a used 2003 Arctic Cat 500 and this helps mesh the driveshafts easily. Rear calipers remain the same but the old brake pads will be replaced with new sintered pads for a better grip and better resistance to heat.



*Figure 117: Arctic Cat 500 Rear Brake Caliper (left) Polaris Hawkeye 300 Brake Pads (middle) and 2003 Arctic Cat Assembly(right)*

### *Throttle Assembly*

In the team's final design for the throttle assembly, the hanging pedal configuration was utilized. It is mounted along the secondary member pipe that the brake assembly is mounted on which is closer to the other end of the chassis. The throttle assembly utilized the same pedal and brake assembly because the team decided to keep the similar feel and resistance when the driver pressed on the brake. The only thing that the team needs to consider is the slight groove on the back of the throttle pedal mount that might have to eventually be raised to best fit the throttle cable during the manufacturing process.

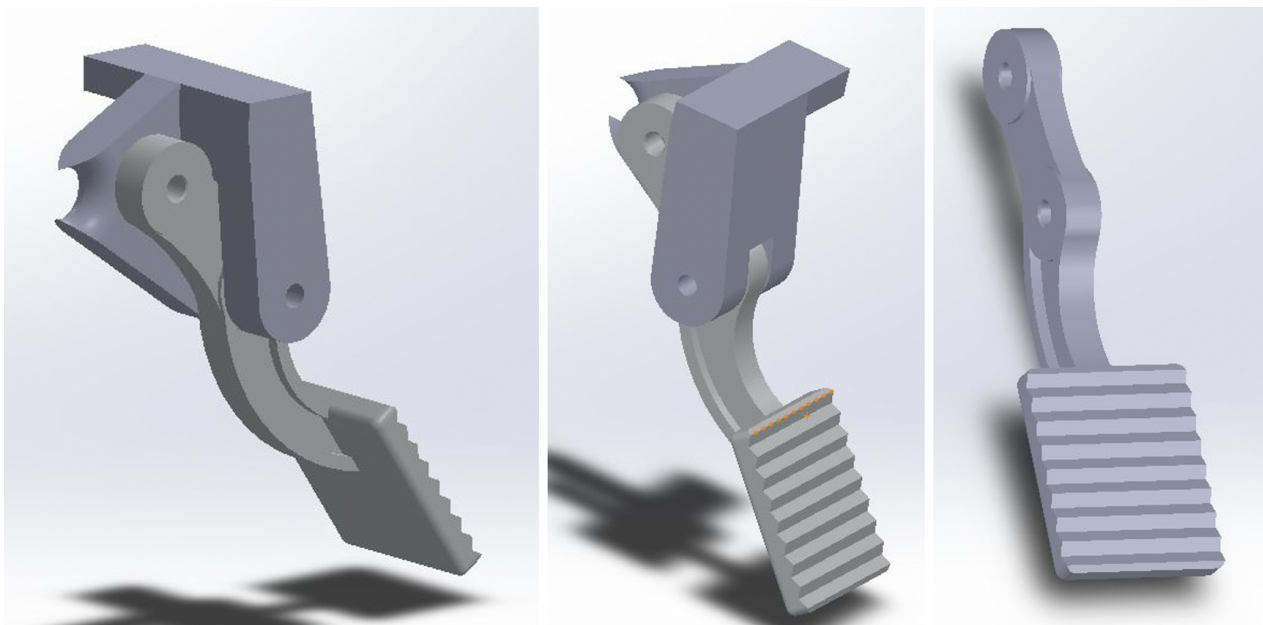


*Figure 118: Final Throttle Assembly on CAD*

## *Recap of Previous Brake Design*

In last year's design there was not a brake assembly implemented so further creating a design had to start from scratch. Available parts were picked up from Grove School of Engineering at City College and the only parts that were there for the assembly was the hub assembly. The calipers and pads were missing therefore a heat analysis could not have been implemented but the future design now has the opportunity too with this new brake assembly design.

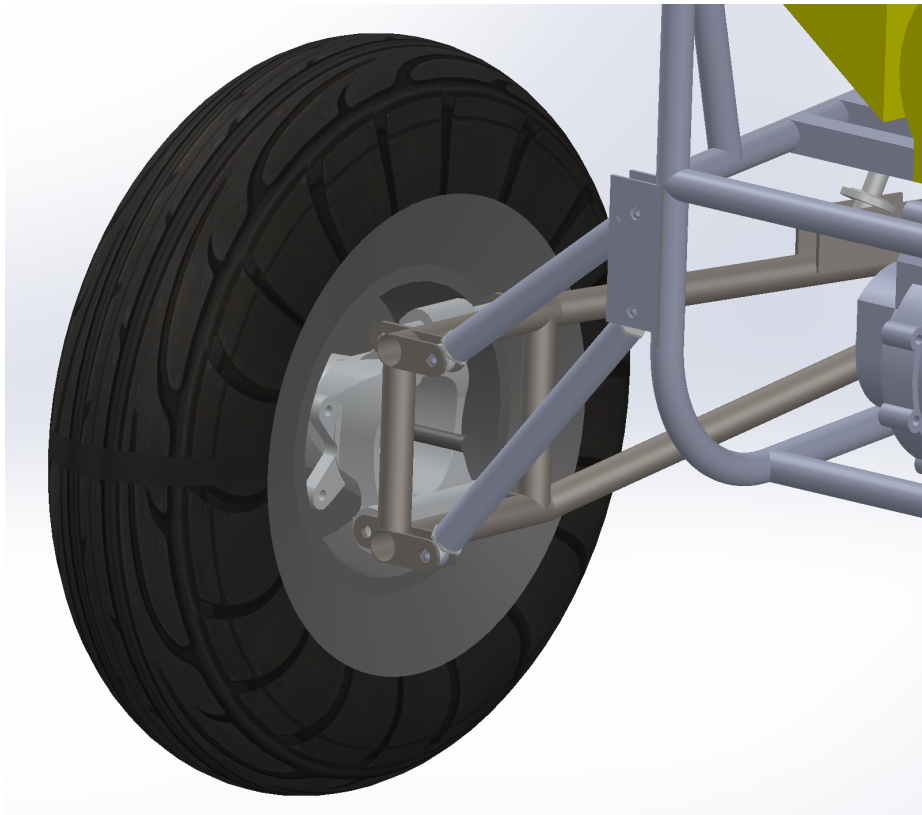


*Figure 119: 2020 miniBaja Design (no brakes)*

The mounting constraints remained the same. The master cylinders with separated with the mounted reservoirs. The parts were not cluster free and the 13.5" clearance from the lower to upper member front side of the chassis.

## *CAD Design*

### *Rotors*

A rotor is a part of a vehicle's braking system. It is roughly shaped like a flat-bottomed bowl with a wide lip at the top. The calipers and pads of the brake press against the sides of the rotor when the brake is applied, causing friction to stop the vehicle. The design of the rotor

allows the heat produced by this process to be evenly dispersed throughout the braking system, so it does not overheat.



Figure 120: Individual parts of brake hub assembly

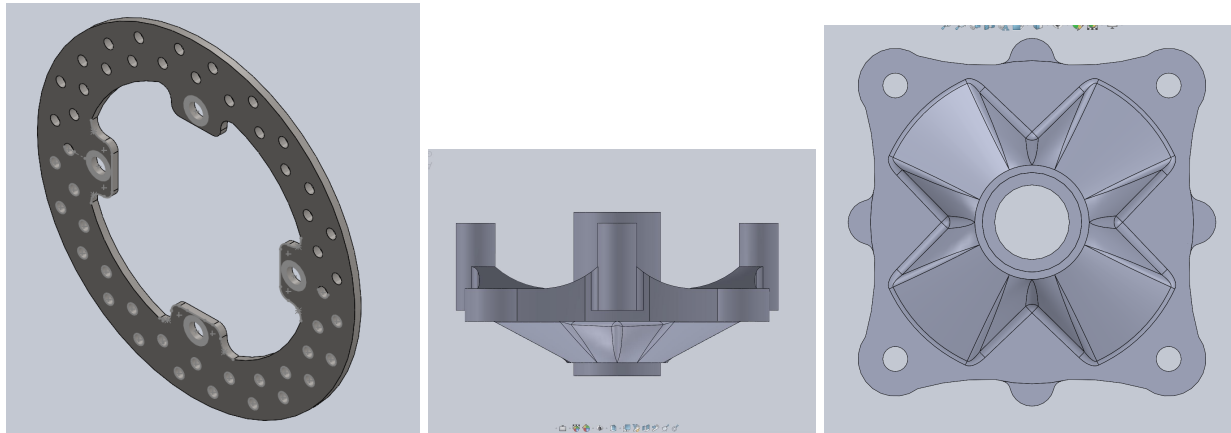


Figure 121: CAD model of parts

#### Assembly:

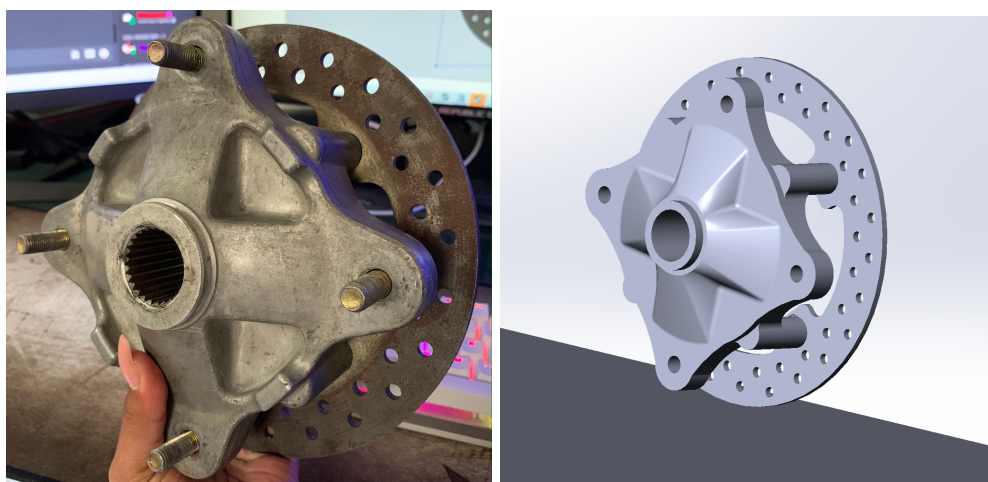


Figure 122: Brake Assembly (left) CAD Assembly (right)

## *Brake System Analysis*

### *Heat Transfer Analysis*

The back-brake disc was studied to get a superior comprehension of the heat transfer of a brake disk in a Baja vehicle; the heat made in the disc under braking conditions, the heat convection rate of the disk to the air, and the conduction of the brake plate to the center were not easy to compute. The assumed speed of the vehicle was utilized to figure the rakish speed of the brake disc before braking. The air speed was thought to be brimming with the rotor speed because of the pivot of the plate giving a positive and negative extraneous speed due to air. For the braking analysis we assumed: steady state, lumped mass, heated volume was equal to three times the contacted section of the disc (due to the area in the center of the disc being empty), convection is uniform across surface, air velocity is to be half the speed of the car, and air flow is turbulent. The energy equation was used in a way to sum up the rate of conduction and the rate of convection heat transfer and that equation is:

$$E_{in} = Q_{conv} + Q_{cond}$$

where,

$E_{in}$  = the braking heat is created by the caliper

$Q_{conv}$  = the about of heat exchanged through convection to the air

$Q_{cond}$  = the about of heat exchanged through conduction to the center point. This can be expressed because of the steady state that has been assumed.

Then the following two equations were used:

$$F_{in} = \mu_k \int F_n(x)dx$$

$$F_{in} = \frac{\mu_k F_n (V_s - V_f)}{2t}$$

where,

$F_{in}$  = the force on the brake disc

$\mu_k$  = the coefficient of kinetic friction

$x$  = the position

$V_s$  = the starting angular velocity

$V_f$  = the final angular velocity

$t$  = time

The bottom equation is used to calculate the total heat produced in the disc from normal braking. Once total heat can be discovered, a convection analysis of the disc to the surrounding air can be

done. The next thing to be done is calculating the convection heat transfer which follow Newton's law of cooling using this equation:

$$Q = hA(T_{disc} - T_{\infty})$$

where,

$T_{disc}$  = the temperature of the surface

$T_{\infty}$  = the temperature of the fluid (air) at infinity

$A$  = the area (assumed to be twice the area of a face of the disc)

$Q$ = the heat transfer rate from the disc to the air

Then, a conduction analysis was also made using Fourier's law using the equation:

$$Q = \frac{Ak_f \Delta T}{\Delta x}$$

Then after combining the equations we have the following:

$$\frac{\mu_k F_n (V_s - V_f)}{2t} = Q = hA(T_{disc} - T_{\infty}) + \frac{Ak_f \Delta T}{\Delta x}$$

The outcomes can be evaluated and tested when determining a  $T_{disc}$  temperature and finding out the surface of the circle with a speed at the beginning as well as time. This can be a nearby estimate that can be utilized to permit further examination of the utilization of different kinds of materials for brake plate in a Baja vehicle, for instance, aluminum.

### ***Brake Force Calculations***

For the design goals:

Braking Distance

$$D_b = 60\text{in} - 80\text{in}$$

Maximum Velocity (before braking)

$$V_{max} = 20 \text{ mph} = 29.33 \text{ fps}$$

Deceleration

$$d = \frac{v}{t} = \frac{8.94 \frac{\text{m}}{\text{s}}}{0.7\text{s}} = 12.78 \frac{\text{m}}{\text{s}^2} = 1.302 \text{ gs}$$

$$F_{zf \text{ dyn}} = (1 - 0.625 + 0.278 * 1.302) * (240) \\ = 176.869 \text{ kg} = 1734.5 \text{ N}$$

$$\Delta_{dynamic \text{ weight transfer}} = X_{aw} \\ = 0.27 * 13.06 * 240 = 846.29 \text{ N}$$

$$a = \mu * g$$

Yielding,

$$\mu = \frac{a}{g} = \frac{13.06 \frac{\text{m}}{\text{s}^2}}{9.81 \frac{\text{m}}{\text{s}^2}} = 1.33 \text{ gs}$$

$$\psi_{zf} = \frac{F_{zf}}{W} = \frac{225}{600} = 0.375$$

$$F_{zf \text{ dyn}} = F_{zf} + \Delta_{dyn} = 1000.85 + 846.29 = 1847.14 \text{ N}$$

$$F_{xf} = \mu * F_{zf \text{ dyn}} = 0.9 * 1847.14 = 1662.43 \text{ N}$$

$$F_{xr} = 0.9 * 708.41 = 632.96 \text{ N}$$

Needed Front Torque for Braking

$$T_{xf} = \frac{F_{xf} * R}{r} = \frac{1662.43 * 11 * 25.4}{1000} = 464.48 \text{ Nm}$$

$$T_{xr} = \frac{F_{xr} * R}{r} = \frac{632.96 * 11 * 25.4}{1000} = 184.89 \text{ Nm}$$

For the existing dimensions from previous miniBaja:

Master Cylinder Bore = 19.05 mm ( $\frac{3}{4}$ "")

$$\text{Area} = 0.000284 \text{ m}^2 = 0.44 \text{ in}^2$$

$$\text{Front Caliper Area} = 1019.34 \text{ mm}^2$$

$$\text{Rear Caliper Area} = 793.55 \text{ mm}^2$$

$$\text{Pedal Force} = 130 \text{ lbf} = 578.2665 \text{ N}$$

$$\text{Pedal Ratio} = 6:1$$

Brakes Leverage efficiency = 0.8 (assumed value)

$$F_{mc} = 2775.68 \text{ N}$$

$$P_{mc} = 9773518.31 \frac{\text{N}}{\text{m}^2}$$

Front and Rear Force on Calipers

$$F_{rc} = 30220.978 \text{ N}$$

$$F_{fc} = 27389.3935 \text{ N}$$

Force on Disk

$$F_{dr} = 5909.36 \text{ N}$$

Torque Generated

$$T_{gf} = 464.48 \text{ Nm(front)}$$

$$T_{gr} = 184.85 \text{ Nm(rear)}$$

NEW	Front	Rear
<b>Torque Needed (Nm)</b>	464.48	184.85
<b>Safety Factor</b>	2.97	12.15

Table 17: Torque needed, generated, and safety factor

A MATLAB code was utilized to calculate the braking force. Equations were used to construct the Matlab code necessary for the brake force calculation and the other variables necessary for the Rotor and Disc Selection. Then, a MATLAB program is composed utilizing M-File for discovering elements raise pivot and front hub powers (Normal reactions) as for vehicle speeding up in 'g' units. A plot is acquired for back hub and front hub powers (Vs) Vehicle deceleration. In this MATLAB program, vehicle load and other vehicle geometry are entered as inputs, the magnitude of above said forces plots are acquired. Another MATLAB program is composed utilizing M-File for discovering dynamic braking power at front and back wheel, created amid sudden braking. In this program, if vehicle stack, vehicle geometry and stopping mechanism equipment information are entered, the greatness of the above said powers and compelling plate span are gotten for the specific load condition. A plot which is given is gotten between unique back and front pivot braking power. A subplot, in which the coefficient of friction between the track surface and the tire is expected as 0.7, is likewise gotten between powerful back hub power and front pivot drive.

$$\frac{M_f}{M} = \Psi$$

where,

$M_f$  = static rear axle load

$M$  = total vehicle mass

$\Psi$  = static axle load distribution

The changes in axle loads during braking bears no relationship to which axles are braked. They only depend on the static laden conditions and the deceleration. Using the equation:

$$(1 - \Psi) + (Xa)M = M_{fdyn}$$

where,

$a$  = deceleration

$M_{fdyn}$  = dynamic front axle load

The max braking force on any axle can be computed before the wheel lock using this equation:

$$F_A = M_{wdyn} \times g \times \mu_r$$

where,

$F_A$  = total possible braking force on axle

$M_{wdyn}$  = dynamic axle mass

$g$  = acceleration due to gravity

$\mu_r$  = coefficient of friction between the road and tire

After choosing the wheel type that will require braking to produce adequate braking power the torque prerequisites of each wheel, for some enactment the conveyance among front and back brakes is set down. This can be accomplished by differing the brake size or almost certain utilizing a valve to lessen the incitation weight. The equation that can be used is:

$$T = \frac{BF_w R}{r}$$

where,

$T$  = brake torque

$BF_w$  = braking force on wheel

$R$  = static laden radius of the tire

$r$  = speed ratio between the wheel and the brake

The effective radius also known as the torque radius of a brake disc is the centre of the brake pads by area. For dry discs it is assumed to use the following equation:

$$r_\theta = \frac{D + d}{4}$$

where,

$r_\theta$  = effective radius

$D$  = disc useable outside diameter

$d$  = disc useable inside diameter

The braking force can only be generated if the wheel does not lock because the friction of a sliding wheel is much lower than a rotating one. For the total braking force, Newton's Second Law can be used and that equation is:

$$B_F = M \times a \times g$$

where,

$B_F$  = total braking force

It was discovered that there was plentiful space to put the pedal in the vehicle in an agreeable position for the driver. To modify inclination, an obtained predisposition bar should be utilized. So as to change inclination rapidly, a remote link will be setup with the goal that it will have the capacity to be balanced by the driver on the fly. The ace barrels will likewise be bought.

Whatever remains of the pieces will be created from a light material with the goal that they are lightweight, remembering the aggregate weight of the vehicle. So as to dissect the powers that the pedal will understand, a driver input constrain should have been expected. To discover this Power- Force, the group set a scale against a divider and sat in a comparable position as in the vehicle with the driver's back against another divider. Each colleague needs to press the scale as hard as possible when it comes to racing time after the manufacturing process. Other than not having all the parts, we managed to create a successful brake assembly - the brakes in the rear and front might possibly differ in the future design as it sets slightly different in the rear.

### *Updated Design with Brake Assembly*

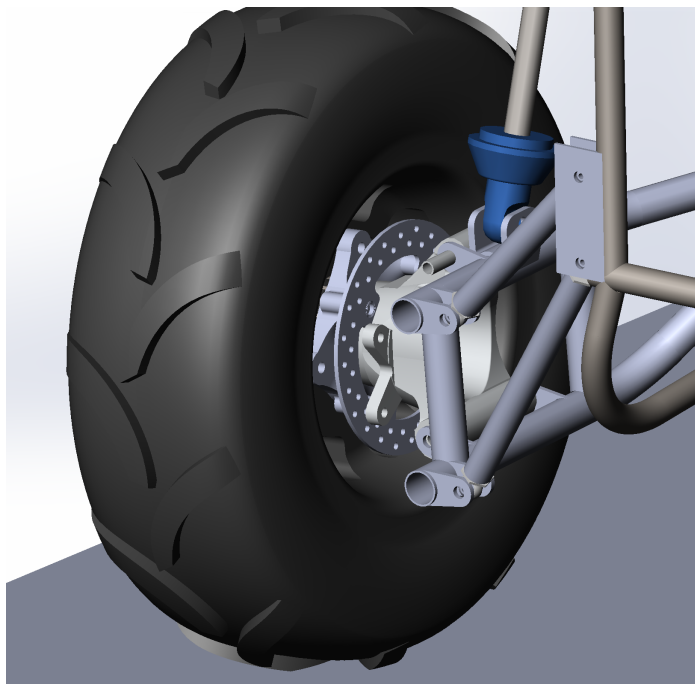


*Figure 123: 2021 miniBaja (with brakes) FINAL ASSEMBLY*

# Electronics

## What is an AWD System?

To incorporate an All-Wheel-Drive (AWD) system in the Baja, the team planned to simulate Nissan's ATTESA ETS System that helps aid the transfer of power from the rear shaft (which receives torque from the rear engine) to the front shaft. The following concept diagram will illustrate the intended design:

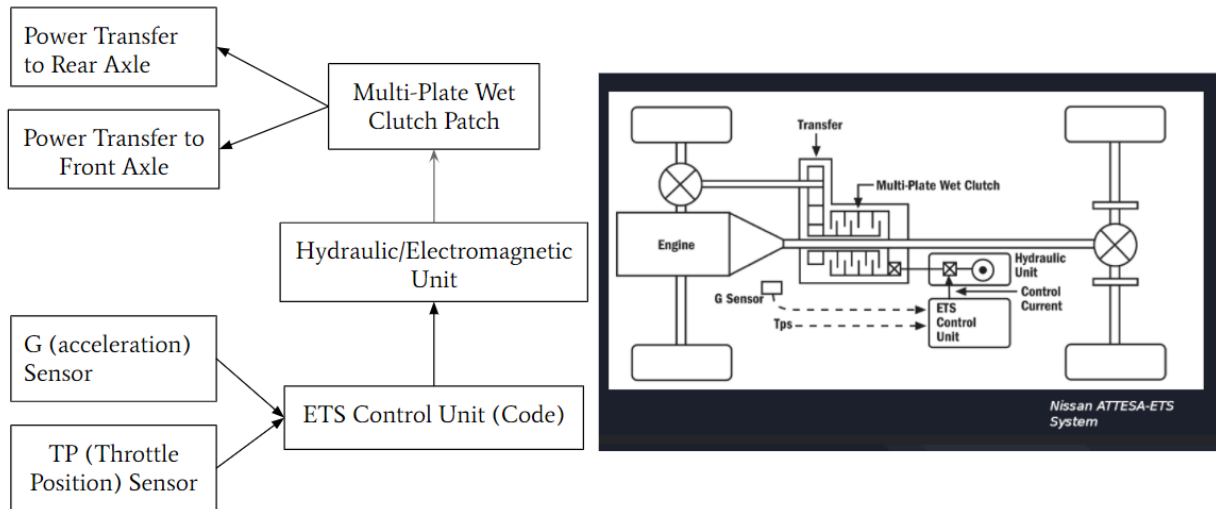


Figure 124: Concept Diagram of Electronics ATTESA Software System

The ATTESA system utilizes sensor information from G (acceleration) and TP (throttle position) sensors from the Baja to activate a Multi-Plate Wet Clutch Pack that transfers a percentage of torque provided from the rear shaft to the front shaft that consequently transfers power to the front wheels using a front differential system. The amount of torque and power transfer is dependent on the amount of normal force that is applied to the friction plates inside the clutch pack, which can be hydraulically or mechatronically activated.

The purpose of implementing Nissan's AWD system is to increase performance incentives, safety, and reliability. It would help prevent unwanted loss of grip on low traction surfaces, limit power loss by not always being in AWD mode, reduce overall wear and tear on powertrain components, and most importantly prevent excessive over/understeer while cornering during a race.

## What is a Clutch Pack & Torque Transfer Theory?

To utilize this AWD system, a multi-plate clutch pack must be used to transfer some, if not all, of the power coming from the rear shaft to the front shaft. This is done by applying a normal force onto a pressure plate that compresses friction and steel plates that would transfer torque from the rear to the front. This can be illustrated by the following figures:

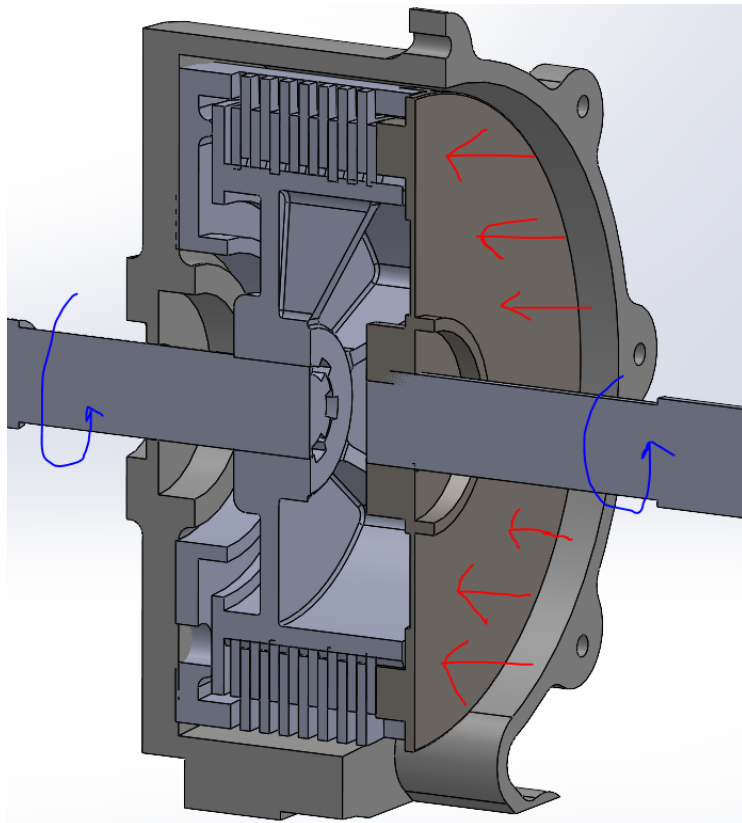


Figure 125: Sectional View of Torque Transfer

## Clutch Pack - Torque Transfer Diagram

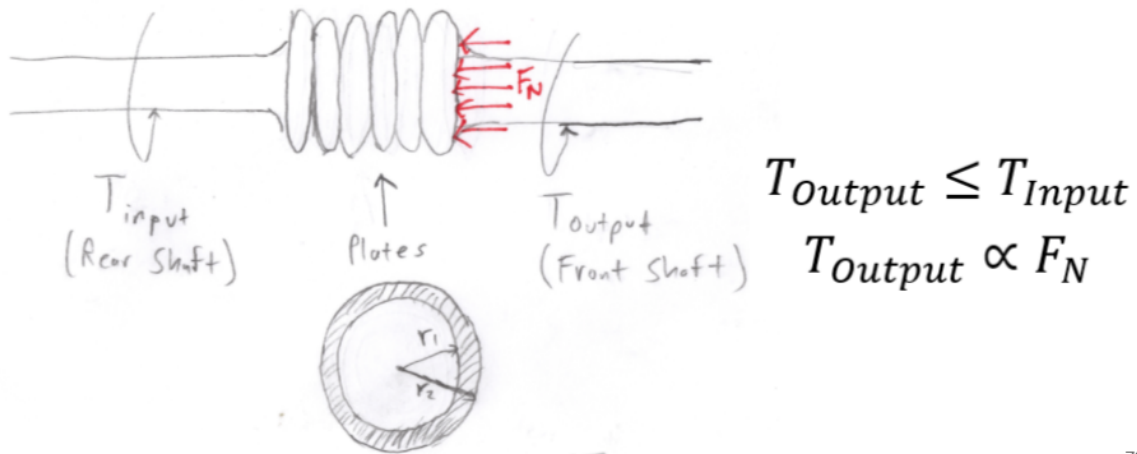


Figure 126: Torque Diagram Conceptualization

73

When the interior plates are compressed, a percentage of torque from the rear shaft is transferred to the front shaft. Maximum torque transfer is dependent on the maximum normal force  $F_N$  needed to compress these plates. In fact, the maximum force can be calculated by using the following torque transfer theory:

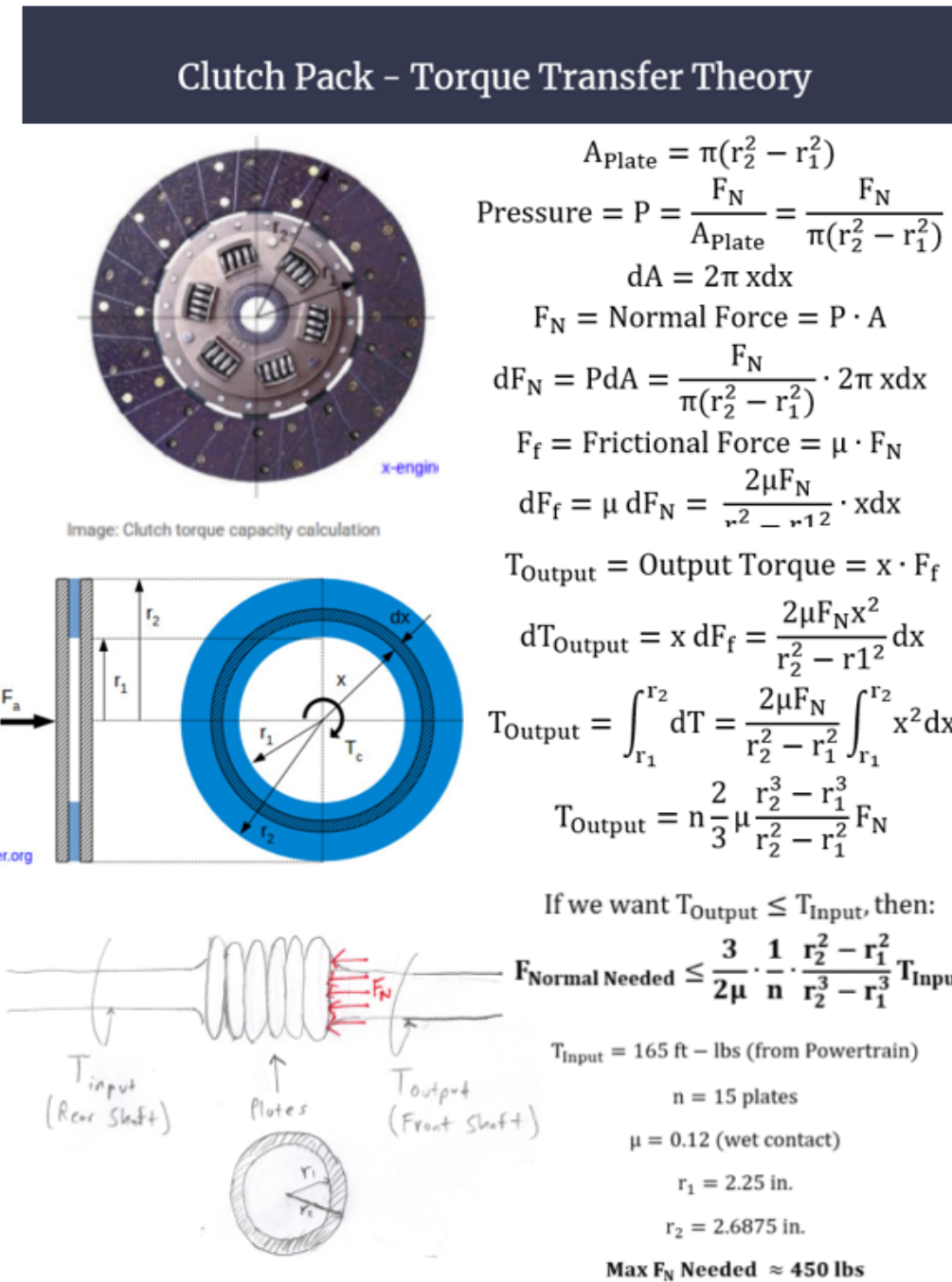


Figure 127: Torque Transfer Theory Calculation

## *Flaws in the Previous EM Clutch Design*

Before the start of the Senior Design, it was originally planned to use a hydraulically powered clutch activation system. However, this would be problematic because of the transitional delay of the movement of hydraulic fluid between the linear actuator that pushes fluid into the clutch pack and the pressure plate that compresses the separator disks and activates the clutch system to transfer power to the front shaft.

It was proposed to run a conceptual idea of modifying the original clutch pack design by activating it electromagnetically, instead of powering it hydraulically. However, the EM clutch design that was worked on last semester (Fall 2020) was flawed because the conceptual understanding of electromagnetism was wrong.

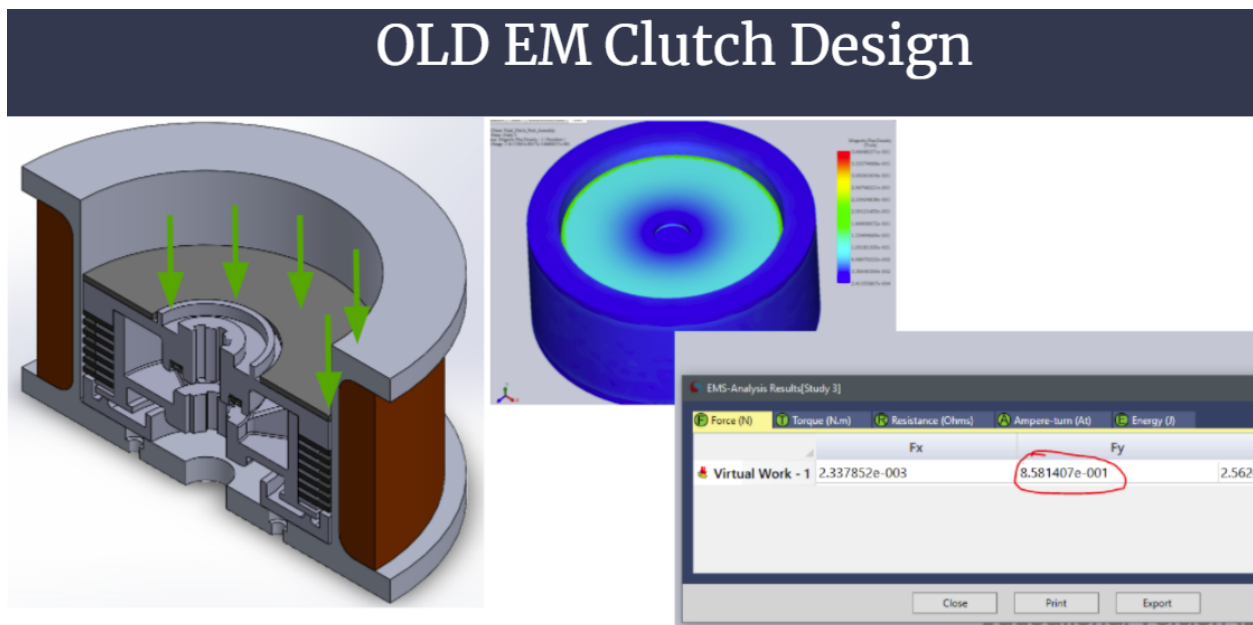


Figure 128: Old Electromagnetic Clutch Design

The previous photo shows the old electromagnetic clutch design that used a solenoid wrapped around the clutch pack that would apply an electromagnetic force onto the steel pressure plate. However, after running an FEA electromagnetic simulation, it shows that the expected amount of force from this design is less than 1 N. As a result, the team's electromagnetism understanding was completely wrong. The following image shows what should have been done:

# Our EM Understanding was Wrong

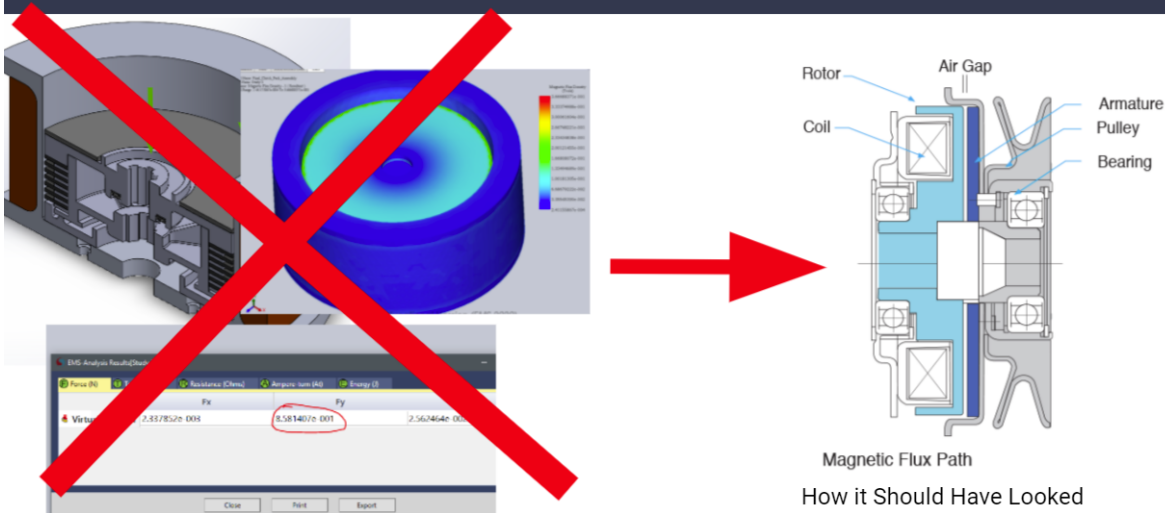
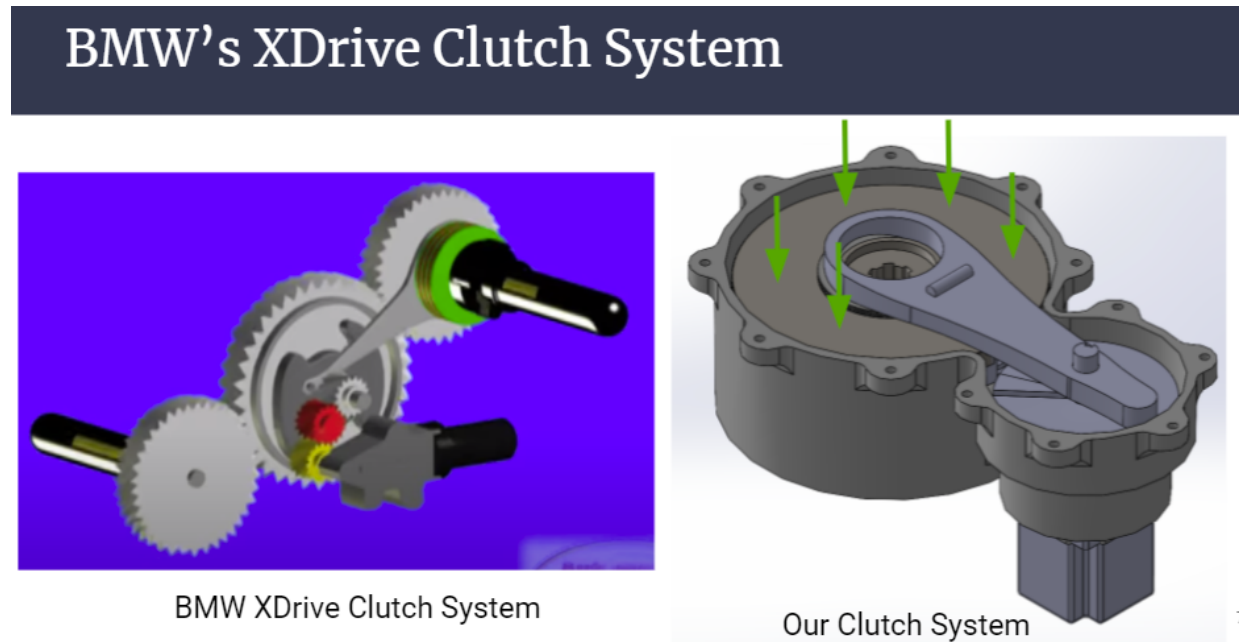


Figure 129: Old EM Clutch Design vs. Industrial Design

What the team should have done was to try to mimic the industrial way of implementing an electromagnetic clutch system. The difference between this and the industries' design is that companies create a rotor that entirely wraps around and houses the coil (to maximize EMF) to magnetically attract the armature to compress the friction plates. However, this implementation would have required an entirely new design, including the clutch pack that the team wanted to utilize for the design to mitigate costs. If the team didn't restrict themselves to reusing old components and came up with an entirely new concept design, then this electromagnetic implementation might have worked. However, because of time constraints and the fact that the team still wanted to use the old clutch pack design, they instead tried a different implementation: BMW's XDrive Clutch System.

## *BMW's XDrive Clutch System*



*Figure 130: Mimicking BMW's XDrive Clutch into Our Design Implementation*

Towards the last quarter of the Senior Design year, the team decided to try to mimic BMW's XDrive clutch system. This design works by converting rotational motion from a stepper motor into vertical, linear motion that would compress the pressure plate on top of the clutch basket:

### BMW's XDrive Clutch System: How It Works

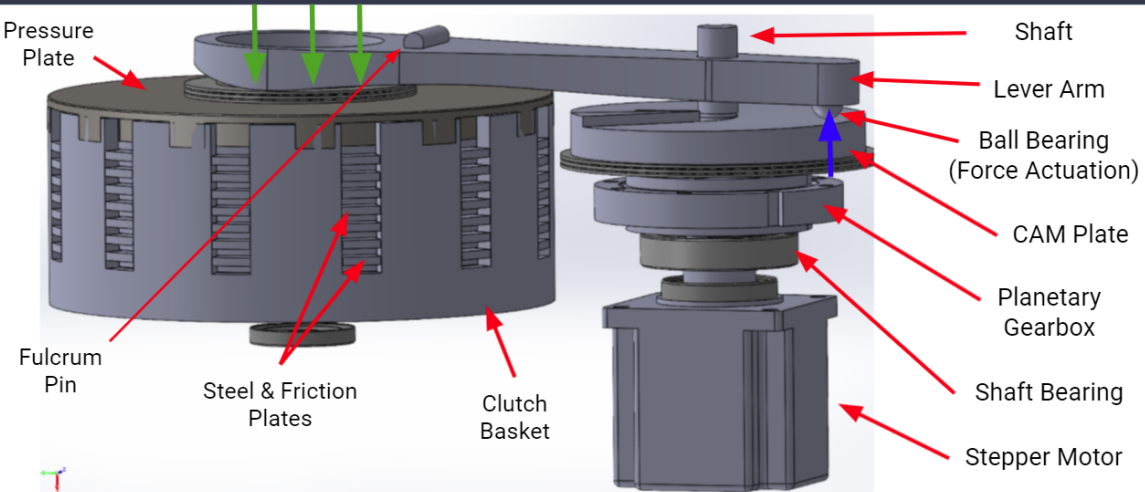


*Figure 131: Interior Clutch Assembly Components & How it Works*

Again, the goal of this design implementation is to create a normal force (green downwards arrows) onto the pressure plate on top of the clutch basket. By creating this force, the steel and friction plates inside the clutch basket would compress and transfer a percentage of the torque coming from the input shaft to the output shaft. This normal force is created by using a stepper motor that provides around 100 N-cm of torque; this torque is then amplified by utilizing a planetary gearbox that reduces rotational speed and increases mechanical torque that would turn the CAM plate in this design. As this CAM plate rotates, an upwards force (blue arrow) is applied onto a ball bearing embedded in the lever arm. Note, there is a hole in the right side of the lever arm to provide clearance for a shaft to radially restrain the gearbox in place (this does NOT hinder the lever arm's movement in any way). Finally, by using a fulcrum pin (which is restrained by a lid enclosing this design), this force is then amplified as well. As a result, this entire electromechanical design utilizes two mechanical advantage systems: Lever Arm and Cylindrical Ramp.

### **Lever Arm Mechanical Advantage**

From the torque transfer theory section, it estimated that the team needed approximately 450 lbs. of compressive normal force on the clutch basket's pressure plate. By utilizing a lever arm, the amount of required force can be less:

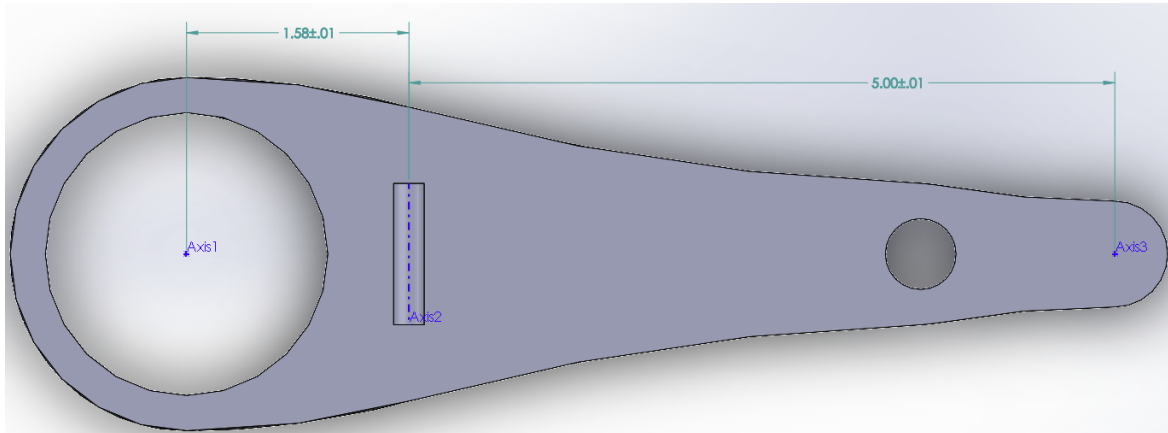


*Figure 132: Lever Arm Dimensions*

$$\text{Max } F_N \text{ Needed} \approx 450 \text{ lbs}$$

$$F_N L_1 = F_2 L_2$$

$$F_2 = \frac{L_1}{L_2} F_N = \frac{1.38 \text{ in}}{5.0 \text{ in}} 450 \text{ lbs}$$

$$F_2 = 142 \text{ lbs}$$

Thus, on the right side of the lever arm, the team only needed approximately 142 lbs. of upwards force.

### Cylindrical Ramp Mechanical Advantage

As the cylindrical CAM plate rotates, it can create the required upwards normal force of 142 lbs. by using frictional torque. This mechanism can be illustrated in the following figure:

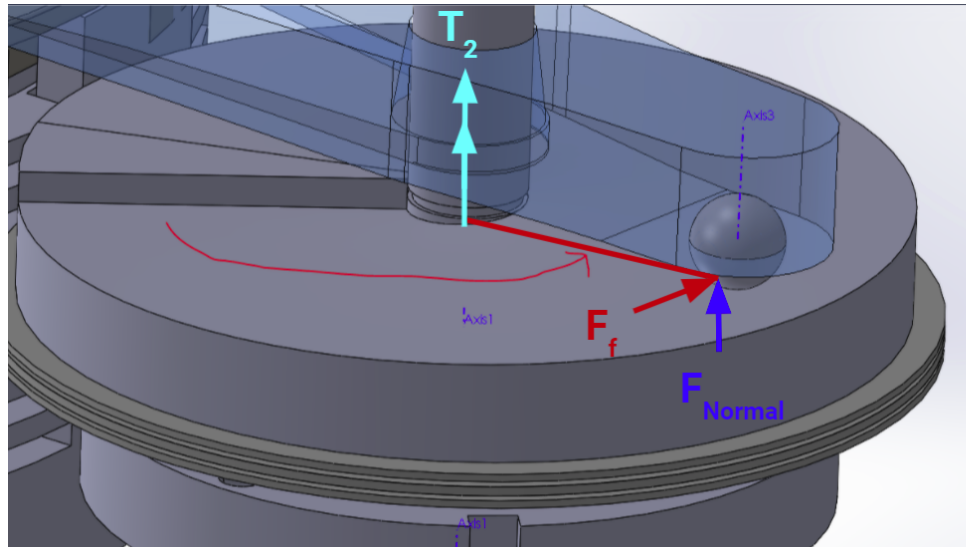
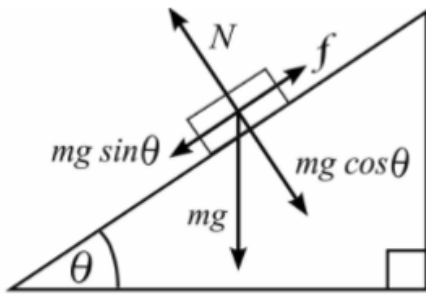


Figure 133: CAM Plate Cylindrical Ramp Mechanism

This frictional torque is dependent on the geometry of the cylindrical inclined plane by conducting the following calculations:



$$\theta = \tan^{-1} \left( \frac{\text{ramp height}}{\text{ramp length}} \right)$$

$$= \tan^{-1} \left( \frac{\text{CAM height}}{\text{CAM Torque Diameter}} \right)$$

$$\theta = 0.83^\circ$$

$$F_{\text{Normal}} = F_2 = 142 \text{ lbs}$$

$$\mu = 0.12$$

$$F_f = \mu F_{\text{Normal}} \cos(\theta)$$

$$F_f = 23 \text{ lbs}$$

$$T_2 = \text{CAM}_{\text{Torque Radius}} F_f$$

$$T_2 = 3.5342 \text{ N-m}$$

In rectangular coordinates, the angle would be calculated by taking the inverse tangent of the ramp height over the ramp length; however, in cylindrical coordinates (since it's a cylindrical inclined plane), this angle would be the CAM's height over the CAM's torque diameter (which is

double the amount of radial distance from the axis of rotation to the point of frictional application on the ball bearing). By using this angle, the amount of frictional force and torque can be calculated, as shown above. Thus, the amount of torque that needs to be applied about the CAM plate's axis is approximately 3.53 N-m to provide enough frictional force that, in return, creates the upwards normal force of 142 lbs.

### **Stepper Motor Requirements**

Because the team needs to apply around 3.53 N-m of torque (which is very high), they decided to utilize a planetary gearbox that would reduce the necessary torque requirement:

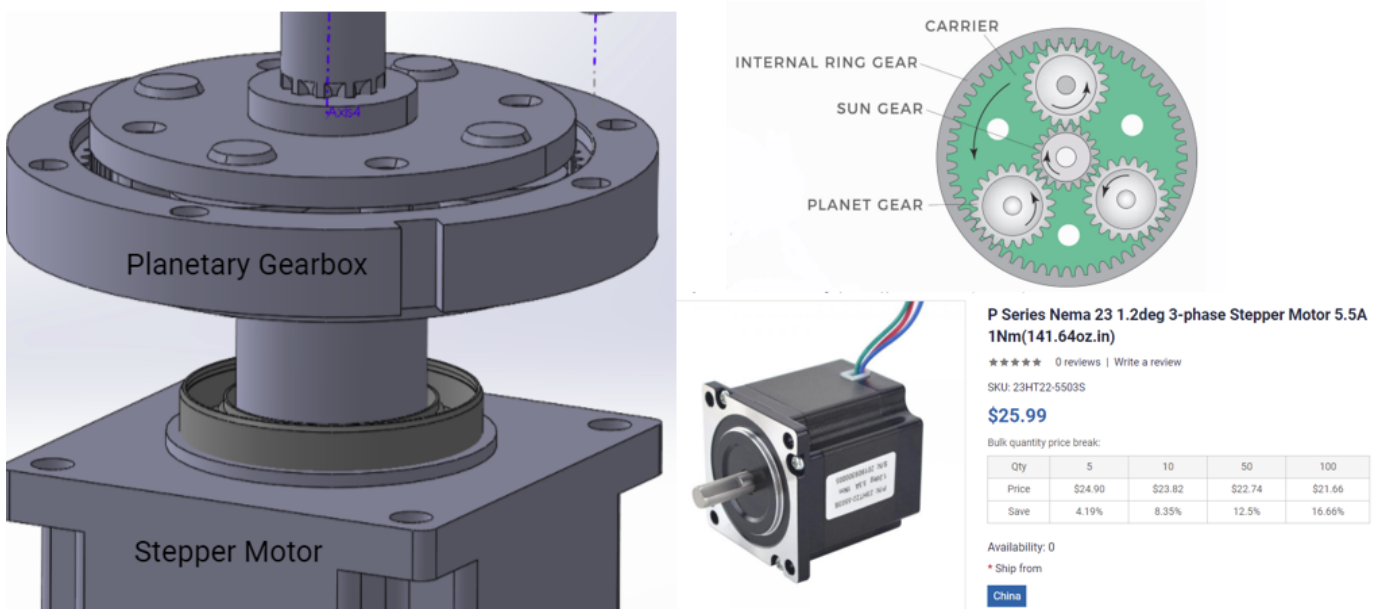


*Figure 134: Stepper Motor-Gearbox Assembly & Specifications*

$$\text{Gear Ratio} = R = 4:1$$

$$T_{\text{Motor}} = \frac{T_2}{R} = \frac{3.5342}{4} = 0.8836 \text{ N-m}$$

$$\text{Angular Accuracy} = 360^\circ \times R = 1440^\circ$$

$$0 \rightarrow 450 \text{ lbs} : 0^\circ \rightarrow 1440^\circ$$

$$3.2 \text{ lbs} : 1^\circ$$

Because the gearbox has a gear ratio of  $R = 4$ , this reduces the necessary amount of torque to approximately 0.88 N-m. This also increases the angular accuracy of the design by 4; instead of applying 0 to 450 lbs. in 1 revolution ( $360^\circ$ ), the gearbox improves this application by 4

revolutions ( $1440^\circ$ ), thus lowering the amount of force per degree of rotation to around 3.2 lb./deg $^\circ$ .

### *Final Assembly of XDrive Clutch Design*

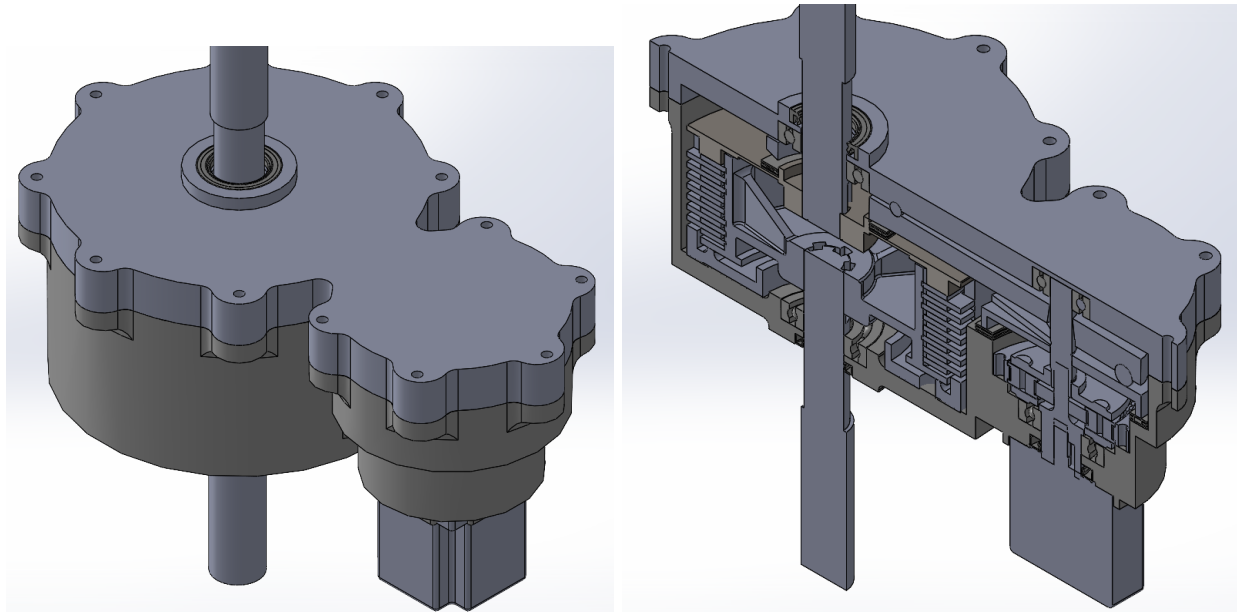


*Figure 135: Full Assembly (Left—Full View & Right—Sectional View)*

### *FEA Analysis*

FEA was only conducted on the lever arm because the cam plate would be secured by a thrust bearing, meaning there would be little moment forces acting on the cam plate and only compressive forces. The lever arm is essentially a simple lever, so a compression-only boundary condition was placed on a contact patch of the lever arm that was over the pressure plate, and a frictionless boundary condition was placed on the pivot point. The force was assumed to be 1000 N or roughly 225 lbs which was an additional safety factor that was put in case the clutch pack would need more force to be actuated.

After refining the mesh and getting results from ANSYS, a singularity had formed on the frictionless boundary condition where the fulcrum would be. The design team decided that this could be ignored due to St. Venant's principle and convergence was found on the thinnest section of the lever arm at approximately 200 MPa, which gives us a safety factor of at least 1.5 if we decide to use cold-drawn 1020 Steel as the material.

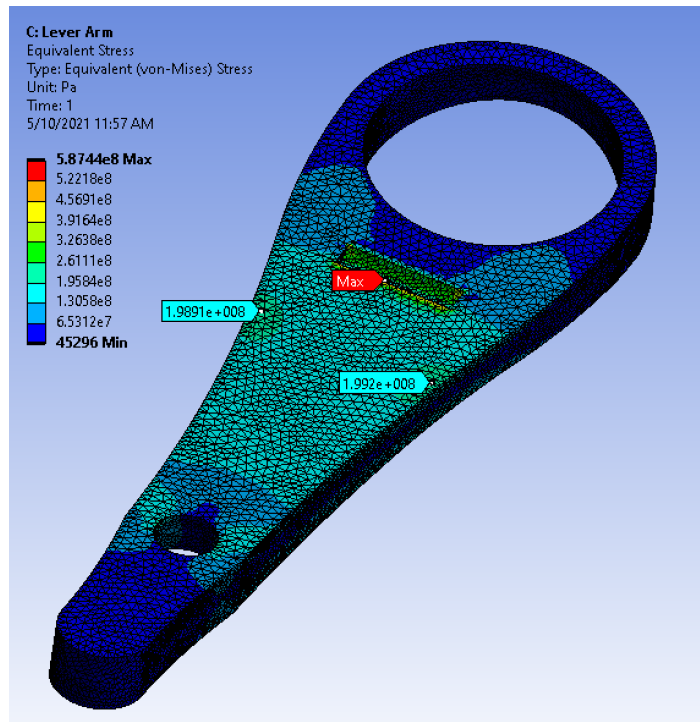


Figure 136: Lever Arm FEA Results

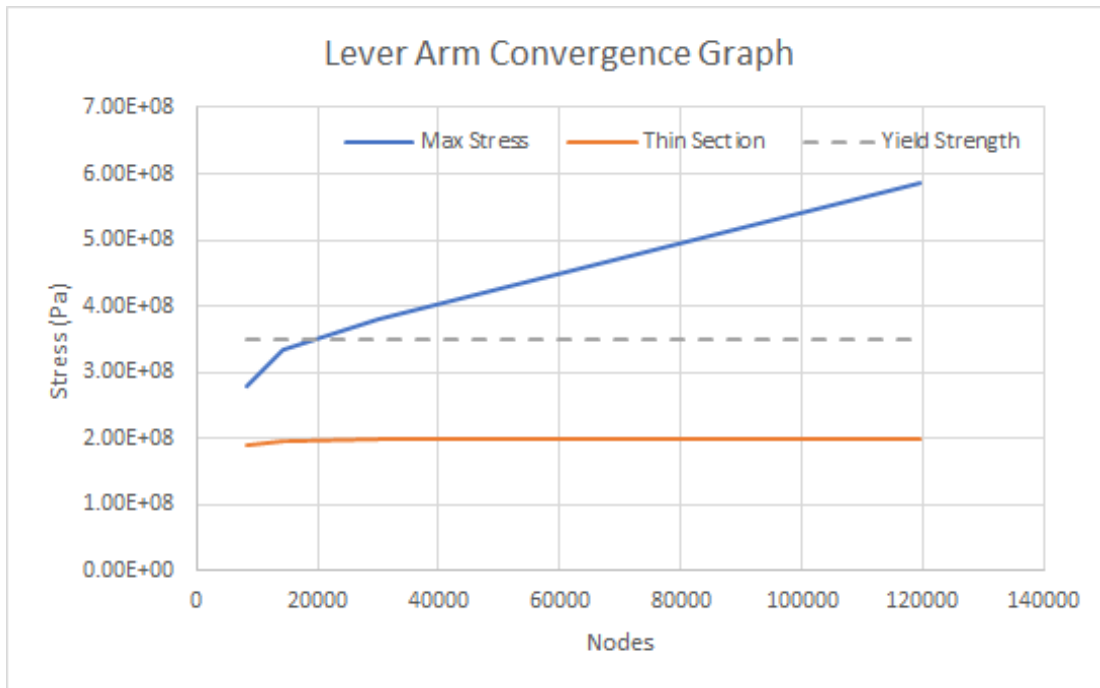
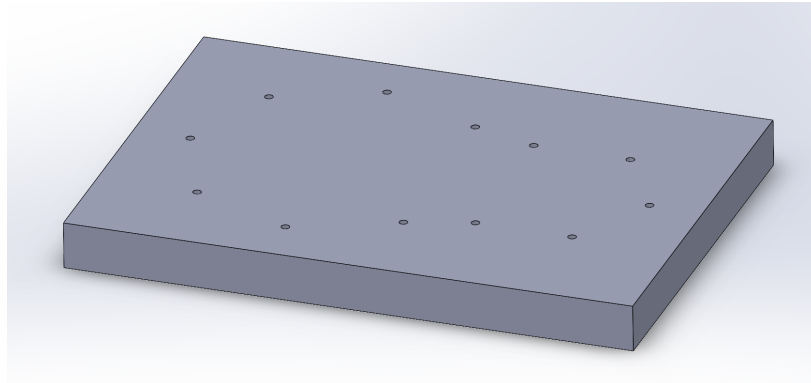


Figure 137: Lever Arm Convergence Graph

## ***Manufacturing Plan***

For the enclosure a manufacturing plan had to be laid out to ensure the smooth production of the enclosure and the lid as they are some of the more complex components that would need to be manufactured. For both models, a fixture plate will be used that the parts can be mounted to during the last operation. Both the stock material and the fixture plate should have parallel and perpendicular faces within 0.001" tolerance across the faces prior to CNC machining. The operations will be as follows:

1. Face off all faces of stock material and fixture plate with parallelism and perpendicularity tolerances of 0.001"
2. Machine Cavities and Bearing Holes on Interior, Tap drilled holes to accommodate fixturing
3. Fasten Enclosure to Fixture Plate and probe rectangular faces on bottom of enclosure to machine oil seals.



*Figure 138: Fixture plate for Machining Second Operations*

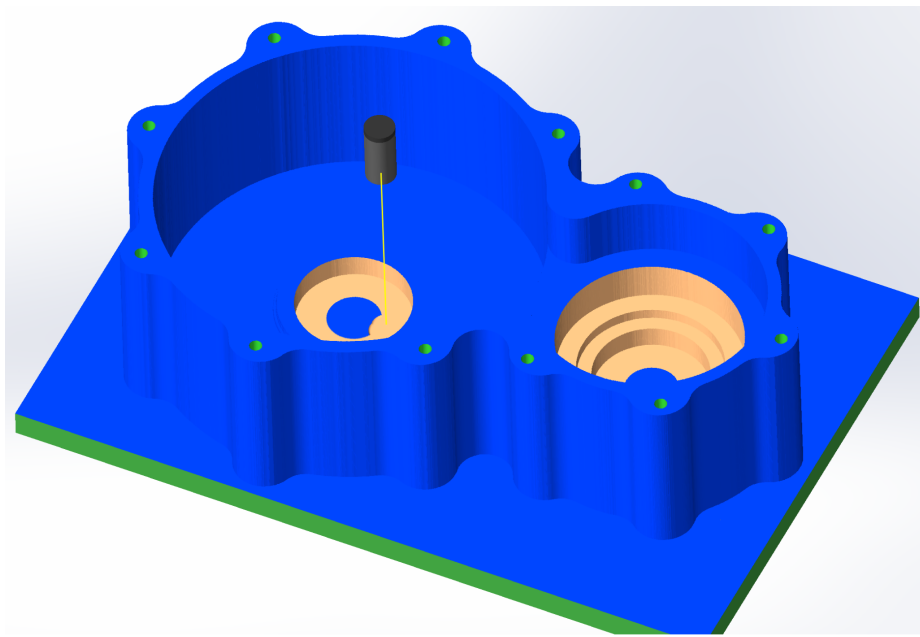


*Figure 139: Operation 2, Machining of Cavities and Bearing Holes, Tap-drilling holes for later tap operation*

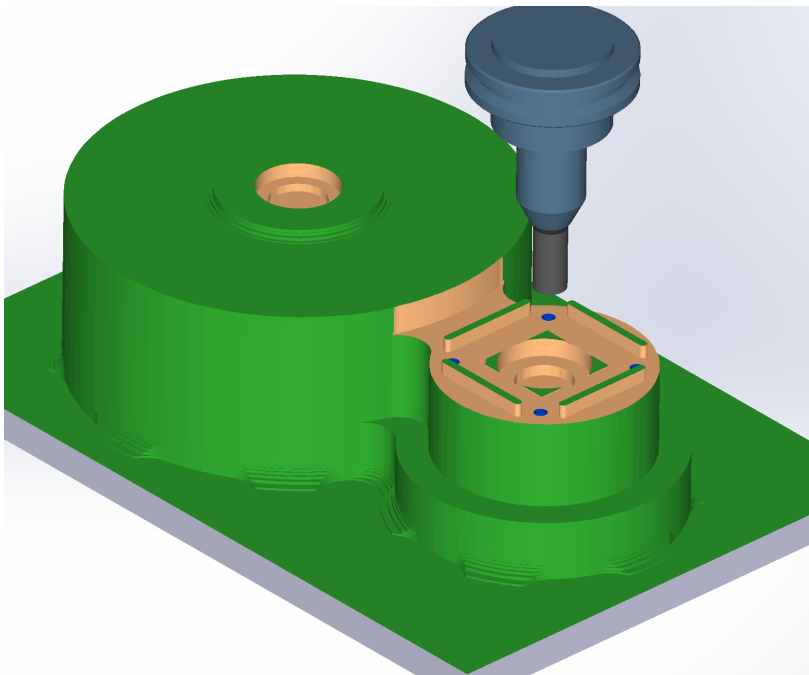


*Figure 140: Operation 3, Machining of second side*

# Conclusion

In general, the powertrain team might want to revise this design as it is overly complex, and many other more reliable systems are out there that can be purchased for much cheaper which is paramount in the team's financial situation. The gear reduction design may still be changed as mounting a gearbox might be easier than mounting a chain and sprocket system as well as the unreliability of a chain and sprocket system. A more robust design should also be made for power delivery both to the front and the rear and a rear differential may have to be chosen again.

The electrical team needs to conduct testing on a control system for AWD to work on the Baja vehicle. If testing cannot be done, AWD will likely be done through manual means or some sort of auto-engaging mechanism rather than through a control system. This would also mean a calibration system to determine how much power is transferred to the front shaft when the EM clutch is activated must be made. Once the calibration system is understood and completed, we then would then need to edit the ATTESA-NYC code using Arduino to program when and how much the clutch should be activated to transfer more power to the front wheels by analyzing data from the accelerometer and hall sensors that would be placed on the Baja. Additionally, we need to also determine the circuitry (i.e., the circuit boards) that would run the ATTESA program, as well as for the brake lights and feedback meters. A side project would be to have strain data acquisition on the suspension components to design more lightweight and robust control arms and knuckles.

For the suspension and steering system, the entire suspension system should be experimentally evaluated in real life to be able to produce actual results using LOTUS. Having a knowledge base on what the positions of certain points affect on turning radius/speed and bump steer would help future designs of the Baja. Ackerman steering also might need to be reoptimized as changes to the front suspension have dramatically altered the steering capability of the vehicle. As a result, the front suspension may need further iterations due to Ackerman steering geometry issues.

The next step for chassis is to continue attempting to get results from ANSYS and manufacturing the chassis. When the next rulebook comes out, it will also have to be reevaluated before going further into manufacturing because rule changes may force changes to the chassis design.

The main goal for the brakes is to see if all of the components can be assembled together, as the current hubs and knuckles may not mate with each other correctly. These should be pulled from wherever the differential is being sourced from, or research should be done on how to design and manufacture knuckle and hub assemblies.

The costs of this project will likely still be the same as last year, where instead of buying many suspension components, more money will be dedicated to the powertrain and electrical systems. Overall the powertrain, electrical, and suspension/steering systems are going to require the most validation work. The goals for next years team are to ensure the designs are within the next year's rulebook standards and the vehicle systems are well validated to prevent failure of any components.

# References

- Acin, Marcos. "Stress Singularities, Stress Concentrations and Mesh Convergence." *Acin*, 2015,  
[www.acin.net/2015/06/02/stress-singularities-stress-concentrations-and-mesh-convergence/](http://www.acin.net/2015/06/02/stress-singularities-stress-concentrations-and-mesh-convergence/).
- Overdrive.in. "How a CVT Works - Everything You Need to Know about Continuously Variable Transmission." *Overdrive*, 19 Sept. 2019,  
[www.overdrive.in/news-cars-auto/features/how-a-cvt-works-everything-you-need-to-know-about-continuously-variable-transmission/](http://www.overdrive.in/news-cars-auto/features/how-a-cvt-works-everything-you-need-to-know-about-continuously-variable-transmission/)
- Mashadi, Behrooz, and David Crolla. *Vehicle Powertrain Systems*. Wiley, 2012.
- Edge.RIT.edu "Glossary of Suspension Terms" RIT Baja,
- Ferrara, Michael. "ATTESA Explained: Understanding Nissan's Electronic Torque Split Technology." *DSPORT Magazine*, 19 Oct. 2018,  
[dsportmag.com/the-tech/education/attesa-explained-understanding-nissans-electronic-torque-split-technology/](http://dsportmag.com/the-tech/education/attesa-explained-understanding-nissans-electronic-torque-split-technology/)
- Parsons, Cameron. "Find Your Center: An Intro to Suspension Geometries." *DSPORT Magazine*, 7 Sept. 2017,  
[dsportmag.com/the-tech/education/find-your-center-an-intro-to-suspension-geometries](http://dsportmag.com/the-tech/education/find-your-center-an-intro-to-suspension-geometries)
- Parsons, Cameron. "Alignment Tech: Optimize Your Handling Performance." *DSPORT Magazine*, 11 June 2016,  
[dsportmag.com/the-tech/extracting-handling-performance-alignment-settings](http://dsportmag.com/the-tech/extracting-handling-performance-alignment-settings).
- Bump Steer | What factors effects bump steer? | How Bump steer can be corrected?  
<https://www.youtube.com/watch?v=Csw6FOHvHhs>
- *Suspension Designer*,  
[www.suspensiondesigner.com/tuning-bump-steer-and-bump-steer-linearity/](http://www.suspensiondesigner.com/tuning-bump-steer-and-bump-steer-linearity/).
- Collins, A. P. (2017, May 20). The Idiot's Guide To Oversteer Vs. Understeer And How To Beat Both. Retrieved from  
<https://jalopnik.com/the-idiots-guide-to-oversteer-vs-understeer-and-how-to-1795389460>
- "Keyfora." *Web Counter Gratis*, [www.keyfora.com/search/oversteering-fwd](http://www.keyfora.com/search/oversteering-fwd).
- "Automobile Suspension Design 101 (Part II)." *YouWheel.com*, 14 Jan. 2015,  
[blogs.youwheel.com/2014/06/12/automobile-suspension-design-101-part-ii/](http://blogs.youwheel.com/2014/06/12/automobile-suspension-design-101-part-ii/).
- Yaeger, Skitter, et al. *DesignJudges.com*, 17 Nov. 2020, [www.designjudges.com/](http://www.designjudges.com/).
- "Electromagnetic Clutches - How It Works." *YouTube*, YouTube, 8 July 2015,  
[www.youtube.com/watch?v=OztP3uFIUII](http://www.youtube.com/watch?v=OztP3uFIUII).
- "Coil Calculator." *Coil Physical Properties Calculator*,  
[production-solution.com/coil-calculator.htm](http://production-solution.com/coil-calculator.htm).
- "How to calculate the torque capacity of a clutch" *X-Engineer*,  
<https://x-engineer.org/automotive-engineering/drivetrain/coupling-devices/calculate-torque-capacity-clutch/>

# Appendix

## *Electronics MATLAB Codes*

### **Lever\_Arm\_Torque\_Motor.m**

```
% Created By: Yusuf Wong
clc; clear; close all;
mew = 0.16;
ramp_height = 0.125; %inch
torque_radius = 1.375; %inch
ramp_length = 2*pi*torque_radius; %inch
ramp_hypotenuse = sqrt(ramp_height^2 + ramp_length^2); %inch
theta = atand(ramp_height/ramp_length)
F_needed = 450; %*4.4482216153;
L1 = 1.58; %*0.0254;
L2 = 5; %*0.0254;
F_applied = F_needed*L1/L2
F_friction = mew*F_applied*cosd(theta)
Torque_1 = F_friction*torque_radius %cam_plate_median_diameter/2
%lb-inch
Torque_1_N_m = Torque_1*0.11298482933333
Gear_Ratio = 4;
Motor_Torque_N_m = Torque_1_N_m/4
```

## *Powertrain MATLAB Codes*

### **Shaft Stress analysis code**

```
clc
clear

rho = 7850;
d = 0.022225;
g = 9.81;
L = 0.635;
r = d/2;
I = (pi*r^4)/4;
A = pi*r^2;
V = A*L;
m_shaft = rho*L*A;
M = (m_shaft*g*L)/2;
sx = (32*M)/(pi*d^3)

T = 223.71;
tauxy = (16*T)/(pi*d^3)

s1 = (sx/2) + sqrt((sx/2)^2 + tauxy^2);
s2 = (sx/2) - sqrt((sx/2)^2 + tauxy^2);

n = 2;
```

```
sqrt((n^2)*(s1^2 - s1*s2 + s2^2))
```